

**REPUBLIC OF TURKEY
YILDIZ TECHNICAL UNIVERSITY
GRADUATE SCHOOL OF NATURAL AND APPLIED SCIENCES**

**THEORETICAL INVESTIGATION OF THE USE OF
NANOREFRIGERANTS IN VARIOUS REFRIGERATION CYCLES**

MELİH AKTAŞ

**MSc. THESIS
DEPARTMENT OF MECHANICAL ENGINEERING
PROGRAM OF HEAT-PROCESS**

**ADVISER
ASSIST. PROF. DR. AHMET SELİM DALKILIÇ**

İSTANBUL, 2014

REPUBLIC OF TURKEY
YILDIZ TECHNICAL UNIVERSITY
GRADUATE SCHOOL OF NATURAL AND APPLIED SCIENCES

**THEORETICAL INVESTIGATION OF THE USE OF
NANOREFRIGERANTS IN VARIOUS REFRIGERATION CYCLES**

A thesis submitted by Melih AKTAŞ in partial fulfillment of the requirements for the degree of **MASTER OF SCIENCE** is approved by the committee on 19.02.2014 in Department of Mechanical Engineering, Heat-Process Program.

Thesis Adviser

Assist. Prof. Dr. Ahmet Selim DALKILIÇ
Yıldız Technical University

Approved By the Examining Committee

Prof. Dr. Hasan HEPERKAN, Member
Yıldız Technical University

Assoc. Prof. Dr. Yasin ÜST, Member
Yıldız Technical University

Assist. Prof. Dr. Ahmet Selim DALKILIÇ, Member
Yıldız Technical University

ACKNOWLEDGEMENTS

Yıldız Technical University is one of the seven government universities situated in İstanbul besides being the 3rd oldest university of Turkey with its history dating back to 1911. It is regarded as one of the best universities in the country as well. Our university has 10 Faculties, 2 Institutes, the Vocational School of Higher Education, the Vocational School for National Palaces and Historical Buildings, the Vocational School for Foreign Languages and more than 25,000 students.

The Istanbul State Engineering and Architectural Academy and affiliated schools of engineering and the related faculties and departments of the Kocaeli State Engineering and Architecture Academy and the Kocaeli Vocational School were merged to form Yıldız University with decree law no.41 dated 20 June 1982 and Law no. 2809 dated 30 March 1982 which accepted the decree law with changes.

The new university incorporated the departments of Science-Literature and Engineering, the Vocational School in Kocaeli, a Science Institute, a Social Sciences Institute and the Foreign Languages, Atatürk Principles and the History of Revolution, Turkish Language, Physical Education and Fine Arts departments affiliated with the Rectorate.

Yıldız Technical University is one of the seven government universities situated in İstanbul besides being the 3rd oldest university of Turkey with its history dating back to 1911. It is regarded as one of the best universities in the country as well.

February, 2014

Melih AKTAŞ

TABLE OF CONTENTS

	Page
LIST OF SYMBOLS	vi
LIST OF ABBREVIATIONS.....	vii
LIST OF FIGURES	viii
LIST OF TABLES.....	x
ABSTRACT.....	xi
ÖZET	xii
CHAPTER 1	
INTRODUCTION	1
1.1 Literature Review	1
1.2 Objective of the Thesis	18
1.3 Hypothesis	18
CHAPTER 2	
THEORETICAL MODEL.....	19
CHAPTER 3	
DATA REDUCTION	23
CHAPTER 4	
RESULTS AND DISCUSSION.....	29
4.1 Results.....	30
4.1.1 Charts	31
4.2 Discussion.....	72
CHAPTER 5	
CONCLUSION.....	76

REFERENCES	78
CURRICULUM VITAE.....	83

LIST OF SYMBOLS

COP	Coefficient of performance
c	Condenser
CNT	Carbon nanotubes
comp	Compressor
e	Evaporator
MO	Mineral Oil
nf	Nanofluid
NP	Nanoparticle
NR	Nanorefrigerant
NSC	Non subcooling
NSH	Non superheating
PR	Pure refrigerant
RE	Refrigerating effect
Q	Heat rate
SC	Subcooling
SH	Superheating
SVFR	Suction vapour flow per refrigeration
vol.	Volume fraction
W	Work
wt.	Mass fraction
ρ	Density
ω	Nanoparticle mass fraction in nanorefrigerant

LIST OF ABBREVIATIONS

YTU Yıldız Technical University

LIST OF FIGURES

		Page
Figure 2.1	P-h diagrams of vapor-compression refrigeration cycle [59].....	19
Figure 2.2	TEM of Al ₂ O ₃ nanolubricant [47]	21
Figure 4.1	Charts of R12 vs R12/Al ₂ O ₃ for non-superheating/subcooling case.....	33
Figure 4.2	Charts of R12 vs R12/Al ₂ O ₃ for 5 °C of superheating/subcooling case ...	35
Figure 4.3	Chart of R12 and R12/Al ₂ O ₃ for non-superheating/subcooling vs. 5 °C of superheating/subcooling	35
Figure 4.4	Charts of R134a vs R134a/Al ₂ O ₃ for non-superheating/subcooling case .	37
Figure 4.5	Charts of R134a vs R134a/Al ₂ O ₃ for 5 °C of superheating/subcooling case	39
Figure 4.6	Chart of R134a and R134a/Al ₂ O ₃ for non-superheating/subcooling vs. 5 °C of superheating/subcooling case.....	39
Figure 4.7	Charts of R430a vs R430a/Al ₂ O ₃ for non-superheating/subcooling case .	41
Figure 4.8	Charts of R430a vs R430a/Al ₂ O ₃ for 5 °C of superheating/subcooling case	43
Figure 4.9	Chart of R430a and R430a/Al ₂ O ₃ for non-superheating/subcooling vs. 5 °C of superheating/subcooling case	43
Figure 4.10	Charts of R436a vs R436a/Al ₂ O ₃ for non-superheating/subcooling case	45
Figure 4.11	Charts of R436a vs R436a/Al ₂ O ₃ for 5 °C of superheating/subcooling case.....	47
Figure 4.12	Chart of R436a and R436a/Al ₂ O ₃ for non-superheating/subcooling vs. 5 °C of superheating/subcooling case.....	47
Figure 4.13	Charts of R600a vs R600a/Al ₂ O ₃ for non-superheating/subcooling case	49
Figure 4.14	Charts of R600a vs R600a/Al ₂ O ₃ for 5 °C of superheating/subcooling case	51
Figure 4.15	Chart of R600a and R600a/Al ₂ O ₃ for non-superheating/subcooling vs. 5 °C of superheating/subcooling case.....	51
Figure 4.16	Charts of R22 vs R22/Al ₂ O ₃ for non-superheating/subcooling case.....	53
Figure 4.17	Charts of R22 vs R22/Al ₂ O ₃ for 5 °C of superheating/subcooling case .	55
Figure 4.18	Chart of R22 and R22/Al ₂ O ₃ for non-superheating/subcooling vs. 5 °C of superheating/subcooling case.....	55
Figure 4.19	Charts of R290 vs R290/Al ₂ O ₃ for non-superheating/subcooling case...	57
Figure 4.20	Charts of R290 vs R290/Al ₂ O ₃ for 5 °C of superheating/subcooling case	59
Figure 4.21	Chart of R290 and R290/Al ₂ O ₃ for non-superheating/subcooling vs. 5 °C of superheating/subcooling case	59
Figure 4.22	Charts of R410a vs R410a/Al ₂ O ₃ for non-superheating/subcooling case	61
Figure 4.23	Charts of R410a vs R410a/Al ₂ O ₃ for 5 °C of superheating/subcooling case.....	63

Figure 4.24	Chart of R410a and R410a/Al ₂ O ₃ for non-superheating/subcooling vs. 5 °C of superheating/subcooling case	63
Figure 4.25	Charts of R431a vs R431a/Al ₂ O ₃ for non-superheating/subcooling case	65
Figure 4.26	Charts of R431a vs R431a/Al ₂ O ₃ for 5 °C of superheating/subcooling case	67
Figure 4.27	Chart of R431a and R431a/Al ₂ O ₃ for non-superheating/subcooling vs. 5 °C of superheating/subcooling case	67
Figure 4.28	Charts of R507a vs R507a/Al ₂ O ₃ for non-superheating/subcooling case	69
Figure 4.29	Charts of R507a vs R507a/Al ₂ O ₃ for 5 °C of superheating/subcooling case	71
Figure 4.30	Chart of R507a and R507a/Al ₂ O ₃ for non-superheating/subcooling vs. 5 °C of superheating/subcooling case	71

LIST OF TABLES

		Page
Table 3.1	Some results from Subramani and Prakash [58]’s study	24
Table 3.2	Finding enthalpy of R134a/Al ₂ O ₃ nanorefrigerant at point 3	24
Table 3.3	Finding enthalpy of R134a/Al ₂ O ₃ nanorefrigerant at point 1	24
Table 3.4	Cycle parameters and calculated values	25
Table 3.5	Calculations of COPs of cycles	25
Table 3.6	Finding enthalpy of R134a/Al ₂ O ₃ nanorefrigerant at point 3	25
Table 3.7	Finding enthalpy of R134a/Al ₂ O ₃ nanorefrigerant at point 1	26
Table 3.8	Calculations of COPs of cycles, $\rho_{\text{Al}_2\text{O}_3} = 2200 \text{ kg/m}^3$	26
Table 3.9	Some results from Bi et al. [12]’s study	26
Table 3.10	Finding enthalpy of R134a/Al ₂ O ₃ nanorefrigerant at point 3	26
Table 3.11	Finding enthalpy of R134a/Al ₂ O ₃ nanorefrigerant at point 1	27
Table 3.12	Cycle parameters and calculated values	27
Table 3.13	Calculations of COPs of cycles	27
Table 3.14	Finding enthalpy of R134a/Al ₂ O ₃ nanorefrigerant at point 3	27
Table 3.15	Finding enthalpy of R134a/Al ₂ O ₃ nanorefrigerant at point 1	28
Table 3.16	Calculations of COPs of cycles	28
Table 4.1	Refrigerant list	29
Table 4.2	Calculation of sample case, $T_c = 45 \text{ }^\circ\text{C}$ and $T_e = -10 \text{ }^\circ\text{C}$, and non- superheating/subcooling	31
Table 4.3	Calculation of sample case, $T_c = 45 \text{ }^\circ\text{C}$ and $T_e = -10 \text{ }^\circ\text{C}$, and $5 \text{ }^\circ\text{C}$ superheating and $5 \text{ }^\circ\text{C}$ subcooling	31
Table 4.4	Temperature vs. heat of evaporation (h_{fg}) of R134a	72
Table 4.5	Comparison of the highest COP enhancement caused adding alumina nanoparticles into R22, R290, R410a, R431a and R507a	73
Table 4.6	Comparison of the lowest COP enhancement caused adding alumina nanoparticles into R22, R290, R410a, R431a and R507a	73

ABSTRACT

THEORETICAL INVESTIGATION OF THE USE OF NANOREFRIGERANTS IN VARIOUS REFRIGERATION CYCLES

Melih AKTAŞ

Department of Mechanical Engineering

MSc. Thesis

Adviser: Assist. Prof. Dr. Ahmet Selim DALKILIÇ

Refrigerant mixtures which the composition of a pure refrigerant and nanoparticles are named nanorefrigerants. Most studies on nanorefrigerants have indicated that adding nanoparticles in pure refrigerant increases heat transfer coefficient, thermal conductivity, refrigeration capacity, and decreases compressor work and energy waste. In this thesis, a prediction model was developed to guess COP of the nanorefrigerant and applied to vapour-compression refrigeration cycles of nanorefrigerants consisted from R12, R134a, R430a, R436a, R600a and R22, R290, R410a, R431a, R507a as base fluid and Al₂O₃ nanoparticles. Alteration in COP was investigated while nanoparticles added to pure refrigerant for various evaporating temperatures and various condensation temperatures by calculating densities and achieving enthalpies of nanorefrigerants on the points of vapour-compression refrigeration cycle. The results pointed that COP enhances with adding nanoparticle to pure refrigerant.

Key words: Nanorefrigerant, vapour compression-refrigeration cycle, nanoparticle

YILDIZ TECHNICAL UNIVERSITY
GRADUATE SCHOOL OF NATURAL AND APPLIED SCIENCES

ÇEŞİTLİ SOĞUTMA ÇEVREMLERİNDE NANOAKIŞKANLARIN KULLANIMININ TEORİK OLARAK İNCELENMESİ

Melih AKTAŞ

Makine Mühendisliği Anabilim Dalı

Yüksek Lisans Tezi

Tez Danışmanı: Yrd. Doç. Dr. Ahmet Selim DALKILIÇ

Saf soğutucu akışkan ve nanoparçacıklardan oluşan soğutucu akışkan karışımlarına nanosoğutkan denir. Nanosoğutkanlar üzerine çok sayıda çalışma saf soğutucu akışkana nanoparçacık eklemenin ısı transfer katsayısını, ısı iletkenliği, soğutma kapasitesini arttırdığı ve kompresör işini ve enerji sarfiyatını azalttığını göstermektedir. Bu tezde, nanosoğutkanların COP'sini tahmin etmek için bir tahmin modeli geliştirildi ve R12, R134a, R430a, R436a, R600a and R22, R290, R410a, R431a, R507a temel akışkanları ve Al₂O₃ nanoparçacıklarından oluşan nanosoğutkanların buhar sıkıştırımlı soğutma çevrimine uygulandı. Çeşitli buharlaşma sıcaklıkları ve çeşitli yoğuşma sıcaklıklarında, saf soğutucu akışkana nanoparçacık ilave edilmesiyle COP'de meydana gelen değişim yoğunluklar hesaplanarak ve nanosoğutkanların buhar sıkıştırımlı soğutma çevrimi noktalarındaki entalpileri elde edilerek araştırıldı. Sonuçlar saf akışkana nanoparçacık eklendiğinde COP'de iyileşme olduğunu gösterdi.

Anahtar Kelimeler: Nanosoğutkan, buhar sıkıştırımlı soğutma çevrimi, nanoparçacık

CHAPTER 1

INTRODUCTION

Most of electric power generation in the world is providing from fossil fuel. CO₂ is one of the outputs of fossil fuel plants and involves global warming as accumulating in the atmosphere. The problem of increase in global warming caused scientists to investigate more environmentally friendly and energy-saving refrigerants using in refrigeration and air-conditioning systems or in other words refrigerants which realize same refrigeration with less CO₂ emission. Nanorefrigerant that composition of nanoparticles (1-100 nanometers) and a pure refrigerant have been advanced as an alternative to traditional refrigerant, because it can be a more efficient refrigerant.

Many investigations have been in progressed about nanorefrigerants and usage of them as refrigerant. The results showed that nanorefrigerant can be a new alternative to conventional refrigerants. However some problems such as settlement of nanoparticles in time, high initial investment cost have not been exactly solved yet. Adding surfactant which suspends the nanoparticles for a while now in mixture and finding new techniques to produce nanoparticles cheaper and charging them into system easier will accelerate the progress of development of refrigeration system which work with nanorefrigerant.

1.1 Literature Review

Xuan and Roetzel [1] investigated the heat transfer phenomenon in nanofluids theoretically by regarding the mixture as single-phase liquid or multiphase nanofluid. These different approaches was due to two different mechanisms took part in nanofluid heat transfer, thermal conductivity increase by suspending nanoparticles and nanoparticle chaotic movement which results in heat transfer acceleration. In single-phase approach, which considers only the thermal conductivity increment, base fluid's heat transfer correlations accepted as nanofluid's, with the exception of thermal

properties which nanofluid properties should be taken. For multiphase approach, Peclet number was used for developing a Nusselt correlation with an unknown parameter which requires experimental study to determine.

Xue [2] presented a model of the effective thermal conductivity for nanofluids, based on Maxwell theory and average polarization theory, considering the interface effect between the solid particles and the base fluid in nanofluids. They found that their theoretical results were in good agreement with the experimental data on the effective thermal conductivity of nanotube/oil nanofluid and water/ Al_2O_3 nanofluid.

Xie et. al. [3] produced nanofluids with multiwalled carbon nanotubes (CNTs) using nitric acid for disentangle process and oxygen-containing groups for hydrophilic surface generation for CNTs. After the treatment, CNTs have been successfully dissolved in water, ethylene glycol and decene. Thermal conductivities of these mixtures have been determined with transient hot-wire system. For nanofluids with 1% volume fraction, 19.6%, 12.7% and 7% increase in thermal conductivity observed for decene, ethylene glycol and distilled water respectively. An increase in thermal conductivity enhancement observed in experiments with increasing volume fraction of CNTs while with increasing thermal conductivity of the base fluid opposite situation occurred. Finally authors compared their measurement data with Hamilton-Crosser and Davis model which resulted in values less than the experimental data.

Liu et. al. [4] performed an experimental thermal conductivity analysis for ethylene glycol and synthetic oil with CNTs. Different CNT volume ratios ranged between 0.2% to 1% for ethylene glycol and 1%-2% for synthetic oil were used. For synthetic oil mixture, N-hydroxysuccinimide used as dispersant and found to have a favorable effect on thermal conductivity. 12.4% and 30% enhancement ratio was obtained for ethylene glycol nanofluid with 0.01 and 0.02 volume fractions respectively. As for the synthetic oil, maximum enhancement ratio of 30.3% was achieved for 2% volume fraction ratio. Authors also noted that there were higher enhancement ratios achieved in previous works. Comparison with the previous studies showed that the enhancement due to CNTs was higher than CuO nanoparticles at same volume fractions with same base fluids. Previous models for predicting thermal conductivity ratio also showed poor performance with underestimating about 3 or 5 times.

Hwang et. al. [5] experimentally investigated the lubrication, thermal conductivity enhancement and stability analysis of nanofluids which use multi wall carbon nanotubes (MWCNT), CuO, fullerene and SiO₂ as nanoparticle with water, ethylene glycol and oil as base fluid. Results showed that the best thermal conductivity increase achieved with MWCNT for water mixtures. MWCNT and CuO nanofluids with oil mixtures achieved higher enhancement ratios than water ones so this lead to conclusion that lower the thermal conductivity of base fluid better enhancement ratios could obtained. Stability tests revealed that fullerene mixture with oil was very stable compared with other nanofluids while MWCNT showed the worst stability performance. Also, additive of surfactant proved to have an improving effect on stability.

Park and Jung [6] performed nucleate boiling heat transfer analysis for CNTs with 1% volume fraction mixed with R134a and R123 using no dispersing agents. At low heat fluxes heat transfer enhancement showed better performance such as 36.6% while at large heat fluxes enhancement ratio decreased. Fouling effect on heat transfer surface was also investigated after 3 weeks and CNTs not found as a major fouling source.

Ding [7] investigated the most recent and available simulation techniques for vapour-compression refrigeration system design. Both conventional and computer simulation models for refrigerator system design were described and benefits of using computational model explained with introduction of simulation methods for most important equipment in refrigerators. As for nanofluids, brief concept of phenomenon was presented and need for an accurate model for predicting nanofluid properties addressed. Recent studies for different prediction models, mainly for thermal conductivity, were also introduced and author emphasized the necessity of other evaluation methods for properties such as viscosity and electric conductivity.

Ding et al. [8] studied on the forced convective heat transfer using aqueous and ethylene glycol-based spherical titanium nanofluids, and aqueous-based titanate nanotubes, carbon nanotubes and nano-diamond nanofluids experimentally. They accomplished to formulate these nanofluid's specifications. They indicated that all the formulated nanofluids performed a higher effective thermal conductivity than that of predicted by the conventional theories. Apart from the ethylene glycol-based titanium nanofluids, all other nanofluids were observed to be non-Newtonian. They said that the convective heat transfer coefficient enhancement was higher than the thermal conduction enhancement substantially. However, they indicated deterioration of the convective heat transfer for

ethylene glycol-based titanium nanofluids at low Reynolds numbers. They recommended on the effective thermal conductivity to be responsible for the experimental observations.

Li and Peterson [9] pointed out that the Brownian motion of the nanoparticles in these suspensions was one of the potential contributors to this enhancement and the mechanisms that could contribute to this subject of considerable discussion and debate. The mixing effect of the base fluid in the immediate vicinity of the nanoparticles caused by the Brownian motion was examined, modeled also compared with the experimental data in the literature. Moreover, simulation results showed that the effective thermal conductivity of nanofluids was affected by this mixing effect.

Avsec and Oblak [10] proposed a mathematical model for the calculation of thermophysical properties of nanofluids on the basis of statistical nanomechanics. In this study, they indicated two calculation methods to describe the properties such as classical and statistical mechanics. It was stated that the classical mechanics had no insight into the microstructure of the substance. On the other hand, it calculates the properties of state both on the basis of molecular motions in a space and on the basis of the intermolecular interactions. On the contrary to the classical mechanics, they suggested that the statistical mechanics calculated the thermomechanic properties of state on the basis of intermolecular interactions between particles in the same system of molecules. According to them, it means that the systems composed of a very large number of particles. The results of the analysis were compared with experimental data and indicated a relatively good agreement.

Bartelt et. al. [11] researched the heat transfer effects of CuO nanoparticles on R134a/POE mixtures in horizontal flow boiling conditions. Although 0,5% nanoparticle by mass mixture showed no effect of enhancement in heat transfer, %1 mass fraction mixture showed 42-82% improvement while nanoparticle fraction of 2% showed 50-101%. The reasons behind this large improvement was not understood clearly however, additional nucleation sites formed by nanoparticles argued to be one of the main factor of it. It is also noted that the saturation temperatures found to be higher with nanofluid mixtures and pressure drop difference is insignificant when compared with base fluid only state.

Bi et al. [12] studied with nanoparticles in the working fluid for observing domestic refrigerator's reliability and performance. They utilized from mineral oil/TiO₂ nanoparticle mixtures such as the lubricant instead of Polyol-ester (POE) oil in the 1,1,1,2-tetrafluoroethane (HFC134a) refrigerator. Researchers analyzed that the refrigerator performance with the use of nanoparticles was enhanced regarding with the energy consumption and freeze capacity. Their results showed that HFC134a and mineral oil with TiO₂ nanoparticles worked normally and securely in the refrigerator. They also observed that the refrigerator had higher performance than the HFC134a and POE oil system, and the use of nanoparticles with 0.1% mass fraction reduced energy consumption 26.1% compared to the HFC134a and POE oil system.

Lu and Fan [13] studied on molecular dynamics simulation method which was applicable for a stationary nanofluids of the volume fractions less than 8%. They used this method to simulate nanofluids' thermophysical properties which included thermal conductivity and viscosity. They compared experimental data with numerical results and obtained good results. They found it very useful to estimate some thermal properties of nanofluids. Their results also showed that thermal conductivity and the viscosity of nanofluids depended on the volume fraction and the size of nanoparticles.

Chen et al. [14] presented the properties of the effective thermal conductivity, their rheological behavior and forced convective heat transfer of the nanofluids. They found that thermal conductivity increased as 3% at 25 °C and 5% at 40 °C for the 2.5 wt.% nanofluid. They observed that nanofluids including spherical titanium nanoparticles had better properties of thermal conductivity and convective heat transfer coefficient. They also suggested new systems to increase the convective heat transfer coefficient.

Ding et al. [15] investigated the influence of original mass of nanoparticles and the mass of refrigerants on the migration characteristics of CuO nanoparticles in pool boiling of R113/CuO nanorefrigerant and R113/CuO/RB68EP nanorefrigerant-oil mixture for 0.0912%, 0.183% and 1.536% volume concentrations at ambient temperature and pressure, experimentally and numerically. It was found that increase in the original mass of CuO the nanoparticles and the mass of the R113 refrigerant made increase the migrated mass of nanoparticles, and increment of volume fraction of nanoparticles made decrease the migration ratio of CuO nanoparticles. The numerical model developed was able to predict influence of the original mass of nanoparticles on the migration mass of nanoparticles in nanorefrigerant and nanorefrigerant-oil mixture with

10.5% and 7.7% average deviation from experimental results, respectively. In addition, it was able to predict influence of the mass of refrigerant on the migration mass of nanoparticles in nanorefrigerant and nanorefrigerant-oil mixture with 32.2% and 38.4% average deviation from experimental results, respectively.

Jiang et al. [16] investigated the influence of diameter and nanoparticle concentration of CNT on thermal conductivity of R113/CNT nanorefrigerants for from 0% to 1.0 wt.% mass fraction, experimentally and compared results with different models. The experiments showed that thermal conductivity of R113/CNT enhanced with increase of the CNT volume fraction or decrease of CNT diameter, especially for 1.0 vol.% thermal conductivities of four different CNT nanorefrigerants increased between 50% and 104% compared with base-fluid R113. The predicting models existed for thermal conductivity of CNT nanorefrigerants could predict results within an average deviation of more than 15%.

Kedzierski [17] investigated the influence of CuO nanoparticles on the boiling characteristics of R134a/CuO/RL68H, refrigerant/nanolubricant mixture for 0.5%, 1%, and 2% mass fractions, on roughened, horizontal flat surface. At 0.5% mass fraction of nanolubricant, CuO nanoparticles enhanced the heat transfer between 50% and 275% compared with pure R134a/polyolester (99.5/0.5). For the R134a/nanolubricant (99/1) mixture, boiling heat transfer enhanced on average 19% compared with the R134a/polyolester (99/1) mixture, and for R134a/nanolubricant (98/2) mixture, enhancement in heat flux was on average 12%. As a result, increase in the thermal conductivity of the lubricant that was caused by CuO nanoparticles enhanced heat transfer 20% of boiling heat transfer. Secondary nucleation and particle mixing might be observed as other effects on enhancement of boiling heat transfer, also.

Naphon et al. [18] investigated the influence of titanium nanoparticle concentration in R11/Ti nanorefrigerant for 0.01%, 0.05%, 0.10%, 0.50% and 1.0% concentrations and the tilt angle of pipe on the efficiency of copper heat pipe. Experimental results showed that the highest efficiency ratios were seen at 0.01% nanoparticle volume fraction, and 60° tilt angle and 50% charge amount of pure refrigerant were optimum values for enhancement of heat transfer in the tests. Finally, it was showed that a significant influence of titanium nanoparticle concentrations on the heat pipe efficiency and heat transfer enhancement.

Peng et al. [19] investigated the influence of concentration of CuO nanoparticles on the heat transfer characteristics of R113-based nanorefrigerant flow boiling inside a horizontal roughness tube experimentally for 0.1 wt.%, 0.2 wt.%, and 0.5 wt.% nanoparticle concentrations, and a correlation was developed to predict heat transfer enhancement of R113/CuO nanorefrigerant. It was observed that dispersing nanoparticles in R113 pure refrigerant enhanced the flow boiling heat transfer of nanofluid, and the maximum enhancement of heat transfer coefficient was 29.7%. The correlation was able to predict heat transfer coefficients agree with 93% of the experimental results within the deviation of $\pm 20\%$.

Peng et al. [20] investigated the influence of the mass fraction of CuO nanoparticles on the frictional pressure drop behavior of R113-based nanofluid flow boiling inside a horizontal roughness copper tube with an outside diameter of 9.52mm and thickness of 0.70 mm experimentally for 0.1 wt.%, 0.2 wt.%, and 0.5 wt.% nanoparticle concentrations, and a correlation was developed to predict the frictional pressure drop of R113/CuO nanorefrigerant. It was observed that dispersing nanoparticles in R113 pure refrigerant increased the frictional pressure drop of nanorefrigerant flow boiling compared with pure R113 refrigerant, and increased with the increase of the mass fraction of nanoparticles and the maximum enhancement of frictional pressure drop was 20.8%. The correlation was able to predict frictional pressure drops agree with 92% of the experimental results within the deviation of $\pm 15\%$. The nanoparticle impact factor FPD decreased with the increment in mass flux for same vapor quality and mass fraction of nanoparticles. The nanoparticle impact factors predicted by the equation agree with 99% of the experimental results within the deviation of $\pm 5\%$.

Trisaksri and Wongwises [21] studied with R141b/TiO₂ nanorefrigerant which contained 21nm average diameter sized nanoparticles at 0.01%, 0.03% and 0.05% volume fractions in order to investigate the effect of the nanoparticle concentrations and pressure on nucleate pool boiling heat transfer of R141b/TiO₂ nanorefrigerant. The results showed that increasing particle volume concentrations decreased the boiling heat transfer coefficient, adding TiO₂ nanoparticles in pure refrigerant deteriorated the pool nucleate boiling heat transfer. In addition, the influence of pressure on boiling heat transfer coefficients decreased with increasing nanoparticle volume concentrations.

Kedzierski [22] investigated the influence of CuO nanoparticles in CuO/RL68H mixtures as previous study, however CuO nanoparticle concentration was 0.5 vol.%, 1

vol.% and 2 vol.% in the nanolubricants. Results were showed that R134a/nanolubricant (99 vol.%/1 vol.%) mixture which the 0.5% CuO volume fraction nanolubricant had on average 140% larger boiling heat flux than the 0.5% volume fraction nanolubricant (0.5 vol.% CuO). Overall, R134a/nanolubricant mixtures with 1 vol.%CuO nanoparticles had larger heat flux than R134a/CuO/RL68H mixtures with 2 vol.%CuO nanoparticles for all nanolubricant volume fractions in measurements, and the boiling heat flux ratio bigger than 1, mostly. Finally, it was realized that the enhancements in the boiling heat transfer were related with nanoparticle interactions.

Jwo et al. [23] studied with R12/Al₂O₃/MO nanorefrigerant at 0.05 wt.%, 0.1 wt.% and 2 wt.% Al₂O₃ in a refrigerator works with R134a originally. R134 was replaced by R12, after POE was replaced by MO and lastly Al₂O₃ nanoparticles added in R12/MO mixture, and measurements were realized for each one. Results showed that system using R12 refrigerant had lower compression ratio compared with R134a and nanorefrigerant contained 0.1 wt.% nanoparticles lowest power consumption with about 2.4% lower than that using R134a in stable condition and had the best performance.

He et al. [24] studied numerically single phase method and combined it with Euler and Lagrange method on the convective heat transfer of TiO₂ nanofluids which were flowing through a straight tube under the laminar flow conditions. They researched the effects of nanoparticles' concentrations, Reynolds number, and various nanoparticle sizes on the flow and the convective heat transfer behavior. It was found that heat transfer of nanofluids increased importantly in the entrance region. The numerical results were in good agreement with the experimental data and a reasonable good agreement was accomplished.

Murshed et al. [25] researched a combined static and dynamic mechanisms based on a model for anticipating the effective thermal conductivity of nanofluids. In their study, the model incorporated the effects of particle size, nanolayer, Brownian motion, particle surface chemistry and interaction potential which were about the static and dynamic mechanisms responsible for the enhanced effective thermal conductivity of nanofluids. Also, the model had logically a good agreement with the experimental results of various types of nanofluids

Wang et al. [26] investigated the usage of nanoparticles in residential air conditioners (RAC) working with R410a as the refrigerant. In the study, the cooling/heating

capacity, the energy efficiency ratio and the power input of RAC were determined. They produced new mineral-based nano refrigeration oil (MNRO), which is composed by mixing some nanoparticles (NiFe_2O_4) into naphthene based oil B32, as an alternative to POE VG 32. The solubility of the MNRO in different refrigerants such as R134a, R407C, R410a and R425a was experimentally investigated. They tested performance of RAC units working with R410a/MNRO, R410a/POE and R22/MO. The results showed that in the residential air conditioners the mixture of R410a/MNRO can be used normally. By using MNRO instead of the Polyol-Ester oil VG 32 in residential air conditioners, energy efficiency ratio increased approximately %6.

Bobbo et al. [27] performed a study in order to clarify the influence of the dispersion of single wall carbon nanohorns (SWCNH) and titanium dioxide (TiO_2) on the tribological properties of commercial POE oil (SW32). The oil having 0.5 g/L nanoparticle concentration was prepared for experiments and they conducted tribological tests and solubility measurements for R134a at various temperatures. According to their study, small addition of nanoparticles to the base lubricant does not affect the tribological behavior of the base lubricant practically. As a result of study, TiO_2 /SW32 oil mixture showed the best performance compared with pure SW32 and SWCNH/SW32 oil mixture.

Henderson et al. [28] investigated heat transfer performance of R134a and R134a/polyolester mixtures with nanoparticles during boiling flow conditions in a horizontal tube. The R134a/ SiO_2 nanorefrigerants having volume concentrations of 0.5% and 0.05% was tested in order to determine effect of nanoparticles. For both volume concentrations, the convective boiling heat transfer coefficient decreased (as much as 55%) compared with pure R134a because of poor dispersion. Also, they conducted experiments with R134a/POE mixtures having CuO nanoparticles volume fraction of 0.02%, 0.04% and 0.08%. It was observed that R134a/CuO/POE nanorefrigerant having volume fraction of 0.02% showed slight enhancement in the heat transfer performance. CuO volume fraction of 0.04% and 0.08% caused an average heat transfer enhancement of 52% and 76% respectively. The heat transfer coefficient variation of R134a/CuO/POE nanorefrigerant having different volumetric concentrations.

Peng et al. [29] investigated the nucleate pool boiling heat transfer characteristics of nanorefrigerant with carbon nanotubes (CNTs) experimentally. In the study, they used

four CNTs having different outside diameter, length and aspect ratio. The prepared R113/CNT/oil mixtures having mass fractions of 0.1 wt.%, 0.2 wt.%, 0.3 wt.%, 0.6 wt.% and 1.0 wt.%. The results showed that R113/oil mixture with CNTs increased nucleate pool boiling heat transfer coefficient up to 61% compared with the R113-oil mixture. It was observed that usage of CNTs having higher length and smaller outside diameter improved nucleate pool boiling heat transfer coefficient. Also, they produced a correlation within a deviation of 10% in order to predict the nucleate pool boiling heat transfer coefficient of refrigerant/oil mixture with CNTs.

Peng et al. [30] performed an experimental study in order to determine nucleate pool boiling heat transfer characteristics of R113/VG68 oil with diamond nanoparticles. In the study, nanoparticles concentration in the R113/Diamond/VG68 oil mixture was 0.05 wt%, 0.1 wt%, 0.15 wt%, 0.25 wt%, 0.3 wt%, 0.45 wt%, 0.5 wt% and 0.75 wt%. They observed that the usage of diamond nanoparticles in R113/VG68 oil mixture increased the nucleate pool boiling heat transfer coefficient up to 63.4%. The enhancement effect of diamond nanoparticles/oil suspension was more than 20% higher than CuO nanoparticles/oil suspension for the nucleate pool boiling heat transfer conditions. They also produced a correlation for prediction of the nucleate pool boiling heat transfer coefficient of refrigerant/oil mixture with nanoparticles and compared predicted results with experimental data.

By using a CFD approach, under constant wall temperature condition in a circular tube, the laminar convective heat transfer of nanofluids was studied in a numerical way in Fard et al [31]'s study. Single phase and two-phase models were used for the determination of the temperature, flow field, and calculation of heat transfer coefficient. The effects of some important parameters such as nanoparticle sources, nanoparticle volume fraction and nanofluid's Peclet number on heat transfer rate were investigated. According to their results, as the particle concentration increased, heat transfer coefficient also increased. According to their simulation results, it was seen that when their model was compared to the single phase model, better predictions for heat transfer rate was obtained from the two phase approach.

In Meibodi et al. [32]'s study, modeling of the thermal conductivity of the suspensions was done by means of the resistance model approach. In this model, Brownian motion and interfacial layer and also a new mechanism were considered. They reported that this model may be used without any adjustable parameter for estimating the upper and lower

limits of nanofluid thermal conductivity. Data of thermal conductivity for CuO nanofluids were acquired experimentally and according to the results, proposed model was consistent with the data. Their model was used to detect the various mechanisms' portions on the thermal conductivity of nanofluids. The results were found to be compatible with the basic knowledge about nanofluids' thermal conductivity mechanism.

Bi et al. [33] used R600a/TiO₂ nanorefrigerants in a domestic refrigerator without any system reconstruction as a working fluid. Effect of nanoparticles on domestic refrigerator performance is investigated by means of energy consumption and freeze capacity tests. The results revealed that usage of 0.1 and 0.5 g/L concentrations of R600a/TiO₂ instead of pure R600a in domestic refrigerator resulted in 5.94% energy consumption saving and 9.60% higher the freezing velocity of nanorefrigerant.

Yu et al. [34] investigated the thermophysical properties and convective heat transfer of Al₂O₃-polyalphaolefin (PAO) nanofluids which included not only the spherical but also the rod-like nanoparticles. They determined the viscosity and thermal conductivity of the nanofluids and compared their predictions with several existing theories in the literature. Their results showed that in a convective flow, the shear-induced alignment and specific motion of the particles should be regarded in order to truly interpret the experimental data of the nanofluids including non-spherical nanoparticles.

Peng et al. [35] used surfactant additives to investigate the nucleate pool boiling heat transfer characteristics of R113/Cu nanorefrigerant having the nanoparticle concentrations of 0.1 wt.%, 0.5 wt.% and 1.0 wt.%. In the study, Sodium Dodecyl Sulfate (SDS), Cetyltrimethyl Ammonium Bromide (CTAB) and Sorbitan Monooleate (Span-80) were selected as surfactant and their effect was determined. Except high surfactant concentrations condition, the usage of surfactants with nanorefrigerant improved the nucleate pool boiling heat transfer performance. By the means of surfactant enhancement ratio (SER), performance of surfactants was evaluated. According to results, the values of SER were in the ranges of 1.12–1.67, 0.94–1.39, and 0.85–1.29 for SDS, CTAB and Span-80, respectively. Also, optimum concentrations for SDS, CTAB and Span-80 were determined and a correlation for predicting the nucleate pool boiling heat transfer coefficient of nanorefrigerant with surfactant was proposed.

Peng et al. [36] conducted experiments in order to determine the impact of nanoparticle type, nanoparticle size, refrigerant type, mass fraction of lubricating oil (RB68EP), heat flux and initial liquid-level height on the migration of nanoparticles during pool boiling. In the study, R113, R141b and n-pentane were used as refrigerant. Cu, Al, Al₂O₃ and CuO nanoparticles having different average diameter were used as nanoparticle. The results revealed that nanoparticle having smaller size had higher migration ratio. The migration ratio of Al nanoparticle was higher than the other nanoparticles used in the study for average the same average diameter of nanoparticle. Also, the decrease of nanoparticle density, dynamic viscosity of refrigerant, mass fraction of lubricating oil or heat flux and the increase of liquid-phase density of refrigerant or initial liquid-level height improved the migration ratio of nanoparticles during the pool boiling of nanorefrigerant.

Peng et al. [37] experimentally investigated effect of nanoparticle size on nucleate pool boiling heat transfer characteristics of refrigerant R113, ester oil VG68, and Cu nanoparticles having three different average diameters. The nanoparticle concentrations in the nanorefrigerants were 0.1 wt.%, 0.2 wt.%, 0.3 wt.%, 0.6 wt.% and 1.0 wt.%. The results showed that the nanoparticle having average diameter of 20 nm had better heat transfer performance (up to 23.8%) compared with the nanoparticle having average diameter of 50 nm and 80 nm. The increase of nanoparticles concentrations in the nanoparticles/oil suspension or the increase of nanoparticles concentrations in the nanoparticles/oil suspension improved the nucleate pool boiling heat transfer coefficient of refrigerant/oil mixture with nanoparticles. Also, by considering the effects of nanoparticle type and size a general nucleate pool boiling heat transfer coefficient correlation agree with 93% of the existing experimental data was developed.

Abdel-Hadi et al. [38] investigated the usage of R134a/CuO nanorefrigerant in the vapour-compression system experimentally. In the study, they conducted experiments in order to clarify effect of heat flux, nanoparticles size and concentration on the evaporating heat transfer coefficient. They determined optimum CuO nanoparticles size and concentration in the nanorefrigerant as 25nm and %0.55 respectively. They also observed that the evaporating heat transfer coefficient increased with increasing heat flux.

Mahbubul et al. [39] focused the frictional pressure drop characteristics of R123/TiO₂ nanorefrigerants flowing in a horizontal circular tube. They tested the nanorefrigerant

having volume concentrations of 0.1 %, 0.2 % and 0.5 % for different local vapour quality and mass fluxes. The results showed that pressure drop increases with the increase of the particle volume fractions.

Peng et al. [40] presented a numerical model to determine the migration characteristics of nanoparticles (from liquid-phase to vapor phase) during the refrigerant-based nanofluid pool boiling. The migration process including departure of bubble from the heating surface, movement of bubble and nanoparticles, capture of nanoparticles by bubble and escape of nanoparticles from the liquid-vapor interface was considered in the model. Also, the effects of nanoparticle type, nanoparticle size, refrigerant type, mass fraction of lubricating oil, heat flux and initial liquid level height on the migration of nanoparticles can be determined by means of developed model which is compatible with 90% of the experimental data.

Kedzierski [41] examined the pool-boiling performance of R134a/Al₂O₃/polyolester nanorefrigerant on a roughened, horizontal flat surface. In the study, the polyolester lubricant having three different mass fractions (0.5%, 1% and 2%) and 1.6% volume fraction of Al₂O₃ nanoparticle in nanorefrigerant was considered. For all mass fractions of lubricant, the heat transfer improvement was observed with the usage of Al₂O₃ instead of R134a/polyolester mixture. According to model they produced, nanoparticles having large volume fraction and small size was capable of enhancing heat transfer.

Ehsan et al. [42] used nanoparticles to investigate the heat transfer mechanisms regarding with the thermal conductivity increase, brownian motion, dispersion, and fluctuation of nanoparticles especially near wall which led to increase in the energy exchange rates and augmented the heat transfer rate between the fluid and the wall of evaporator section. Their experimental results showed that addition of silver nanofluid in methanol led to energy saving around 8.8-31.5% for cooling and 18-100% for reheating the supply air stream in an air conditioning system.

Kumar et al. [43] conducted experimental studies in order to reveal effect of R134a/Al₂O₃/PAG oil mixture on energy consumption test and freeze capacity of vapour-compression refrigeration system. The system used Al₂O₃ nanorefrigerant with 0.2% concentration as working fluid consumed 10.32% less energy compared with R134a/PAG oil mixture. Also, they observed that the usage of nanorefrigerant in the

refrigerant system increased COP and minimized the length of capillary tube and cost effective.

Padmanabhan and Palanisamy [44] intended to increase COP and exergy efficiency of a vapour-compression refrigeration system by using refrigerant, TiO_2 and lubricant (mineral oil (MO) and Polyol-ester (POE) oil) mixture. R134a, R436A (R290/R600a-56/44-wt.%) and R436B (R290/R600a-52/48-wt.%) were used as refrigerant in the study. They investigated irreversibility at different processes. The COP of vapour-compression refrigeration systems using R134a/ TiO_2 /MO nanorefrigerant showed higher COP value when compared to R436A/MO/ TiO_2 and R436B/ TiO_2 /MO nanorefrigerants. The COPs of vapour-compression refrigeration systems using both R436A/POE oil and R436B/ POE oil mixtures were higher when compared to R134a/POE oil mixture. It is revealed that the total irreversibility of R436A/ TiO_2 /MO and R436B/ TiO_2 /MO nanorefrigerants was higher than R134a/ TiO_2 /MO. In addition; it is observed that the exergy efficiency of R134a/ TiO_2 /MO mixture was lower than R436A/ TiO_2 /MO and R436B/ TiO_2 /MO/ mixtures at lower air temperature in the freezer.

Sabareesh et al. [45] presented an experimental study in order to improve the coefficient of performance (COP) of a vapor compression refrigeration system. They also investigated the viscosity and lubrication characteristics of pure mineral oil lubricant and mineral oil lubricant with TiO_2 nanoparticle. They tested nanoparticles having volumetric concentrations of 0.05%, 0.010%, 0.015 and defined the optimum nanoparticle volumetric concentration as 0.01% considering viscosity, friction coefficient and surface roughness measurements. According to their results, the usage of nanorefrigerant comprised of R12/ TiO_2 /MO in the vapor compression refrigeration system (instead of R12/MO mixture) decreased compressor work 11% while increasing COP and the average heat transfer rate 17% and 3.6% respectively.

Kedzierski [46] investigated influence of diamond nanolubricant on heat transfer characteristics of R134a pool boiling as using R134a/Diamond/RL68H mixtures at 0.5 wt.% , 1 wt.% and 2 wt.% Diamond/RL68H (2.6 vol.%/97.4 vol.%) mass fractions. Measurements got for three different condition following: First one was measurement made over the first 3 days where the surface was initially exposed to diamond nanoparticles, second one was measurements resulted in an average gain of approximately 0.2 K in superheat relative to the previous day's measurements and the

third one was measurements that were made over the next 3 days after the surface was cleaned, between approximately 10 kW/m^2 and 80 kW/m^2 heat flux. R134a/nanolubricant mixture at 2% nanolubricant mass fraction had the least nanoparticle agglomeration. As result, average 98% enhancement in boiling heat transfer which was the best was seen mixture at 0.5% nanolubricant mass fraction, compared with R134a/polyolester and the worst enhancement was got with R134a/nanolubricant mixture at 2% nanolubricant mass fraction, 19% on average.

Kedzierski [47] used a rectangular finned surface in order to investigate the effect of Al_2O_3 nanoparticles on the pool boiling performance of R134a/polyolester lubricant (RL68H) mixture. The test section was copper, horizontal, flat, rectangular-finned surface (the overall height and tip-width of a fin were 0.76 mm and 0.36 mm, respectively.) Al_2O_3 volume fractions in the nanolubricant were 1.0%, 2.3%, and 3.6% in the study. The experimental results revealed that the usage of nanoparticle in R134a/polyolester lubricant (RL68H) mixture enhanced boiling performance up to 113% on a rectangular finned surface. Also they defined that passively enhanced surfaces required higher nanoparticle to obtain similar heat transfer enhancement compared with smooth surface.

Mahbubul et al. [48] investigated the viscosity of R123/ TiO_2 nanorefrigerant having concentrations of 0.5 vol.%, 1 vol.%, 1.5 vol.% and 2 vol.%. In the study, horizontal smooth tube was used as test section and experiments were conducted at 5°C , 10°C , 15°C , 20°C and 25°C . The increase of temperature resulted in decrease in viscosity of nanorefrigerant for all volume concentrations. It was also observed that the nanorefrigerant having higher nanoparticle volumetric concentration had higher viscosity.

Bobbo et al. [49] showed some viscosity data for nanofluids. They used water as base fluid and two different primary nanofluids such as single wall carbonnanohorn (SWCNH) and titanium dioxide (TiO_2). They determined viscosity of nanofluids using arhometer experimentally and benefitted from the function of the nanoparticles' mass fraction and the shear rate therefore they accounted the possible non-Newtonian behavior for the nanofluid. As a result, different empirical correlations were proposed in their study.

Cheng et al. [50] made a study about nucleate pool boiling and flow boiling of nanorefrigerant and nanolubricants as making a wide literature research. Various

experimental and theoretical studies were investigated in the point of enhancement of heat transfer, reduction of energy consumption, pressure drop and theory of mechanisms of nanofluids in heat transfer. In conclusion, discordant results, prediction methods and correlations were found in these studies, especially in similar ones. It was realized that many new studies in heat transfer and boiling of refrigerant-based nanofluids were needed to explain heat transfer and boiling mechanisms, physical properties of nanofluids and correlations and prediction methods.

Javadi and Saidur [51] studied with domestic refrigerators to compare effect of TiO₂-R134a/TiO₂/MO and R134a/Al₂O₃/MO those had 0.06% and 0.1% mass fractions of nanoparticles as nanorefrigerants with R134a/POE oil on energy consumption and emissions of greenhouse gasses in tropical climate, and calculated emission reduction up to energy consumption. It is found that 0.1% R134a/TiO₂/MO nanorefrigerant had the best enhancement with (25%) energy saving in experiments on the contrary 0.06% Al₂O₃ nanorefrigerant had less energy consumption than 0.06% TiO₂.

Kedzierski [52] investigated liquid kinematic viscosity and density of an Al₂O₃ nanoparticle added synthetic polyolester-based nanolubricant for 0 wt.%, 5.6 wt.%, 15.0 wt.%, 24.4 wt.%, 24.8 wt.% and 25 wt.% mass fractions at atmospheric pressure over the temperature range 288 K – 318 K.

$$\frac{\nu}{\nu_0} = \exp \left(A_0 + \frac{A_1}{T_r} + A_2 \ln(T_r) + A_3 T_r^{A_4} \right) \quad (2.3)$$

A new correlation (2.3) which was able to predict the kinematic viscosity of the nanolubricant within $\pm 15\%$ of the measurement was developed by summing the viscosities of the nanoparticle, the surfactant and the base lubricant.

Mahbubul et al. [53] investigated thermal conductivity and viscosity of Al₂O₃/R141b nanorefrigerant at 0.5% to 2% volume concentrations for the temperature range of 5 to 20 °C as measuring with most reliable measuring instruments and compared with results of other predict models. The highest viscosity and thermal conductivity were found out 179 times and 1.626 times greater than R141b for nanorefrigerant that had 2% volume concentration of Al₂O₃.

Mahbubul et al. [54] made same investigation for the thermal conductivity and viscosity of R141b/Al₂O₃ nanorefrigerant at 0.1% to 0.4% volume concentrations for the temperature range of 5 to 20 °C. In both study, the viscosity increased with the increase of the particle volume fractions and decreased with the increase in temperature. Then,

the thermal conductivity was enhanced with both increase volume fraction and temperature.

Mahbubul et al. [55] also studied R141b/Al₂O₃ nanorefrigerant for from 1 vol.% to 5 vol.% nanoparticle concentrations at constant mass flux of 100 kgm⁻²s⁻¹, vapor qualities from 0.2 to 0.7, temperature at 25°C and 0.078535 MPa pressure experimentally to investigate heat transfer and pressure drop behavior of nanorefrigerant. 1755.82 kW/m²K was the highest and 4.68 kW/m²K was the lowest heat transfer coefficient at vapor quality of 0.2 with 5% volume fraction of Al₂O₃ nanoparticles and at vapor quality of 0.3 with 1% volume fraction of nanoparticles, respectively. It means with 1% volume fraction, the minimum heat transfer coefficient enhancement was 383 % relative to pure R141b refrigerant. 464.27 kPa was the highest frictional pressure drop while it was 5.5kPa for pure R141b at vapor quality of 0.7 with 5% volume fraction and 3.34 kPa was the lowest frictional pressure drop at vapor quality of 0.2 with 1% volume fraction of nanoparticles. Thus, with 1% volume fraction, the minimum pressure drop enhancement was 181 % relative to pure R141b refrigerant.

Mahbubul et al. [56] investigated experimentally heat transfer coefficient, viscosity, pressure drop and pumping power enhancement of R134a/Al₂O₃ nanorefrigerants those had 1 to 5 vol.% and the 30 nm average diameter of Al₂O₃ particles over temperature range 300 – 325 K and developed a new model that predicts the results with the deviations of ±5%. Correlation of pool boiling heat transfer coefficient of the model is follows:

$$h_{\text{pool}} = 207 \frac{k_r}{d_b} \frac{q'' d_b}{k_r T_r}^{0.745} \frac{\rho_G}{\rho_{r,L}}^{0.581} Pr_r^{0.533} \quad (2.4)$$

Nanorefrigerants were tested as flowing them in horizontal tube with 5 m/s flow rate and the vapor quality is from 0.2 to 0.7. Coefficient of the convective heat transfer was increased with nanoparticle volume concentration of 1 to 5 % from 298.92 W/m² K to 304.3546 W/m² K, the thermal conductivity enhancement is about 43% at 325 K with 5 % volume fraction of nanoparticle and the highest pressure drop was 301.22 kPa which 79W of pumping power required with 5 % volume fraction of Al₂O₃ nanoparticles. In conclusion, it was found that there was the increment in the thermal conductivity, the convective heat transfer coefficient and flow boiling heat transfer coefficient and viscosity with increasing nanoparticle concentration.

Sun et al. [57] studied with R141b/Cu, R141b/Al, R141b/Al₂O₃, and R141b/CuO as nanorefrigerant for 0.1 wt.%, 0.2 wt.%, and 0.3 wt.% mass fractions in a computer aided test section to investigate the effect of material difference and vapor quality to flow boiling heat transfer inside the horizontal tube. For the same mass fraction, Cu-R141b nanorefrigerant had the biggest average heat transfer coefficient, after R141b/Al followed. R141b/Al₂O₃ had less heat transfer coefficient than R141b/Al and R141b/CuO had the least heat transfer coefficient. The heat transfer coefficient of four nanorefrigerants in tests increased and reached the maximum when $x = 0.5-0.6$ with increasing vapor quality.

1.2 Objective of the Thesis

The experimental studies on nanorefrigerants have showed that adding nanoparticles in pure refrigerant enhanced heat transfer rate and thermophysical specifications. Enhancement in COP was theoretically investigated by calculating enthalpies of points of refrigeration cycle depending on density of nanorefrigerant in this thesis and compared with experimental results in order to check accuracy of prediction approach to calculation of COP of nanorefrigerants mixtures.

1.3 Hypothesis

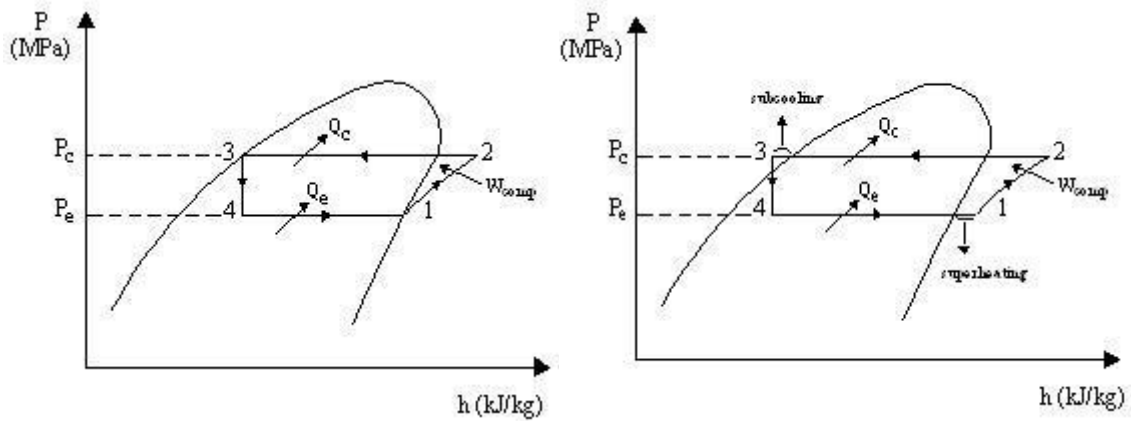
Enthalpies which are required to calculate COPs of refrigeration cycles of R12, R134a, R430a, R436a, R600a and R22, R290, R410a, R431a, R507a refrigerants added Al₂O₃ nanoparticles can predict by using Mollier Diagram of pure refrigerant. You can calculate the density of nanorefrigerant, and get the enthalpy of nanorefrigerant in refrigeration cycle from the pure refrigerant's enthalpy values as it was pure fluid by using the density calculated and pressure or temperature of the point, with acceptable deviation.

THEORETICAL MODEL

Refrigeration is the process of removal of heat from an region, or from a material, and transferring it to a place permanently. The vapour-compression refrigeration is a variety of refrigeration treatment. Generally, the system of a vapour-compression refrigeration includes a condenser, an expansion valve, an evaporator and a compressor.

The vapour-compression refrigeration cycle consist from four process:

- 1 – 2 Compressing refrigerant in compressor isentropically
- 2 – 3 Condensation at constant pressure
- 3 – 4 Adiabatic expanding in expansion valve
- 4 – 1 Evaporation at constant pressure



a) Non-superheating/subcooling case

b) Superheating/subcooling case

Figure 2.1 P-h diagrams of vapor-compression refrigeration cycle [59]

The pressure-enthalpy diagram prepared for theoretical data for two different cases is shown in Fig. 2.1. It should be noted that state 1 in Fig. 2.1a is saturated vapour at the evaporator temperature and state 3 in the same figure is saturated liquid at the condenser

temperature. This situation shows the two-phase region, mostly liquid obtained by a throttling device in turbines or a length of small-diameter tubing, during the isentropic expansion process from 3 to 4. This means that there will be negligible work output from this process. Saturated vapour in state 1 goes into the compressor at low pressure and is exposed to a reversible adiabatic compression during the process from 1 to 2 in Figure 2.1. In process 2–3, while the heat is rejected in the condenser at constant pressure, the working fluid changes its phase to saturated liquid at the exit of the condenser. Then, there is an adiabatic process during the process of 3–4 as explained above and the evaporation of refrigerant occurs at constant pressure during the process of 4–1 to complete the cycle. It is known that the actual refrigeration cycle systems have some deviations from the ideal one due to pressure losses of fluid flow and heat transfer exchange between the environment. The superheated state of vapour exists at the inlet part of the compressor as shown in Figure 2.1b, the pressure of the liquid at the exit part of the condenser is lower than the pressure at the inlet part of it, there is a pressure drop greater than the ideal one between the condenser and expansion valve, and also a larger pressure drop occurs on the evaporation line.

Working fluid in evaporator is colder than region will be cooled so heat transfers to working fluid from refrigerated zone. Because the refrigerant in evaporator is at saturation pressure corresponds to its temperature, it changes phase from liquid to gas, in another saying refrigerant evaporates. Refrigerant removes heat which equals to amount of the vapouring heat multiply mass rate. Completely vapourized refrigerant enters the compressor and its pressure and temperature increases by compressing. Working fluid at compressor outlet, or in other words working fluid at condenser inlet is warmer than environment that the condenser was placed. Heat transfers to environment from the condenser warmer than it. Temperature of the working fluid decreases up to saturation line. When the refrigerant is at the saturation pressure for its temperature, it starts to condense. It is desired that working fluid at condenser outlet is completely liquid. The refrigerant exited from condenser enters expansion valve. In expansion valve, pressure of refrigerant decreases and its velocity increases, and some of refrigerant change phase from liquid to gas adiabatically. Working fluid enters the evaporator with a drying rate between 0 and 1.

The heat transfer rate of the evaporator (Q_e), is calculated as follows:

$$Q_e = h_1 - h_4 \quad (2.1)$$

The heat transfer rate of the condenser (Q_c), is calculated as follows:

$$Q_c = h_2 - h_3 \quad (2.2)$$

Isentropic compression work of the compressor (W_{comp}) is expressed as follows:

$$W_{comp} = h_2 - h_1 \quad (2.3)$$

Isentropic efficiency of compressor is calculated follows:

$$\eta_{isen} = \frac{\text{Isentropic compressor work}}{\text{Actual compressor work}} \quad (2.4)$$

$$\eta_{isen} = \frac{h_{2s} - h_1}{h_{2a} - h_1} \quad (2.5)$$

The performance of refrigerators is determined in terms of the coefficient of performance (COP). COP is defined as follows:

$$\text{COP} = \frac{Q_e}{W_{comp}} = \frac{h_1 - h_4}{h_2 - h_1} \quad (2.6)$$

Particles with at least one dimension less than 100 nm is called nanoparticles. Nanoparticles have started to use in refrigeration systems in order to enhance the performance and COP. However, mixing the refrigerant with nanoparticle directly has been a difficult process, still. Further, that adding nanoparticles to lubricant of system is easier. The nanoparticles transfer into vapour phase of the refrigerant from nanolubricant as explained with migration mechanism explained in study of Ding et al. (2009). Mixture of lubricant and nanoparticles is named nanolubricant.

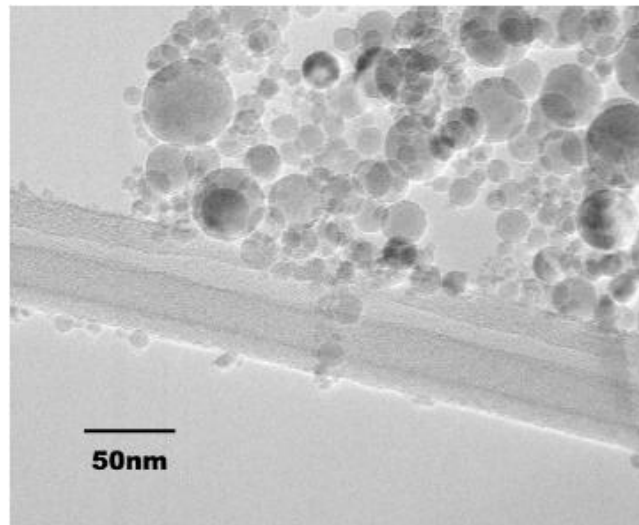


Figure 2.2 TEM of Al_2O_3 nanolubricant [47]

Effects of the nanoparticles to performance of refrigeration changes with variety, shape and concentration (ω) of the particles. Al, Al₂O₃, CuO, SiO₂, Ti, TiO₂ are some of nanoparticle varieties. Generally, spheric and cylindrical types of nanoparticles are produced and used. Further, nanorefrigerants contains at most 4 wt. % mass fraction of nanoparticle. Settlement and dispersion problems are shown when used in excess of 4 wt. % mass fraction of nanoparticle in refrigerants.

Principally, reason of enhancement in COP while nanoparticles are added into system can be explain as follows:

Conductivity and convectional heat transfer of nanorefrigerant is bigger than its pure refrigerant. Enhancement of these physical specifications causes increasing in degree of subcooling and superheating. Because dimensions of refrigeration system are not changed, nanorefrigerant removes more heat for same heat transfer area. Put another way, removed heat is more than evaporation heat of working fluid, degree of subcooling and superheating increases and less compressor work is needed for the same refrigeration load (2.1) or same mass rate. The heat rate of evaporator is able to increase with increase in mass rate. However, it is difficult to be possible as increasing mass rate increases compressor work. Further, a nanoparticle relocates heat as the amount of its heat capacity, during heating and cooling. However, the heat capacity of the nanoparticles are very small and it can be slighted when it is considered mass of nanoparticles in nanorefrigerant.

Prediction model approximates the enhancement in COP that caused using nanorefrigerant by taking advantage of change in density while nanoparticle dispersed in pure refrigerant. A new COP different from cycle of pure refrigerant can determine by using enthalpy at saturation line which correspond to calculated density.

DATA REDUCTION

In present study, a vapour-compression refrigeration cycle for ten different refrigerants and nanorefrigerants consisted 0.06% mass fraction Al_2O_3 nanoparticles compared to each refrigerant are used in order to investigate theoretically the change in performance. The effects of the base parameters of refrigeration cycle such as refrigerant type and degree of subcooling and superheating on the refrigerating effect (RE) and coefficient of performance (COP) are investigated for various evaporating temperatures and various condensation temperatures.

The refrigeration effect (RE), in other words, the heat transfer rate of the evaporator (Q_e), is calculated as follows:

$$\text{RE} = Q_e = h_1 - h_4 \quad (3.1)$$

Suction vapour flow per kW of refrigeration can be determined as:

$$\text{SVFR} = 1000 / (\rho_1 \cdot \text{RE}) \quad (3.2)$$

Mass fraction of nanoparticles in nanorefrigerant is found as follows [19]:

$$\omega = \frac{m_{\text{NP}}}{m_{\text{PR}} + m_{\text{NP}}} \quad (3.3)$$

Density of mixture of nanoparticles and the base fluid can be determine as follows [1]:

$$\rho_{\text{NR}} = \omega \rho_{\text{NP}} + (1 - \omega) \rho_{\text{PR}} \quad (3.4)$$

Subramani and Prakash [58] studied with R134a/ Al_2O_3 nanorefrigerant experimentally and found that there is an enhancement in COP while nanoparticles adding to the system. They determined COP of system theoretically for both R134a and R134a/ Al_2O_3 and measured, as well. Table 3.1 summarized the results of Subramani and Prakash [58]'s study.

Table 3.1 Some results from Subramani and Prakash [58]'s study

	T₁ (°C)	P₁ (bar)	T₂ (°C)	T₃ (°C)	P₃ (bar)	T₇ (°C)	COP	COP (theoretical)
R134a	19	2	82	45	12	-7	1.6	1.95
R134a/ Al ₂ O ₃	4	2	80	38	12	-6	1.78	2.14

Subramani and Prakash [58] reported that COP of cycle used R134a increased 11.25% while R134a/Al₂O₃ mixture used in actual refrigeration cycle and enhancement ratio was 9.74% when COP determined theoretically.

Density of nanorefrigerant can be a parameter to get enthalpy of working fluid. Mollier charts of pure refrigerant can be used to get enthalpy values corresponding to the density and temperature or pressure at cycle point, because of that there is no chart or correlation for nanorefrigerants. Density of Al₂O₃ was accepted 3690 kg/m³ [52]. Table 3.2 summarized the determination of enthalpy of point 3.

Table 3.2 Finding enthalpy of R134a/Al₂O₃ nanorefrigerant at point 3

T_{PR3} (°C)	ρ_{PR3} (kg/m ³)	h_{PR3} (kJ/kg)	ω	ρ_{Al2O3} (kg/m ³)	ρ_{NR3} (kg/m ³)	T_{NR3} (°C)	h_{NR3} (kJ/kg)
45	1125.05	263.44	0.0006	3690	1126.59	44.65	262.94

First, temperature (T_{PR3}) and saturation pressure (P_{PR3}) corresponds to T_{PR3} is specified 45 °C and 11.60 bar, respectively. Then density was read from Mollier chart of R134a. Density of nanorefrigerant (ρ_{NR}) is calculated by replacing nanoparticle mass fraction in nanorefrigerant (ω), ρ_{NP} and ρ_{PR} in equation (4.4). Then saturation temperature and pressure, and enthalpy of nanorefrigerant are read from chart R134a for point 3. Enthalpy at point 3 is decreased to 262.94 kJ/kg from 263.44 kJ/kg.

Similarly to the determination of enthalpy of nanorefrigerant at point 3, enthalpy of nanorefrigerant at point 1 can be found.

Table 3.3 Finding enthalpy of R134a/Al₂O₃ nanorefrigerant at point 1

T_{PR1} (°C)	ρ_{PR1} (kg/m ³)	h_{PR1} (kJ/kg)	ω	ρ_{Al2O3} (kg/m ³)	ρ_{NR1} (kg/m ³)	T_{NR1} (°C)	h_{NR1} (kJ/kg)
-7	11.23	394.47	0.0006	3690	13.43	-2.03	397.42

Temperature (T_{PR1}) and saturation pressure (P_{PR1}) corresponds to T_{PR1} is specified -7 °C and 2.26 bar, respectively. Then density was read from chart of R134a. Density of nanorefrigerant (ρ_{NR}) is calculated by replacing nanoparticle mass fraction in nanorefrigerant (ω), ρ_{NP} and ρ_{PR} in equation (3.4). Then saturation temperature and

pressure, and enthalpy of nanorefrigerant are read from chart R134a for point 1. Enthalpy at point 1 is increased to 394.70 kJ/kg from 394.47 kJ/kg.

It is shown that ρ_{NR1} and ρ_{NR3} is bigger than ρ_{PR1} and ρ_{PR3} . Kedzierski [52] reported that density of nanorefrigerant had been measured bigger than pure refrigerant's, as well.

h_2 and h_4 in a refrigeration cycle can be determined by using specifications at point 1 and point 3 of cycle like pressure, entropy etc.

At the inlet of evaporator, h_4 must equal to h_3 because of adiabatic expanding in expansion valve.

h_1 is read from chart by making use of s_1 and saturation pressure at point 3. At the outlet of the compressor, if isentropic efficiency is 1 and the refrigeration cycle is ideal, s_1 and s_2 must be equal, and P_3 and P_2 must be in same, respectively. For this calculation, isentropic efficiency is 0.51 .

Table 3.4 Cycle parameters and calculated values

	T_1 (°C)	h_1 (kJ/kg)	s_1 (kJ/kgK)	T_3 (°C)	$P_3 = P_2$ (bar)	$h_3 = h_4$ (kJ/kg)	h_2 (kJ/kg)	T_2 (°C)
R134a	-7	394.47	1.7313	45	11.60	263.44	461.41	81.21
R134a/ Al ₂ O ₃	-2.03	397.42	1.7282	44.65	11.49	262.94	456.26	76.23

Table 3.5 Calculations of COPs of cycles

	h_1 (kJ/kg)	h_2 (kJ/kg)	h_3 (kJ/kg)	h_4 (kJ/kg)	Q_e (kJ/kg)	Q_c (kJ/kg)	W_{comp} (kJ/kg)	COP
R134a	394.47	461.41	263.44	263.44	131.03	197.97	66.94	1.96
R134a /Al ₂ O ₃	397.42	456.26	262.94	262.94	134.48	193.32	58.84	2.29

COP enhancement is 16.76% when density of Al₂O₃ nanoparticles was supposed 3690 kg/m³. If we suppose that density of Al₂O₃ nanoparticles was 2200 kg/m³, results calculated are follows:

Table 3.6 Finding enthalpy of R134a/Al₂O₃ nanorefrigerant at point 3

T_{PR3} (°C)	ρ_{PR3} (kg/m ³)	h_{PR3} (kJ/kg)	ω	ρ_{Al2O3} (kg/m ³)	ρ_{NR3} (kg/m ³)	T_{NR3} (°C)	h_{NR3} (kJ/kg)
45	1125.05	263.44	0.0006	2200	1125.70	44.85	263.23

Table 3.7 Finding enthalpy of R134a/Al₂O₃ nanorefrigerant at point 1

T_{PR1} (°C)	ρ_{PR1} (kg/m³)	h_{PR1} (kJ/kg)	ω	ρ_{Al2O3} (kg/m³)	ρ_{NR1} (kg/m³)	T_{NR1} (°C)	h_{NR1} (kJ/kg)
-7	11.23	394.47	0.0006	2200	12.54	-3.96	396.28

Table 3.8 Calculations of COPs of cycles, ρ_{Al₂O₃} = 2200 kg/m³

	h₁ (kJ/kg)	h₂ (kJ/kg)	h₃ (kJ/kg)	h₄ (kJ/kg)	Q_e (kJ/kg)	Q_c (kJ/kg)	W_{comp} (kJ/kg)	COP
R134a	394.47	461.41	263.44	263.44	131.03	197.97	66.94	1.96
R134a /Al ₂ O ₃	396.28	458.30	263.23	263.23	133.05	195.07	62.02	2.15

Enhancement in COP is 9.6% when density of Al₂O₃ nanoparticles was supposed 2200 kg/m³. If density of Al₂O₃ is regarded as 2200 kg/m³, results of calculations approximates Subramani and Prakash [58]'s theoretical results with 99.87% accuracy and experimental COP enhancement with 98.52% accuracy.

If density of Al₂O₃ is regarded as 3690 kg/m³ which is its actual density, results of calculations approximates Subramani and Prakash [58]'s theoretical results with 93.61% accuracy and experimental COP enhancement with 95.05% accuracy.

Bi et al. [12] studied with R134a/Al₂O₃ nanorefrigerant experimentally with a refrigerator reported that energy saving of refrigerator using R134a/Al₂O₃ (0.06% wt.) mixture was 23.24% and enhancement in COP is 18.30%.

Table 3.9 Some results from Bi et al. [12]'s study

	T₁ (°C)	P₁ (bar)	T₂ (°C)	T₃ (°C)	P₃ (bar)	Energy Consumption (kWh/day)	On-time ratio (%)
R134a	-28.90	0.882	47.85	32.08	9.996	1.077	44.89
R134a/ Al ₂ O ₃	-28.78	0.770	39	30.83	9.09	0.8267	35.96

Table 3.10 Finding enthalpy of R134a/Al₂O₃ nanorefrigerant at point 3

T_{PR3} (°C)	ρ_{PR3} (kg/m³)	h_{PR3} (kJ/kg)	ω	ρ_{Al2O3} (kg/m³)	ρ_{NR3} (kg/m³)	T_{NR3} (°C)	h_{NR3} (kJ/kg)
32.08	1179.25	245.11	0.0006	3690	1180.76	31.70	244.58

First, temperature (T_{PR3}) and saturation pressure (P_{PR3}) corresponds to T_{PR3} is specified 32.08 °C and 8.17 bar, respectively. Then density was read from chart of R134a. Density of nanorefrigerant (ρ_{NR}) is calculated by replacing nanoparticle mass fraction in nanorefrigerant (ω), ρ_{NP} and ρ_{PR} in equation (3.4). Then saturation temperature and

pressure, and enthalpy of nanorefrigerant are read from chart R134a for point 3. Enthalpy at point 3 is decreased to 244.58 kJ/kg from 245.11 kJ/kg.

Similarly to the determination of enthalpy of nanorefrigerant at point 3, enthalpy of nanorefrigerant at point 1 can be found.

Table 3.11 Finding enthalpy of R134a/Al₂O₃ nanorefrigerant at point 1

T_{PR1} (°C)	ρ_{PR1} (kg/m³)	h_{PR1} (kJ/kg)	ω	ρ_{Al2O3} (kg/m³)	ρ_{NR1} (kg/m³)	T_{NR1} (°C)	h_{NR1} (kJ/kg)
-28.9	4.65	381.01	0.0006	3690	6.86	-19.73	386.72

Temperature (T_{PR1}) and saturation pressure (P_{PR1}) corresponds to T_{PR1} is specified -28.9 °C and 0.89 bar, respectively. Then density was read from chart of R134a. Density of nanorefrigerant (ρ_{NR}) is calculated by replacing nanoparticle mass fraction in nanorefrigerant (ω), ρ_{NP} and ρ_{PR} in equation (3.4). Then saturation temperature and pressure, and enthalpy of nanorefrigerant are read from chart R134a for point 1. Enthalpy at point 1 is increased to 386.72 kJ/kg from 381.01 kJ/kg. For calculation of COP of cycle, isentropic efficiency is supposed 0.9.

Table 3.12 Cycle parameters and calculated values

	T₁ (°C)	h₁ (kJ/kg)	s₁ (kJ/kgK)	T₃ (°C)	P₃ = P₂ (bar)	h₃ = h₄ (kJ/kg)	h₂ (kJ/kg)	T₂ (°C)
R134a	-28.9	381.01	1.7502	32.08	8.173	245.11	432.27	47.80
R134a/ Al ₂ O ₃	-19.7	386.72	1.7411	31.70	8.09	244.58	428.18	43.65

Table 3.13 Calculations of COPs of cycles

	h₁ (kJ/kg)	h₂ (kJ/kg)	h₄ (kJ/kg)	Q_e (kJ/kg)	Q_c (kJ/kg)	W_{comp} (kJ/kg)	COP
R134a	381.01	432.27	245.11	135.9	187.16	51.26	2.651
R134a/ Al ₂ O ₃	386.72	428.18	244.58	142.14	183.6	41.46	3.428

COP enhancement is 29.32% when density of Al₂O₃ nanoparticles was supposed 3690 kg/m³. If we suppose that density of Al₂O₃ nanoparticles was 2200 kg/m³, results calculated are follows:

Table 3.14 Finding enthalpy of R134a/Al₂O₃ nanorefrigerant at point 3

T_{PR3} (°C)	ρ_{PR3} (kg/m³)	h_{PR3} (kJ/kg)	ω	ρ_{Al2O3} (kg/m³)	ρ_{NR3} (kg/m³)	T_{NR3} (°C)	h_{NR3} (kJ/kg)
32.08	1179.25	245.11	0.0006	2200	1179.86	31.93	244.90

Table 3.15 Finding enthalpy of R134a/Al₂O₃ nanorefrigerant at point 1

T_{PR1} (°C)	ρ_{PR1} (kg/m³)	h_{PR1} (kJ/kg)	ω	ρ_{Al2O3} (kg/m³)	ρ_{NR1} (kg/m³)	T_{NR1} (°C)	h_{NR1} (kJ/kg)
-28.9	4.65	381.01	0.0006	2200	5.97	-23.11	384.63

Table 3.16 Calculations of COPs of cycles

	h₁ (kJ/kg)	h₂ (kJ/kg)	h₃ (kJ/kg)	h₄ (kJ/kg)	Q_e (kJ/kg)	Q_c (kJ/kg)	W_{comp} (kJ/kg)	COP
R134a	381.01	432.27	245.11	245.11	135.9	187.16	51.26	2.65
R134a /Al ₂ O ₃	384.63	428.18	244.90	244.90	142.14	183.6	41.46	3.10

Enhancement in COP is 17.05% when density of Al₂O₃ nanoparticles was supposed 2200 kg/m³. If density of Al₂O₃ is regarded as 2200 kg/m³, results of calculations approximates Bi et al. [12]'s results with 98.94% and if value of density 3690 kg/m³ for Al₂O₃ nanoparticles, results of calculations approximates Bi et al. [12]'s results with 90.68%.

RESULTS AND DISCUSSION

Prediction approach of analyzing performance of nanorefrigerants is applied to ten different pure refrigerant and ten nanorefrigerants summarized in Table 4.1.

Table 4.17 Refrigerant list

Base Refrigerant	Pure Refrigerant (PR)		Nanorefrigerant (NR)	
	Nanoparticle	Mass Fraction (wt.%)	Nanoparticle	Mass Fraction (wt.%)
R12	-	-	Al ₂ O ₃	0.06
R134a	-	-	Al ₂ O ₃	0.06
R430a	-	-	Al ₂ O ₃	0.06
R436a	-	-	Al ₂ O ₃	0.06
R600a	-	-	Al ₂ O ₃	0.06
R22	-	-	Al ₂ O ₃	0.06
R290	-	-	Al ₂ O ₃	0.06
R410a	-	-	Al ₂ O ₃	0.06
R431a	-	-	Al ₂ O ₃	0.06
R507a	-	-	Al ₂ O ₃	0.06

The prediction approached developed was applied to non-superheating/subcooling and superheating/subcooling (5°C) cases with each working fluid.

4.1 Results

COP enhancement for at various evaporating temperatures and various condensing temperatures was calculated as follows :

First, temperature (T_{PR3}) and saturation pressure (P_{PR3}) at T_{PR3} is specified. Then density is read from Mollier chart of R134a. Density of nanorefrigerant (ρ_{NR}) is calculated by replacing nanoparticle mass fraction in nanorefrigerant (ω), ρ_{NP} and ρ_{PR} in equation (3.4). Density of Al_2O_3 was accepted 3690 kg/m^3 [52]. Then saturation temperature and pressure, and enthalpy of nanorefrigerant are read from chart of refrigerant for point 3. The evaporation temperature and pressure of refrigerant increases, and the condensation temperature and pressure of refrigerant decreases when density of the refrigerant increases.

h_2 and h_4 in the refrigeration cycle can be determined by using specifications at point 1 and point 3 of cycle like pressure, entropy etc.

At the inlet of evaporator, h_4 must equal to h_3 because of adiabatic expanding in expansion valve.

h_1 is read from Mollier chart of refrigerant by making use of s_1 and saturation pressure at point 3. At the outlet of the compressor, if isentropic efficiency is 1 and the refrigeration cycle is ideal, s_1 and s_2 must be equal, and P_3 and P_2 must be in same, respectively. For all calculation, isentropic efficiency is 0.51.

The heat transfer rate of the evaporator (Q_e), is calculated by using equation (2.1), the heat transfer rate of the condenser (Q_c), is calculated by using equation (2.2), isentropic compression work of the compressor (W_{comp}) is expressed by using equation (2.3), Isentropic efficiency of compressor is calculated by using equation (2.5) and the COP is defined as by using equation (2.6).

Some samples of calculation used to plot charts are given in Table 4.2 for non-superheating/subcooling case and Table 4.3 for $5 \text{ }^\circ\text{C}$ of superheating/subcooling case.

Table 4.18 Calculation of sample case, $T_c = 45\text{ }^\circ\text{C}$ and $T_e = -10\text{ }^\circ\text{C}$, and non-superheating/subcooling

	ρ_{PR3} (kg/m^3)	ρ_{NR3} (kg/m^3)	T_c ($^\circ\text{C}$)	ρ_{PR1} (kg/m^3)	ρ_{NR1} (kg/m^3)	T_e ($^\circ\text{C}$)	$Q_{e(PR)}$ (kJ/kg)	$W_{comp(PR)}$ (kJ/kg)	$Q_{e(NR)}$ (kJ/kg)	$W_{comp(NR)}$ (kJ/kg)	COP_{PR}	COP_{NR}	COP Increase (%)
R12	1234.05	1235.52	44.64	12.92	15.13	-5.23	103.24	56.04	105.78	49.87	1.842	2.121	15.13
R134a	1125.05	1126.59	44.65	10.04	12.25	-4.61	129.23	71.78	132.95	62.81	1.801	2.117	17.56
R430a	714.69	716.48	44.30	6.23	8.44	-1.23	205.98	111.33	214.57	88.79	1.850	2.417	30.62
R436a	487.20	489.13	43.80	4.48	6.69	2.10	239.28	155.49	257.74	116.71	1.539	2.208	43.51
R600a	523.07	524.97	43.64	3.00	5.22	6.28	229.73	126.42	255.03	97.51	1.817	2.615	43.93

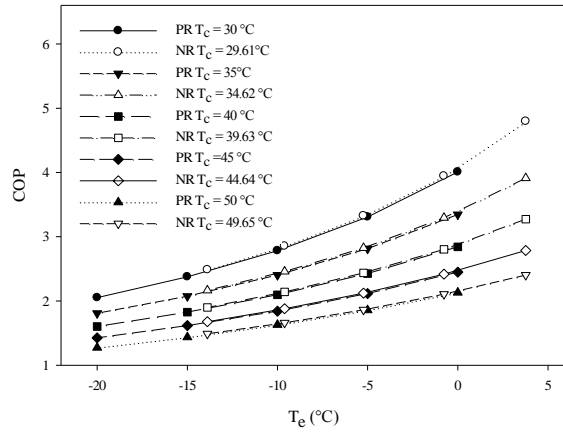
Table 4.19 Calculation of sample case, $T_c = 45\text{ }^\circ\text{C}$ and $T_e = -10\text{ }^\circ\text{C}$, and $5\text{ }^\circ\text{C}$ superheating and $5\text{ }^\circ\text{C}$ subcooling

	ρ_{PR3} (kg/m^3)	ρ_{NR3} (kg/m^3)	T_c ($^\circ\text{C}$)	ρ_{PR1} (kg/m^3)	ρ_{NR1} (kg/m^3)	T_e ($^\circ\text{C}$)	$Q_{e(PR)}$ (kJ/kg)	$W_{comp(PR)}$ (kJ/kg)	$Q_{e(NR)}$ (kJ/kg)	$W_{comp(NR)}$ (kJ/kg)	COP_{PR}	COP_{NR}	COP Increase (%)
R22	1106.00	1107.55	44.66	15.32	17.53	-5.96	154.82	80.83	156.90	72.90	1.915	2.152	12.37
R290	458.03	459.97	43.95	7.64	9.85	-1.72	262.54	141.00	275.12	113.40	1.862	2.426	30.29
R410a	946.79	948.43	44.76	21.90	24.10	-7.16	161.59	88.68	163.09	82.40	1.822	1.979	8.63
R431a	653.71	655.53	44.35	7.70	9.91	-2.87	221.66	131.36	228.86	109.89	1.687	2.083	23.41
R507a	935.46	937.12	44.75	23.37	25.57	-7.30	104.86	60.29	106.70	56.38	1.739	1.893	8.82

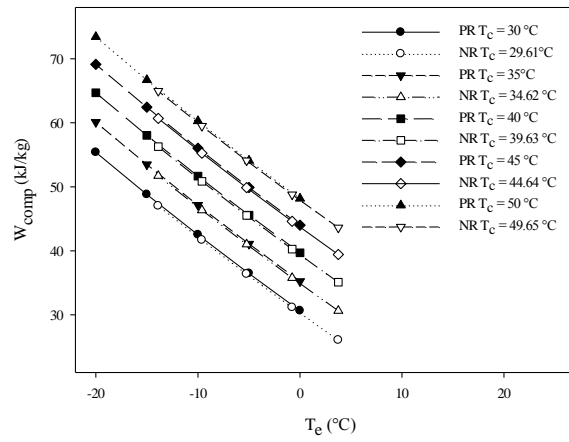
4.1.1 Charts

Figure 4.1 – Figure 4.30 are the result of calculation applied prediction model for R12, R134a, R430a, R436a, R600a and R22, R290, R410a, R431a, R507a refrigerants and nanorefrigerants which they used as base fluid added Al_2O_3 nanoparticles. Enthalpy, pressure and temperature at saturation, and pressure and temperature at defined density got from Mollier Diagrams of pure refrigerants.

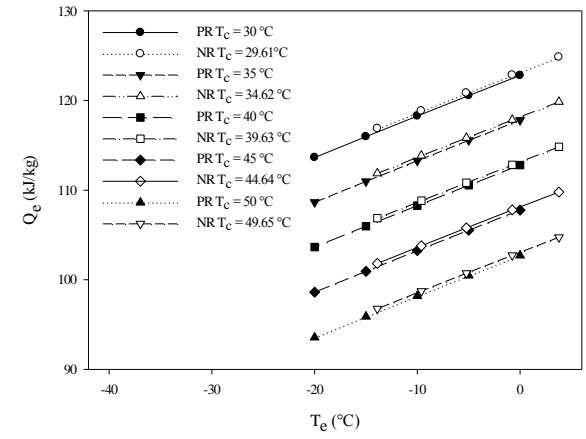
a) T_e vs. COP



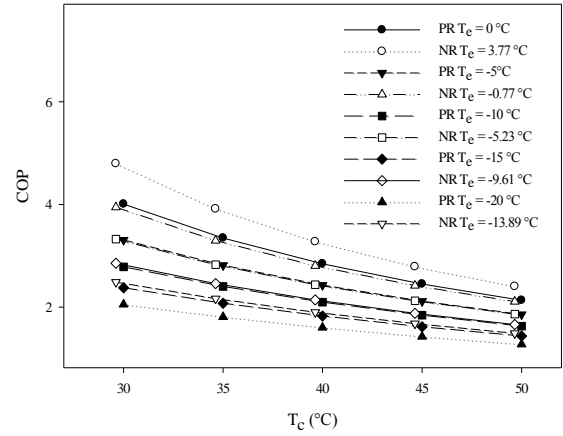
b) T_e vs. W_{comp}



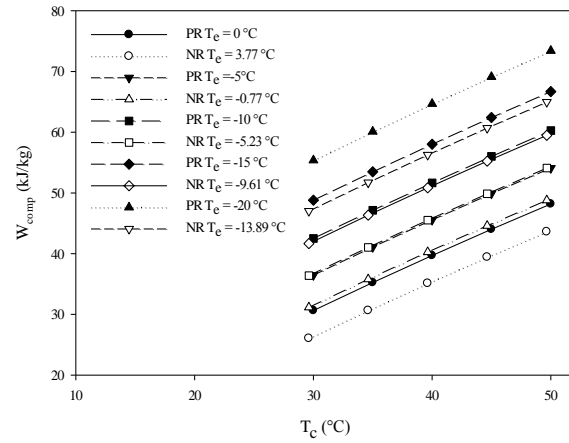
c) T_e vs. Q_e



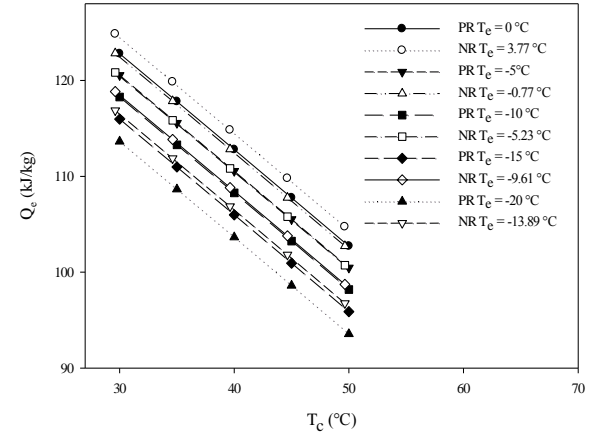
d) T_c vs. COP



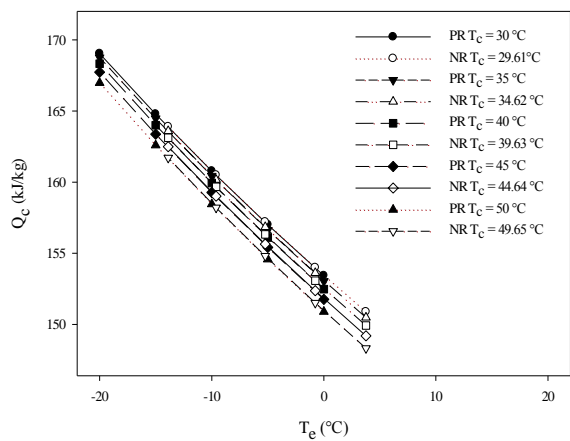
e) T_c vs. W_{comp}



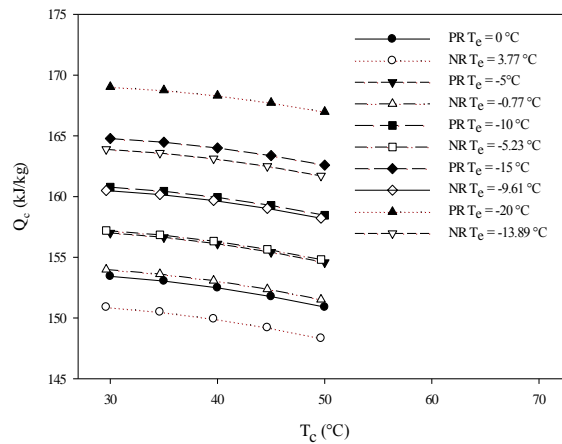
f) T_c vs. Q_e



g) T_e vs. Q_c



h) T_c vs. Q_c



i) T_e vs. SVFR

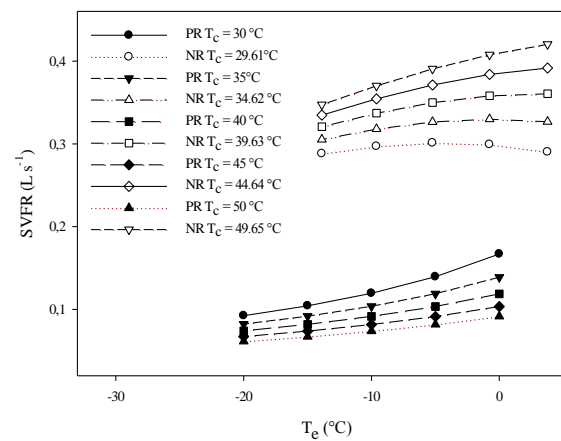
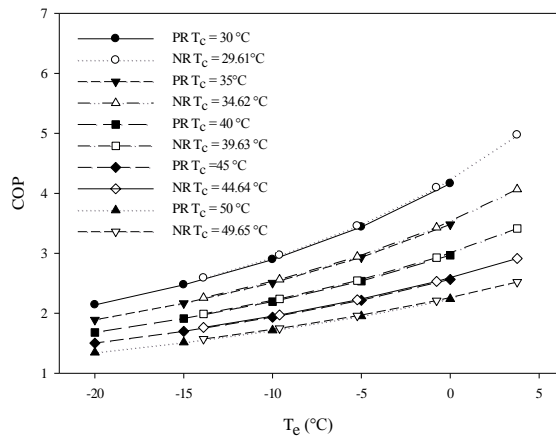
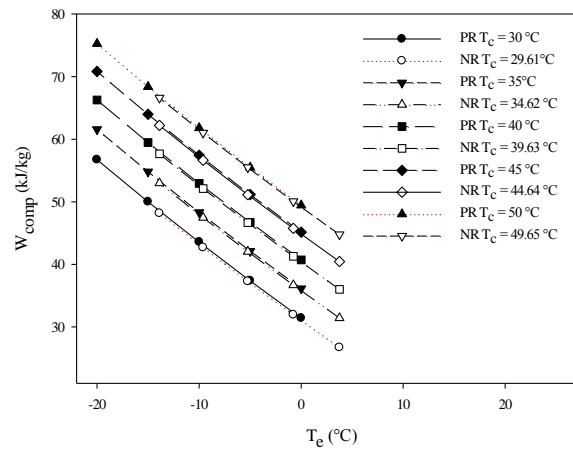


Figure 4.3 Charts of R12 vs R12/Al₂O₃ for non-superheating/subcooling case

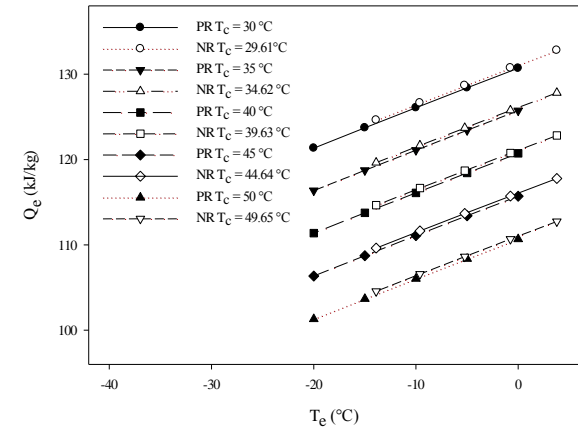
a) T_e vs. COP



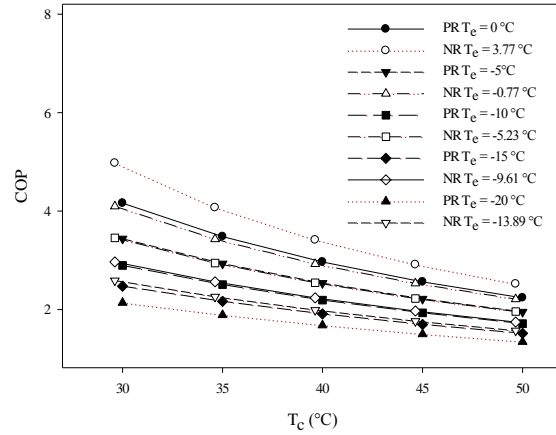
b) T_e vs. W_{comp}



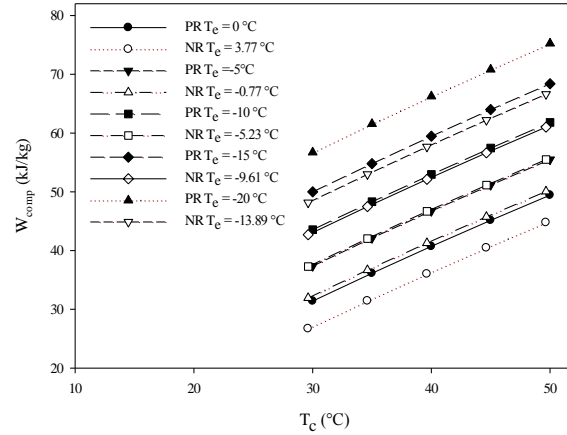
c) T_e vs. Q_e



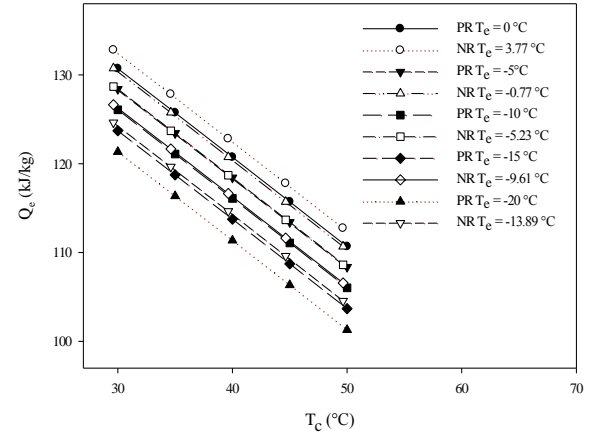
d) T_c vs. COP



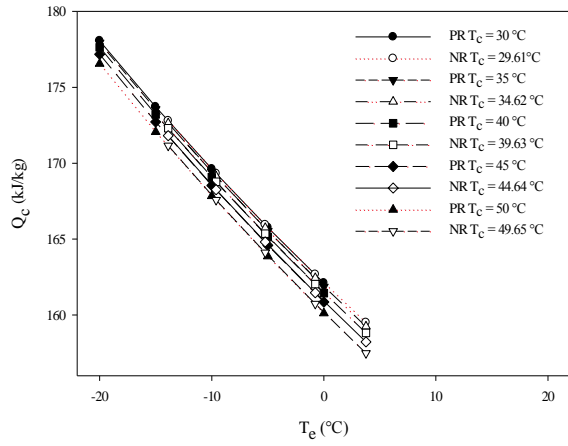
e) T_c vs. W_{comp}



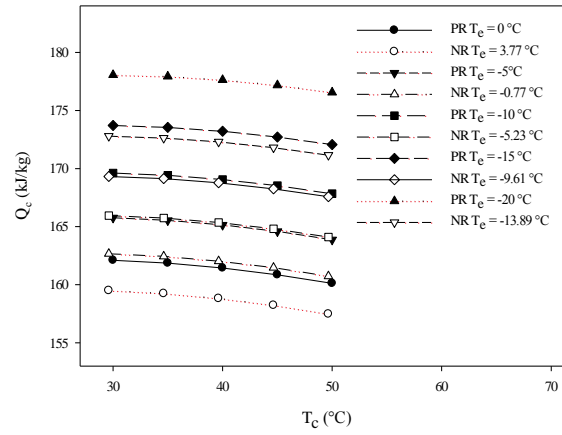
f) T_c vs. Q_e



g) T_e vs. Q_c



h) T_c vs. Q_c



i) T_e vs. SVFR

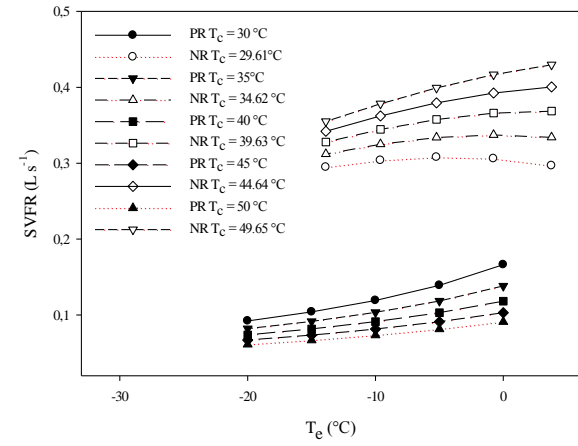


Figure 4.4 Charts of R12 vs R12/Al₂O₃ for 5 °C of superheating/subcooling case

35

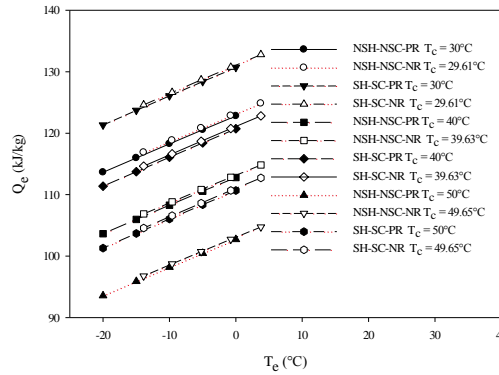
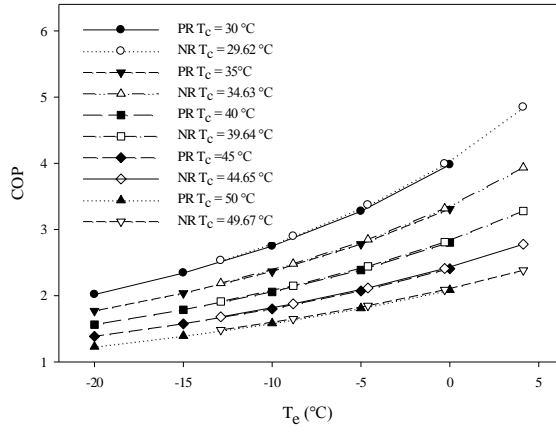
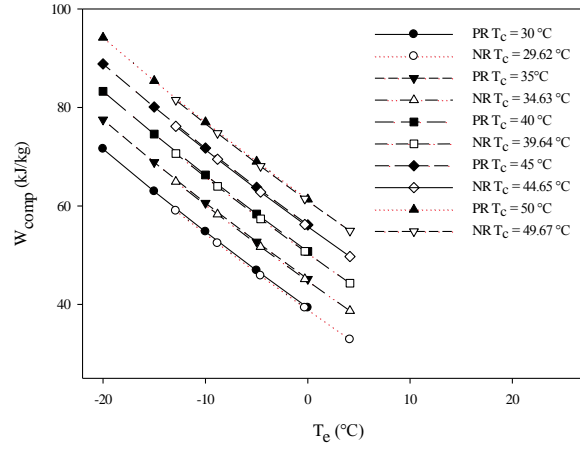


Figure 4.5 Chart of R12 and R12/Al₂O₃ for non-superheating/subcooling vs. 5 °C of superheating/subcooling

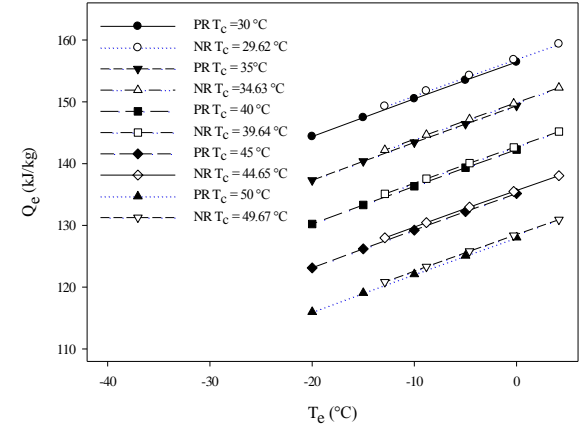
a) T_e vs. COP



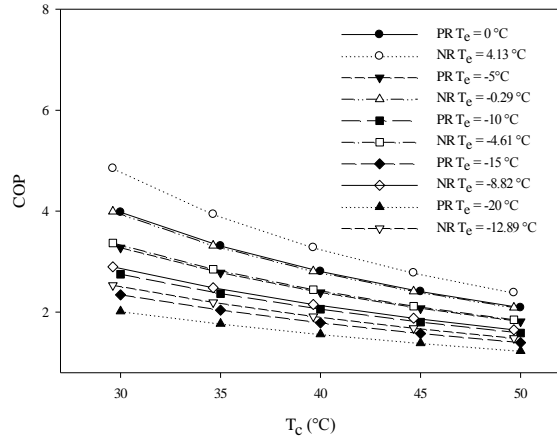
b) T_e vs. W_{comp}



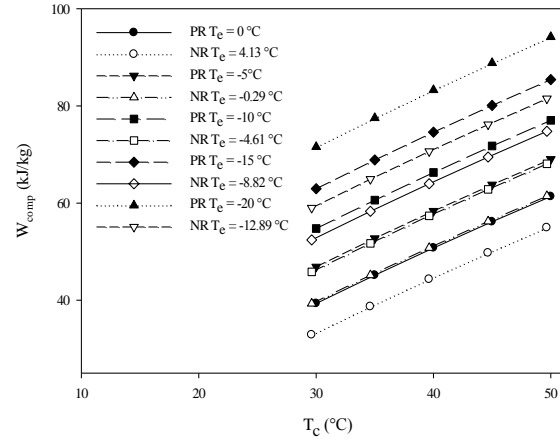
c) T_e vs. Q_e



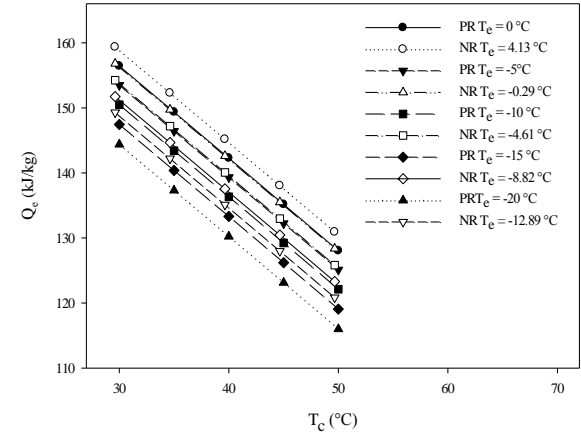
d) T_c vs. COP



e) T_c vs. W_{comp}



f) T_c vs. Q_e



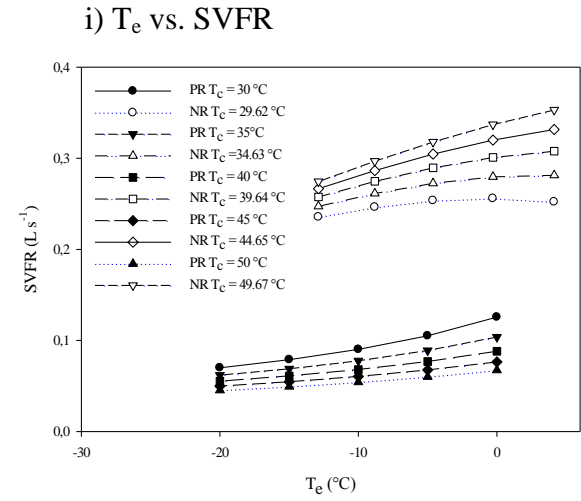
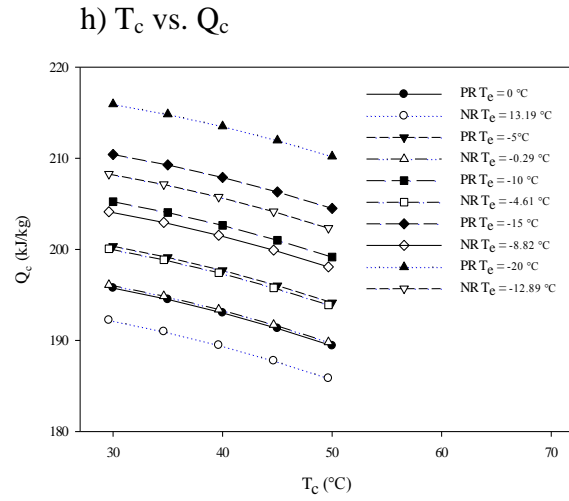
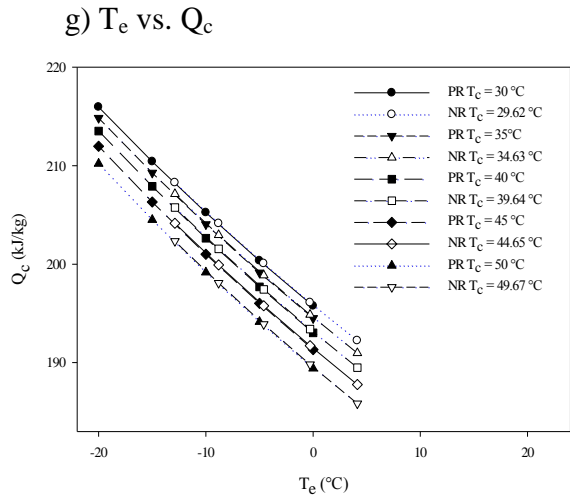
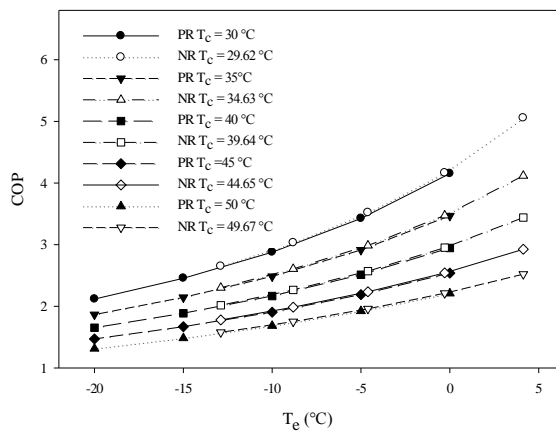
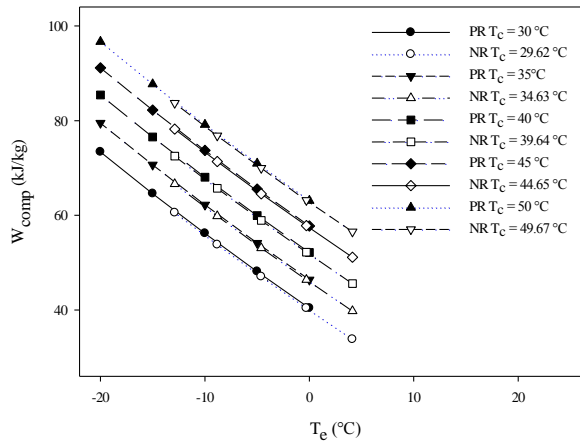


Figure 4.6 Charts of R134a vs R134a/Al₂O₃ for non-superheating/subcooling case

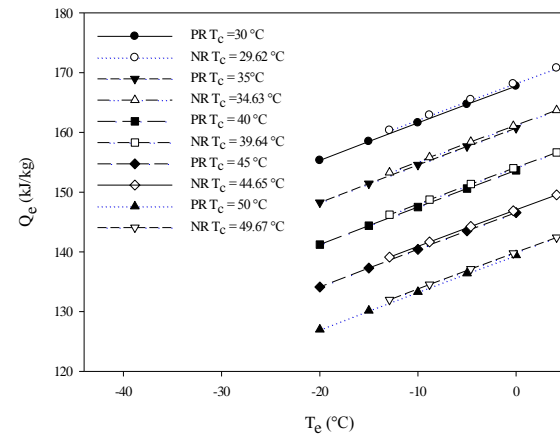
a) T_e vs. COP



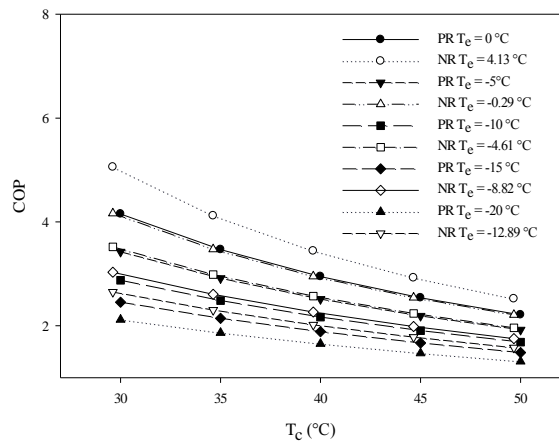
b) T_e vs. W_{comp}



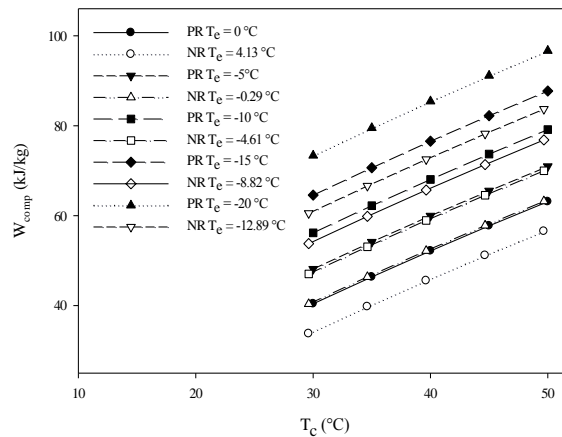
c) T_e vs. Q_e



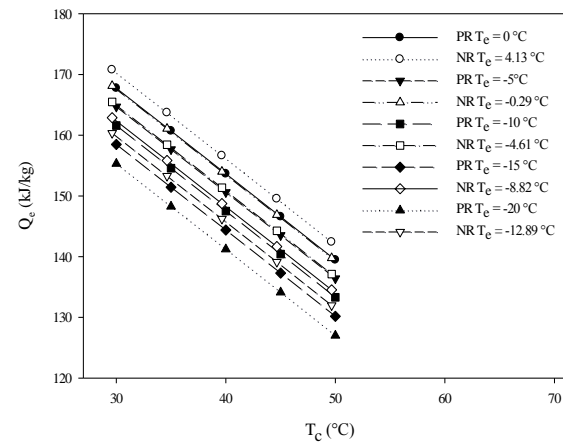
d) T_c vs. COP



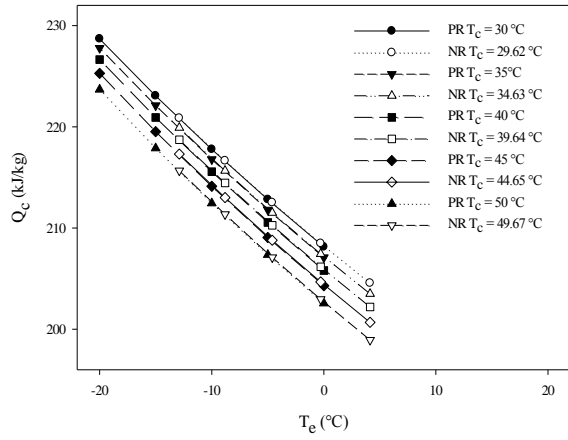
e) T_c vs. W_{comp}



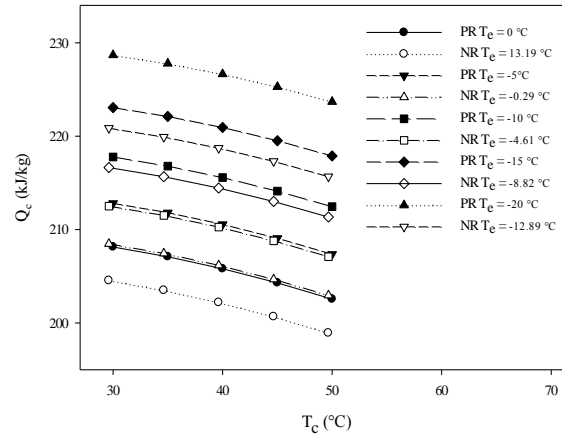
f) T_c vs. Q_e



g) T_e vs. Q_c



h) T_c vs. Q_c



i) T_e vs. SVFR

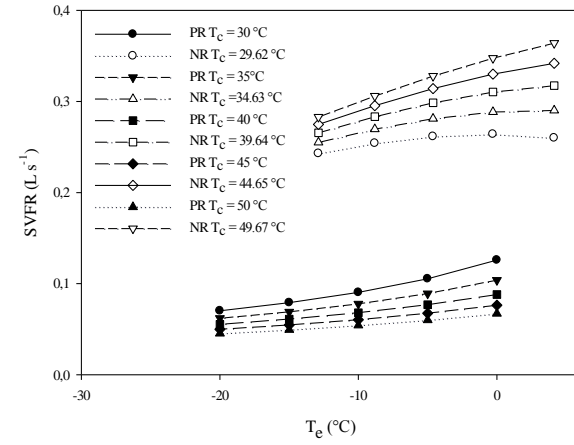


Figure 4.7 Charts of R134a vs R134a/Al₂O₃ for 5 °C of superheating/subcooling case

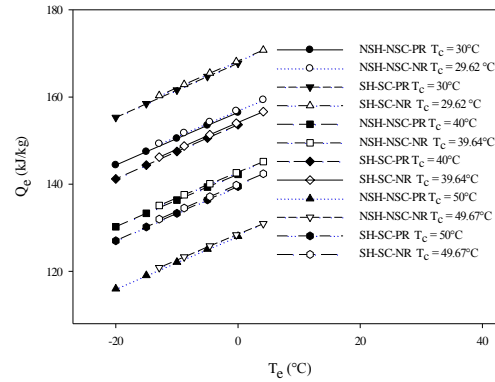
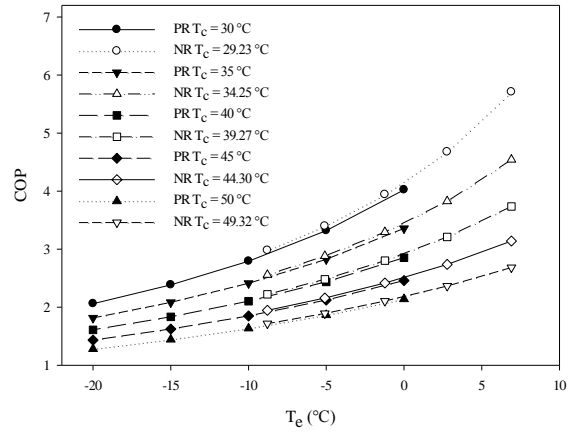
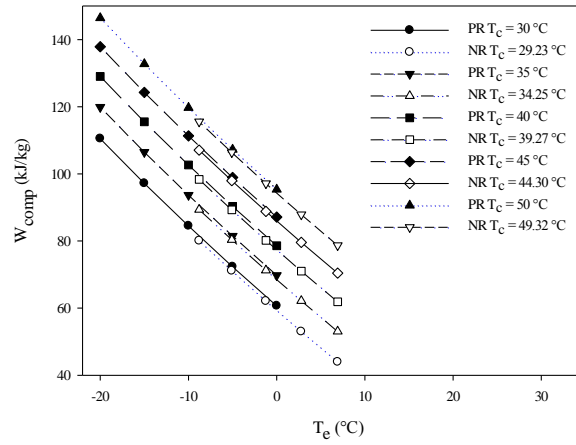


Figure 4.8 Chart of R134a and R134a/Al₂O₃ for non-superheating/subcooling vs. 5 °C of superheating/subcooling case

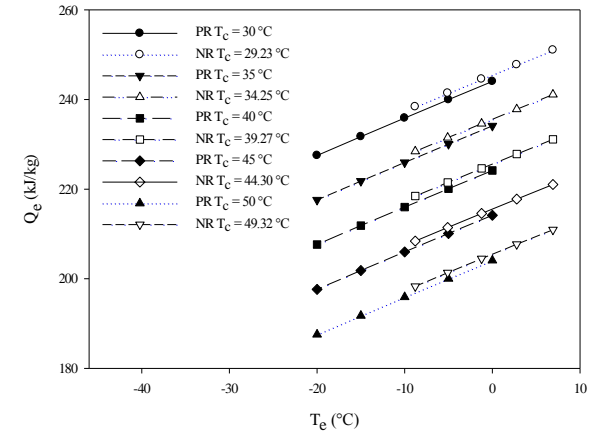
a) T_e vs. COP



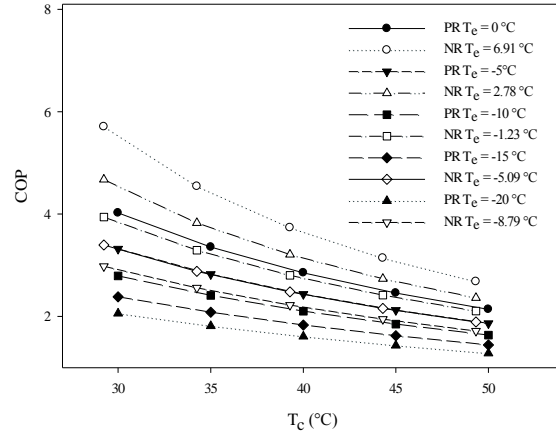
b) T_e vs. W_{comp}



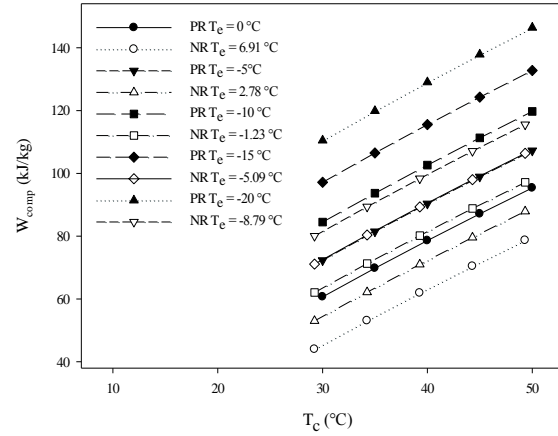
c) T_e vs. Q_e



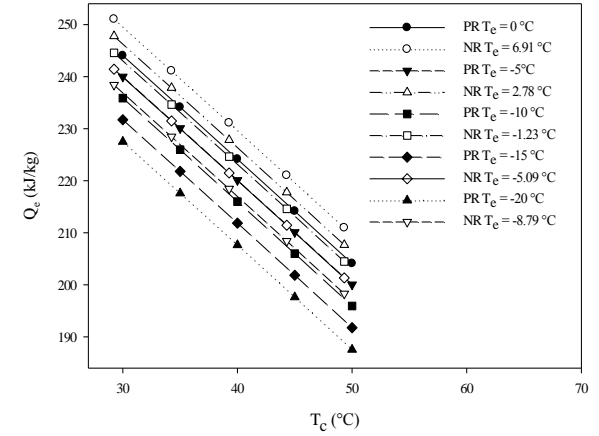
d) T_c vs. COP



e) T_c vs. W_{comp}



f) T_c vs. Q_e



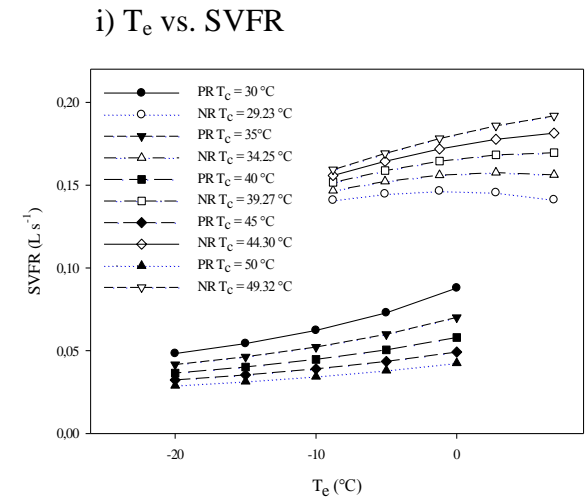
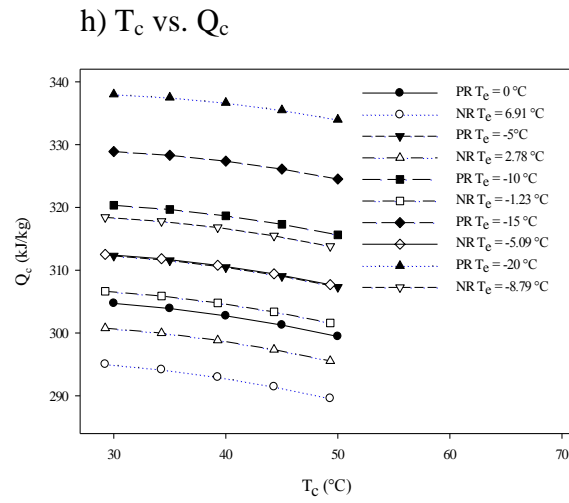
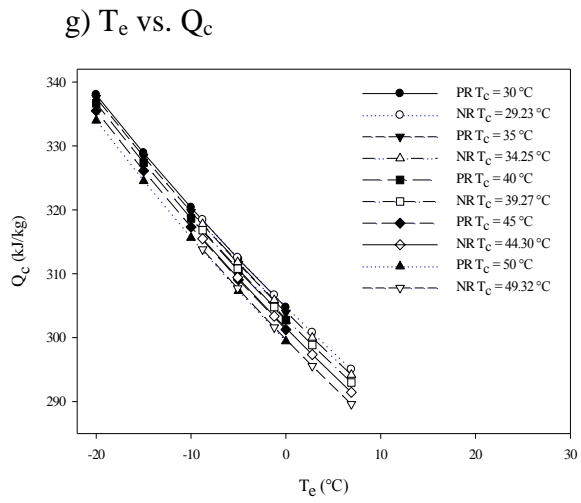
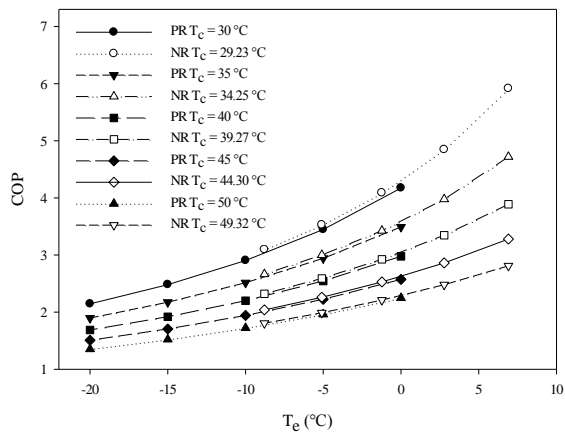
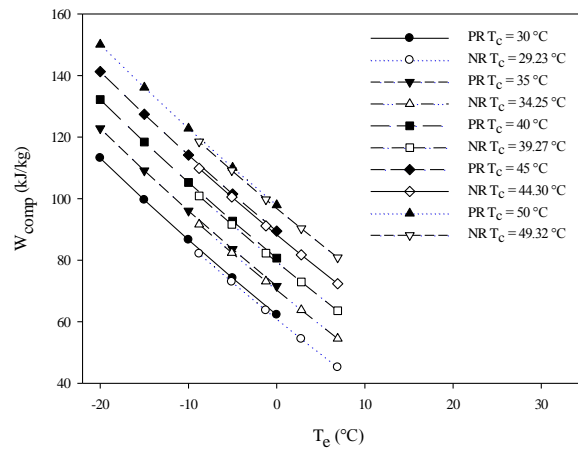


Figure 4.9 Charts of R430a vs R430a/Al₂O₃ for non-superheating/subcooling case

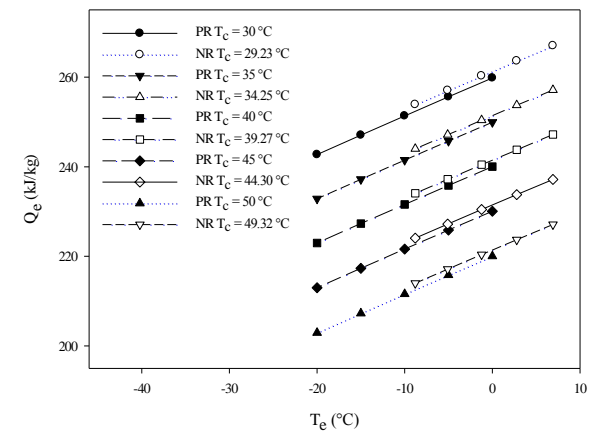
a) T_e vs. COP



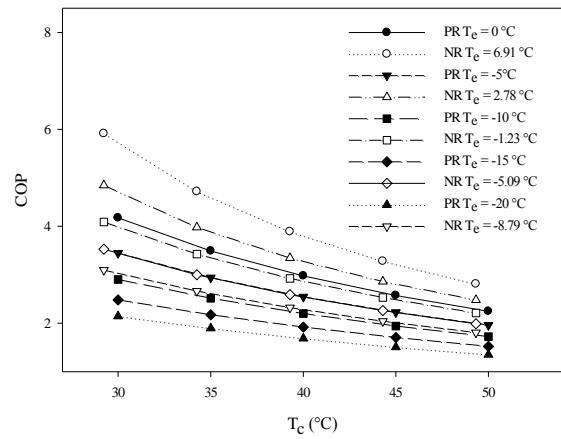
b) T_e vs. W_{comp}



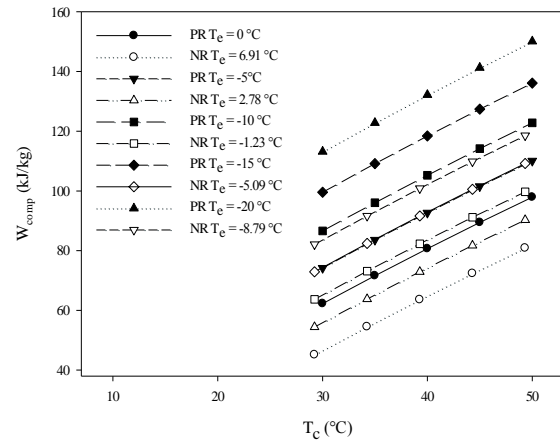
c) T_e vs. Q_e



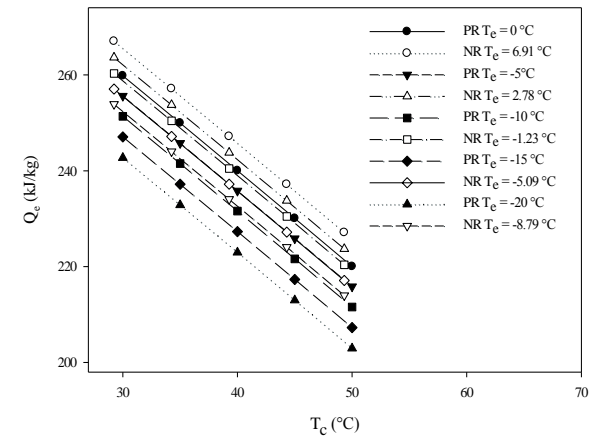
d) T_c vs. COP



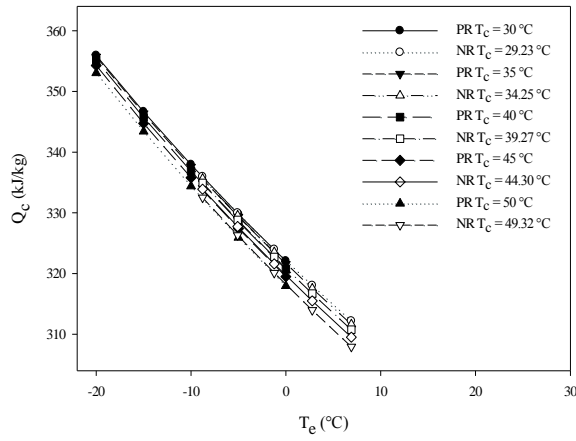
e) T_c vs. W_{comp}



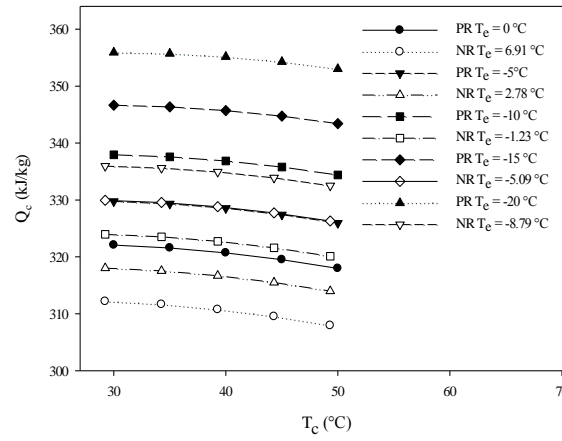
f) T_c vs. Q_e



g) T_e vs. Q_c



h) T_c vs. Q_c



i) T_e vs. SVFR

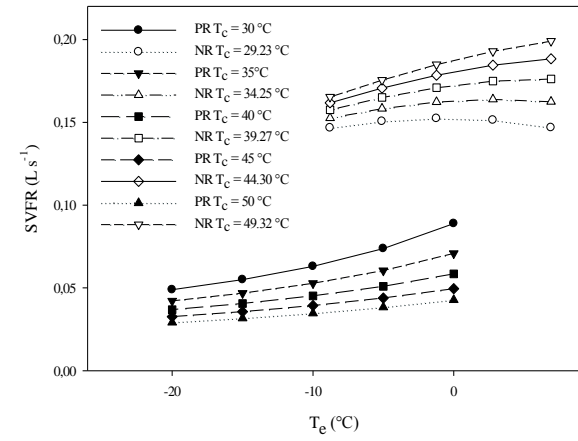


Figure 4.10 Charts of R430a vs R430a/Al₂O₃ for 5 °C of superheating/subcooling case

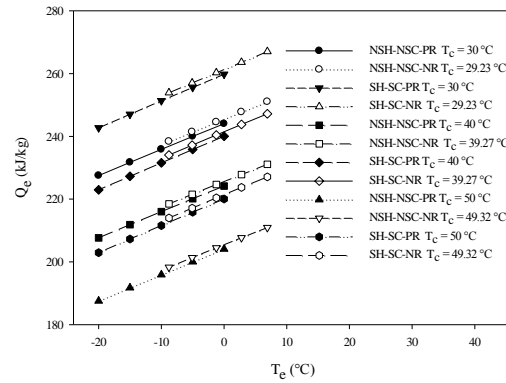
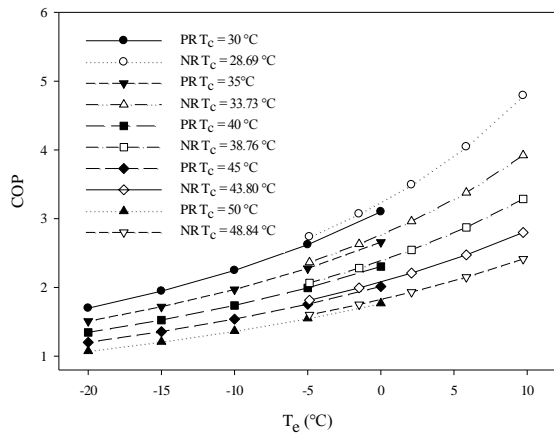
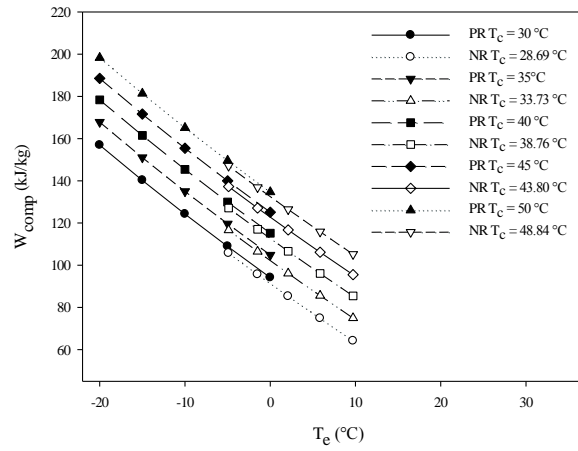


Figure 4.11 Chart of R430a and R430a/Al₂O₃ for non-superheating/subcooling vs. 5 °C of superheating/subcooling case

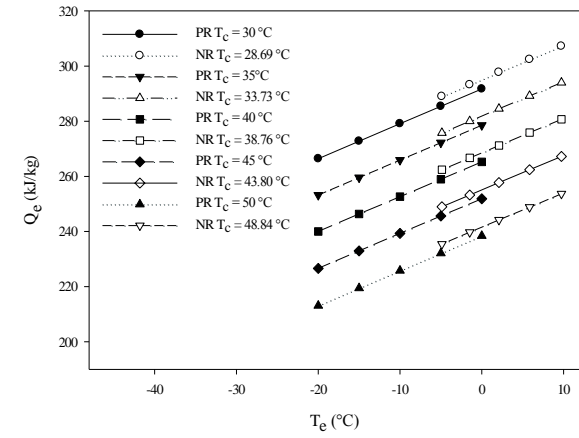
a) T_e vs. COP



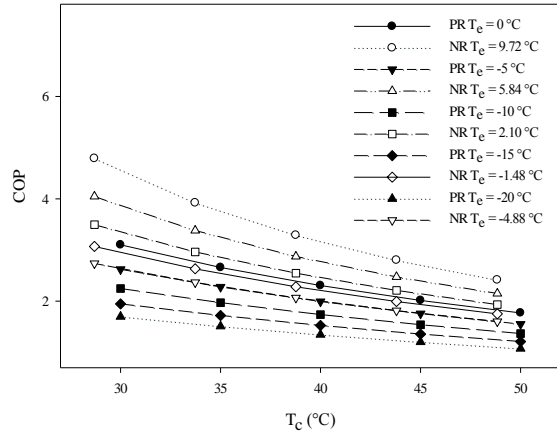
b) T_e vs. W_{comp}



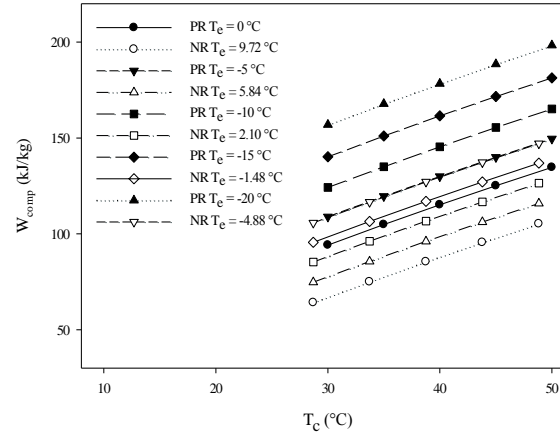
c) T_e vs. Q_e



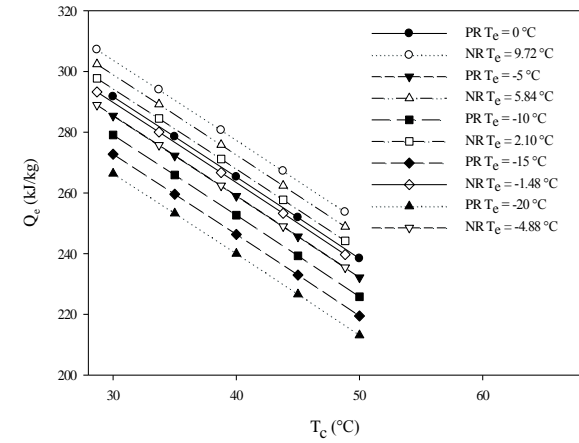
d) T_c vs. COP



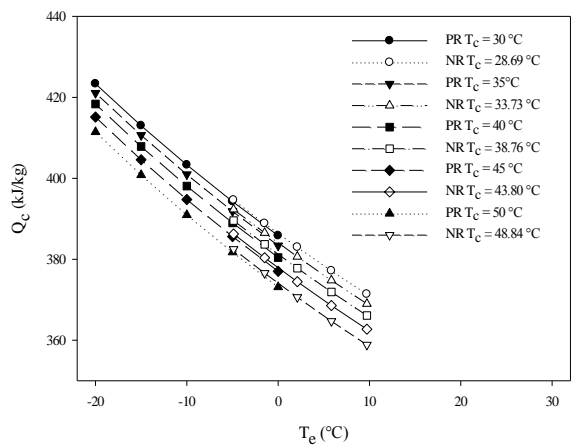
e) T_c vs. W_{comp}



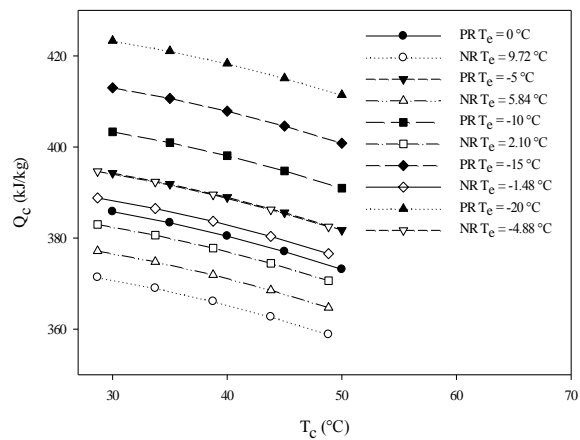
f) T_c vs. Q_e



g) T_e vs. Q_c



h) T_c vs. Q_c



i) T_e vs. SVFR

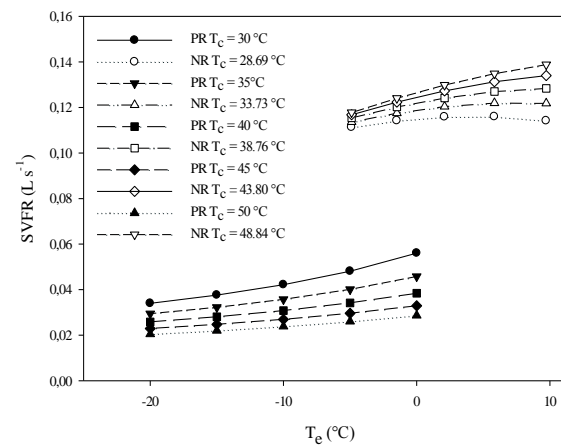
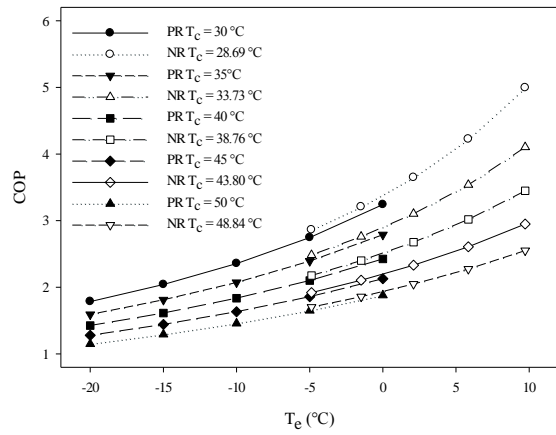
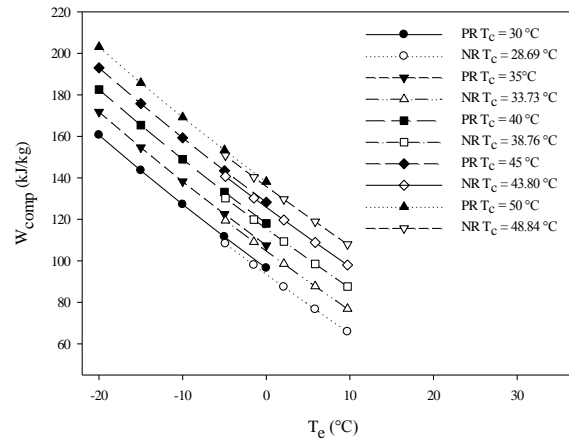


Figure 4.12 Charts of R436a vs R436a/Al₂O₃ for non-superheating/subcooling case

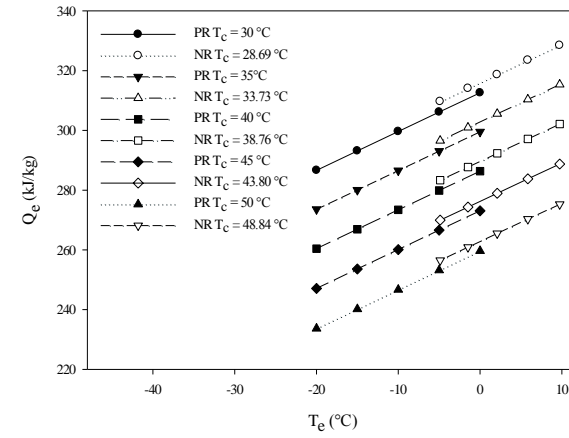
a) T_e vs. COP



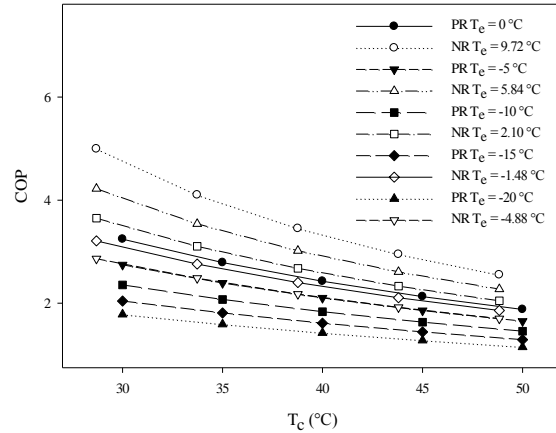
b) T_e vs. W_{comp}



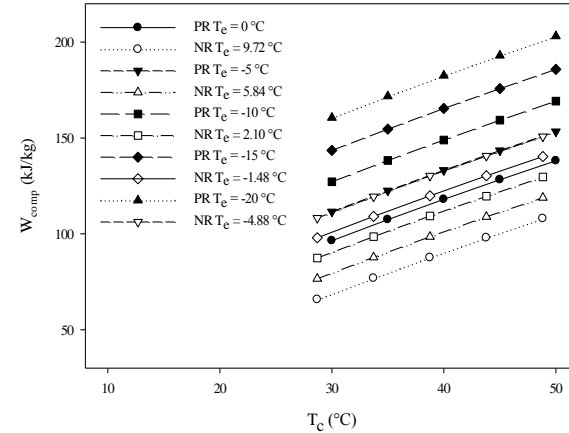
c) T_e vs. Q_e



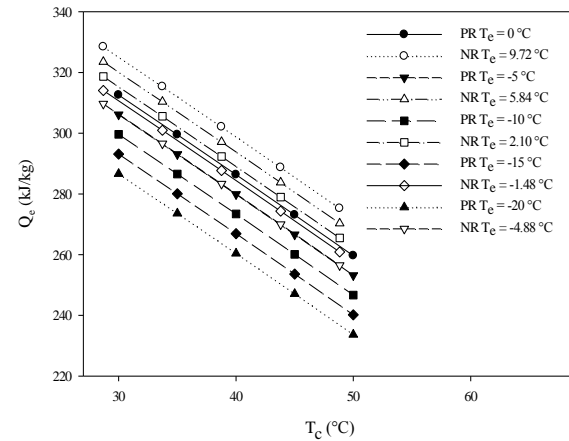
d) T_c vs. COP



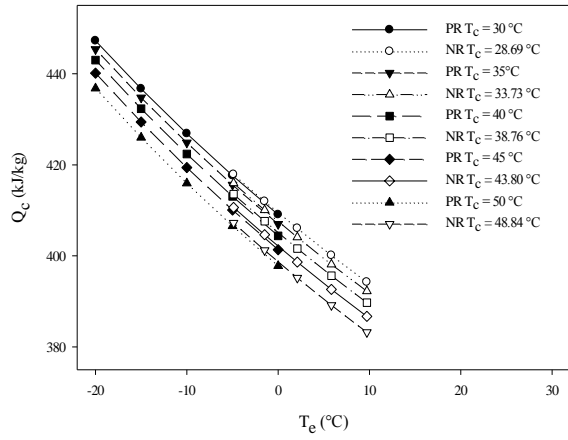
e) T_c vs. W_{comp}



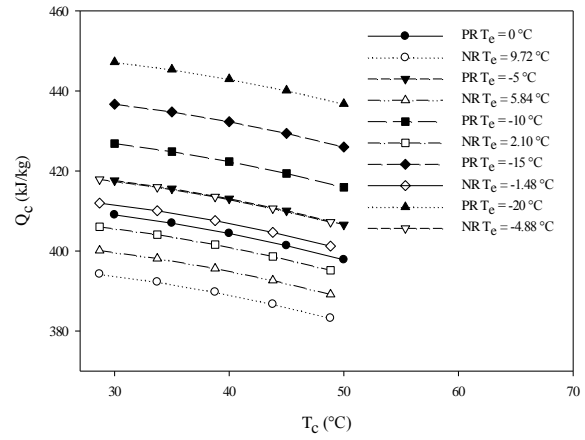
f) T_c vs. Q_e



g) T_e vs. Q_c



h) T_c vs. Q_c



i) T_e vs. SVFR

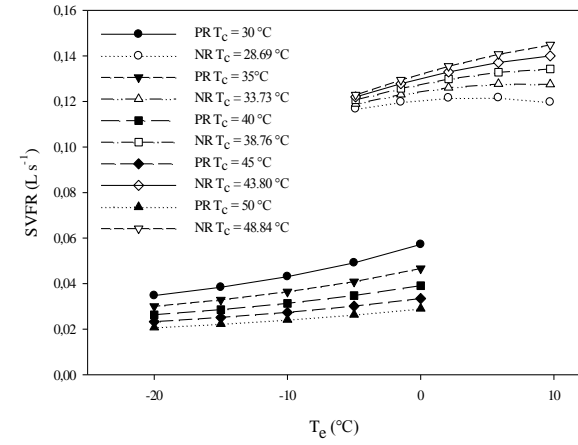


Figure 4.13 Charts of R436a vs R436a/Al₂O₃ for 5 °C of superheating/subcooling case

47

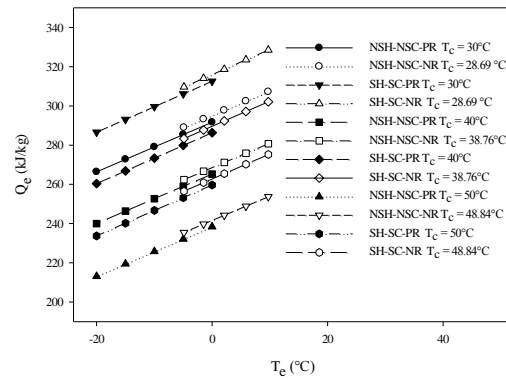
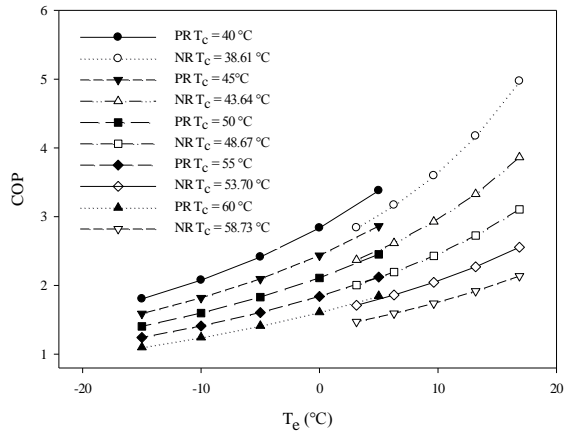
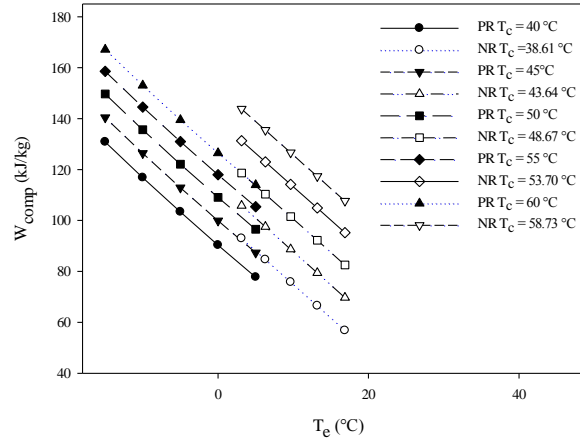


Figure 4.14 Chart of R436a and R436a/Al₂O₃ for non-superheating/subcooling vs. 5 °C of superheating/subcooling case

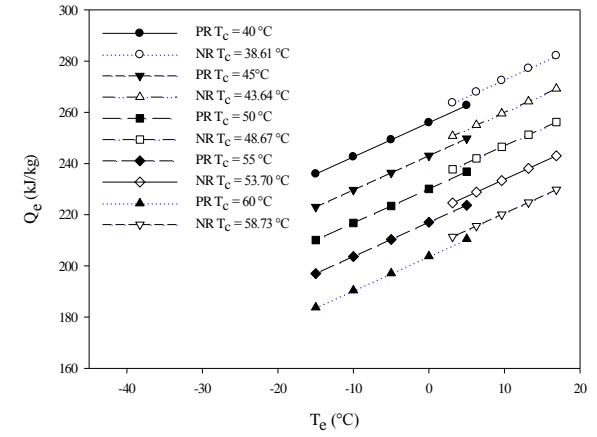
a) T_e vs. COP



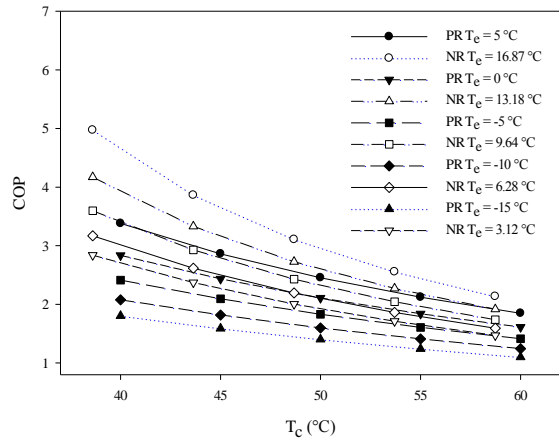
b) T_e vs. W_{comp}



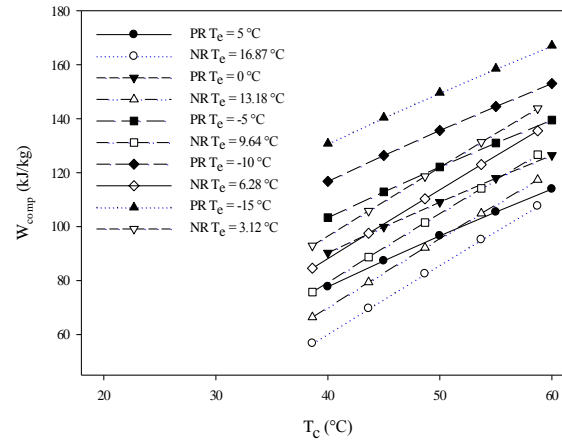
c) T_e vs. Q_e



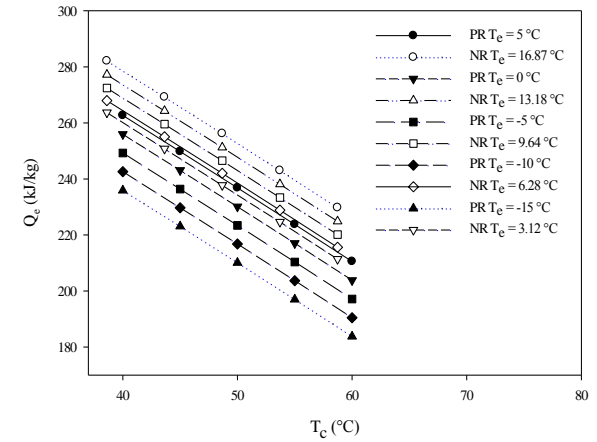
d) T_c vs. COP



e) T_c vs. W_{comp}



f) T_c vs. Q_e



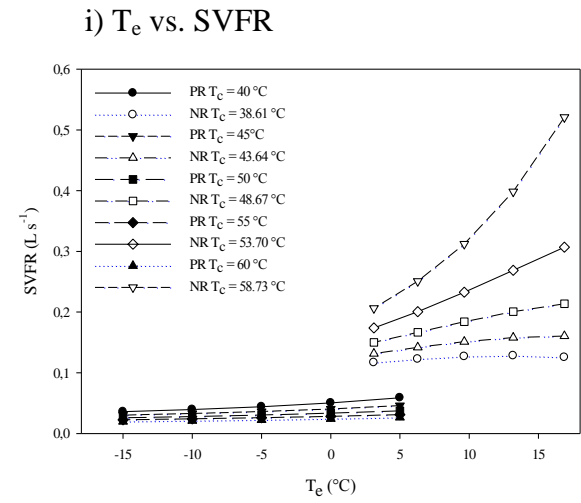
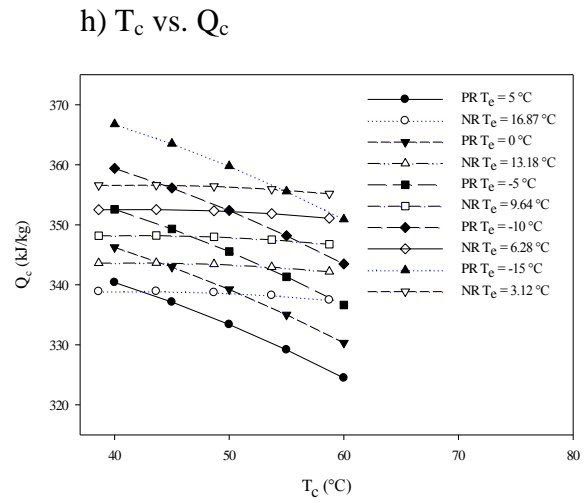
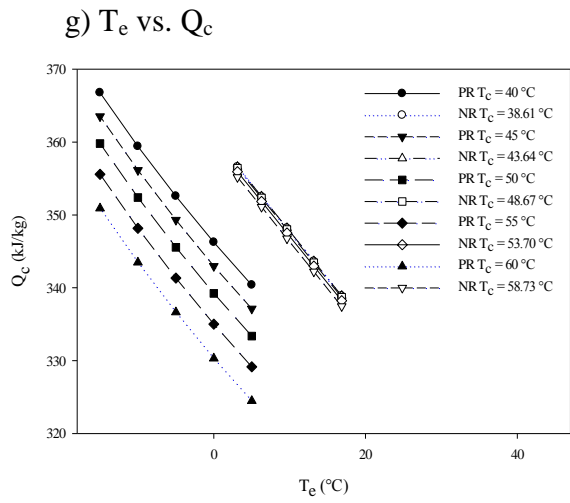
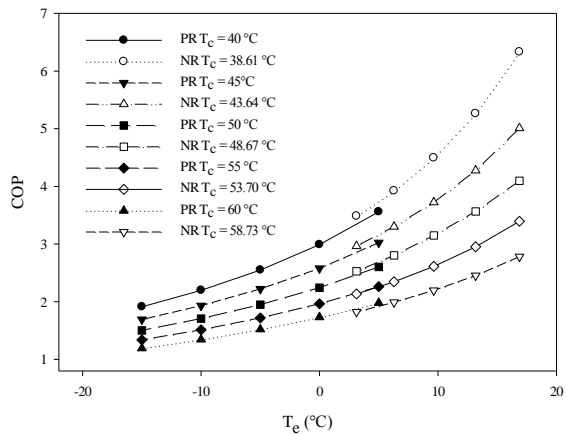
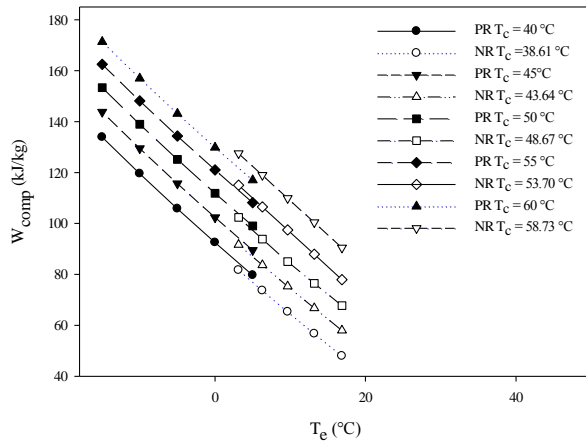


Figure 4.15 Charts of R600a vs R600a/Al₂O₃ for non-superheating/subcooling case

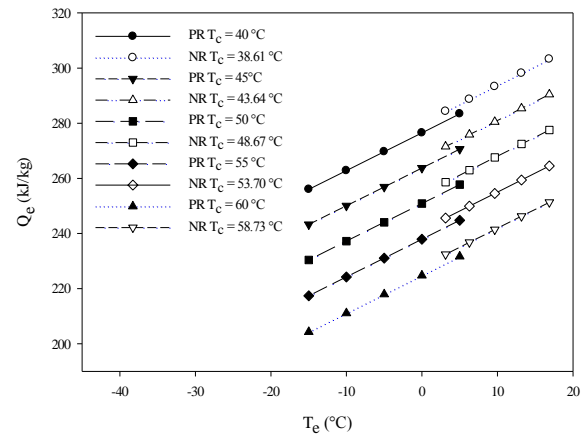
a) T_e vs. COP



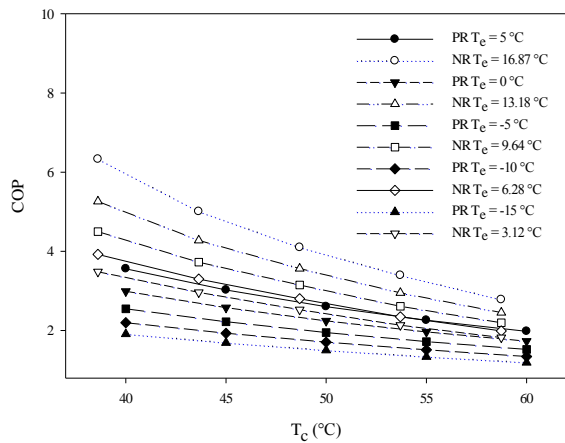
b) T_e vs. W_{comp}



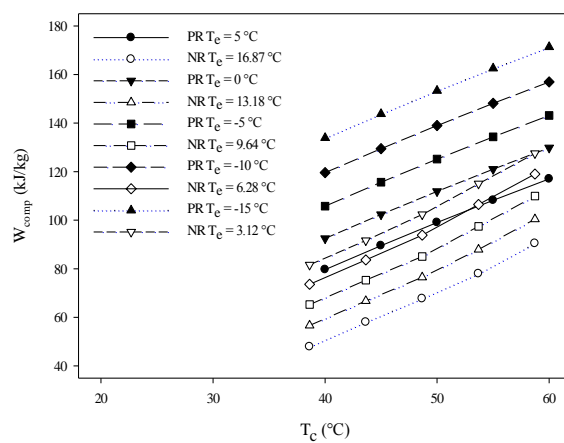
c) T_e vs. Q_e



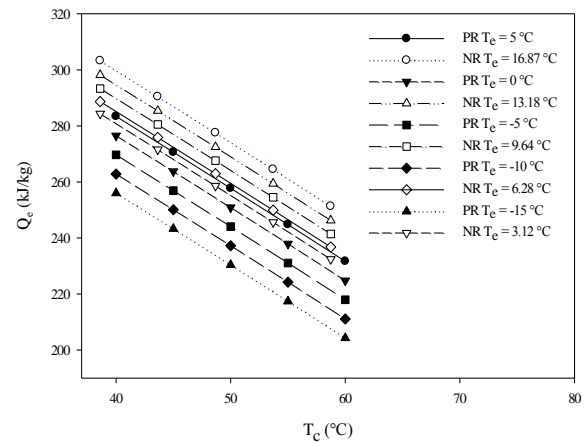
d) T_c vs. COP



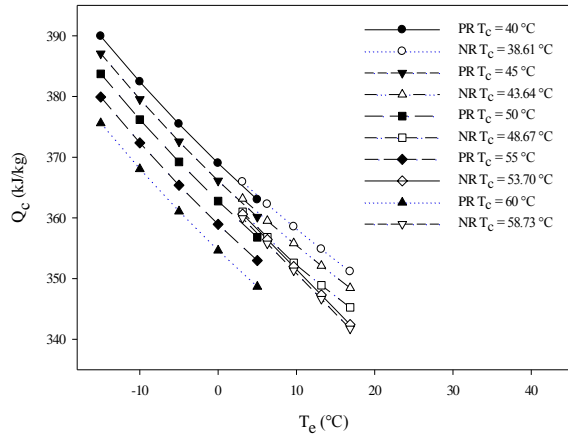
e) T_c vs. W_{comp}



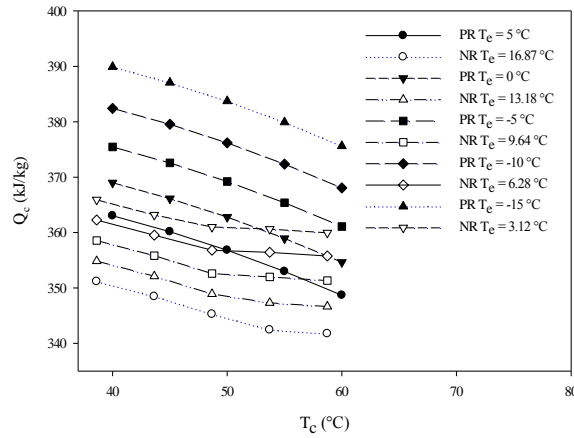
f) T_c vs. Q_e



g) T_e vs. Q_c



h) T_c vs. Q_c



i) T_e vs. SVFR

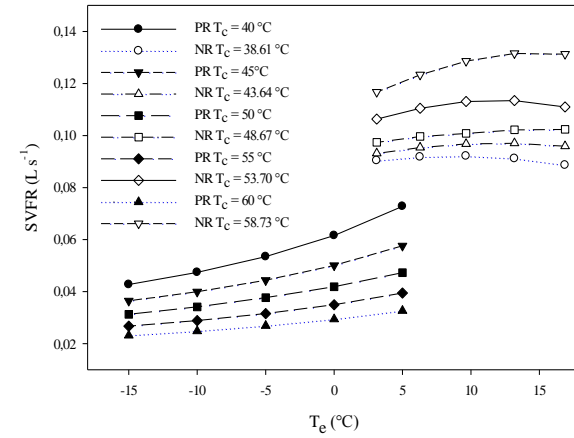


Figure 4.16 Charts of R600a vs R600a/Al₂O₃ for 5 °C of superheating/subcooling case

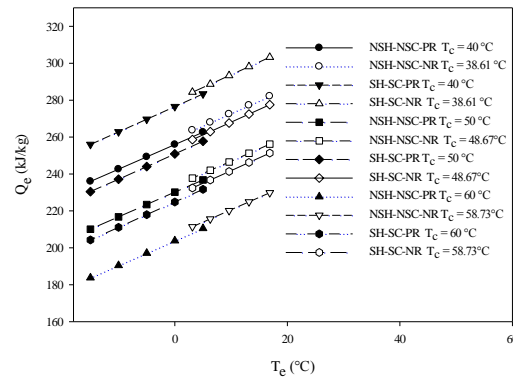
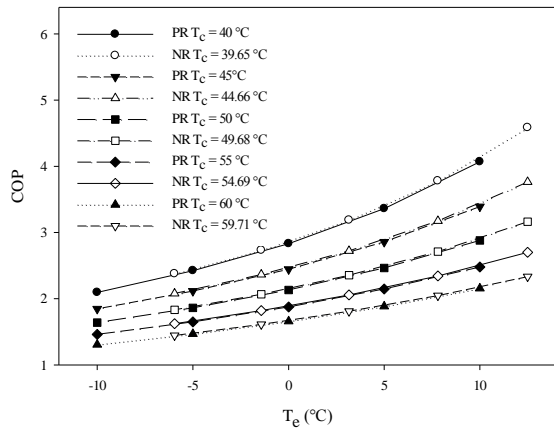
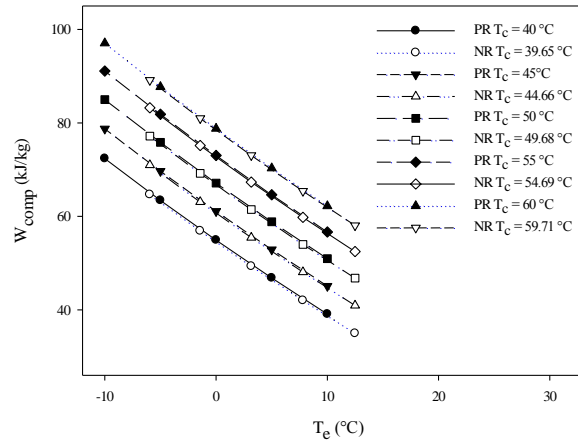


Figure 4.17 Chart of R600a and R600a/Al₂O₃ for non-superheating/subcooling vs. 5 °C of superheating/subcooling case

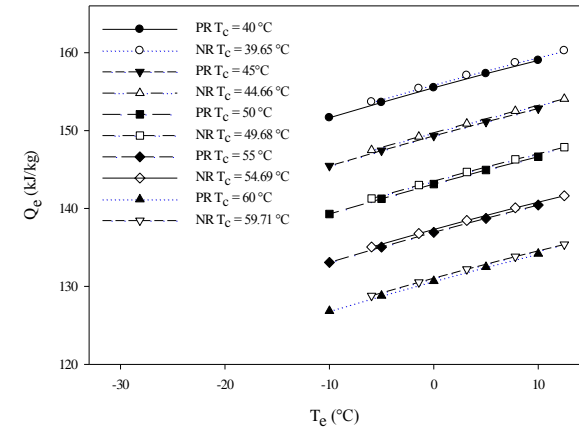
a) T_e vs. COP



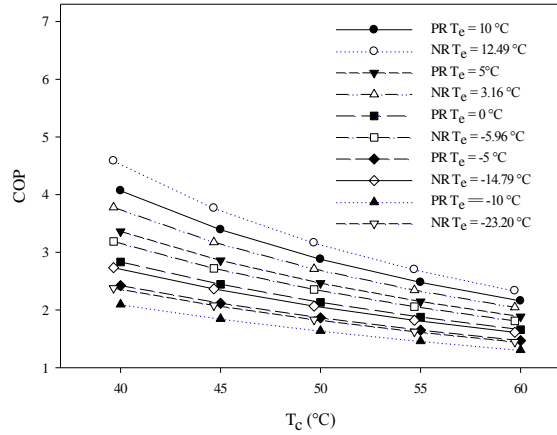
b) T_e vs. W_{comp}



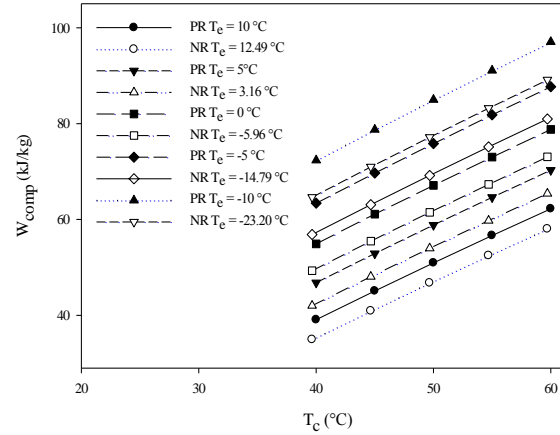
c) T_e vs. Q_e



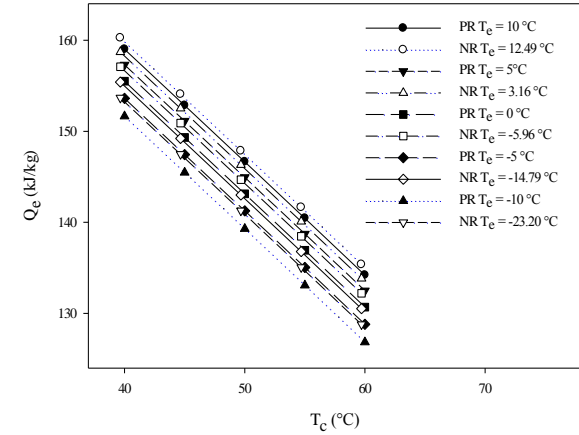
d) T_c vs. COP



e) T_c vs. W_{comp}



f) T_c vs. Q_e



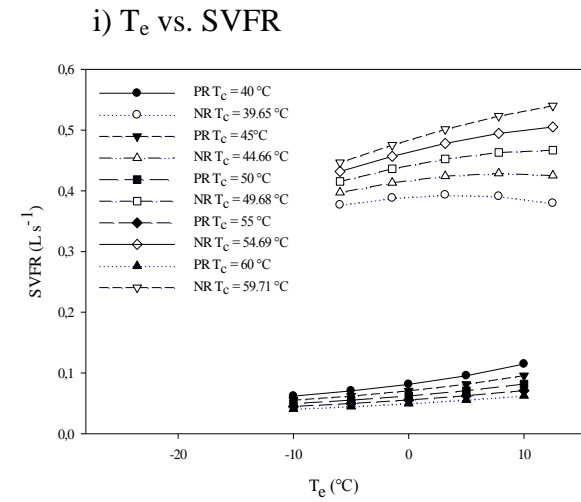
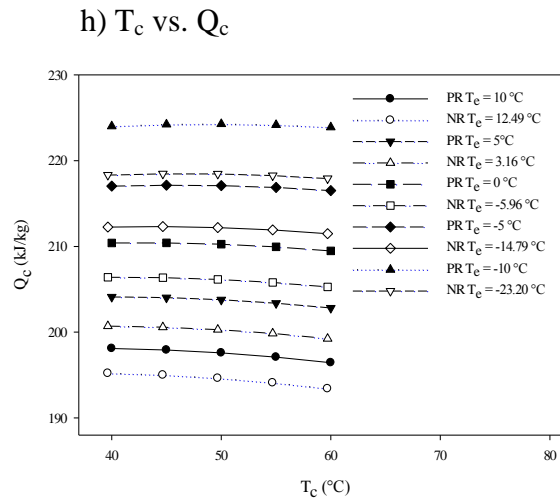
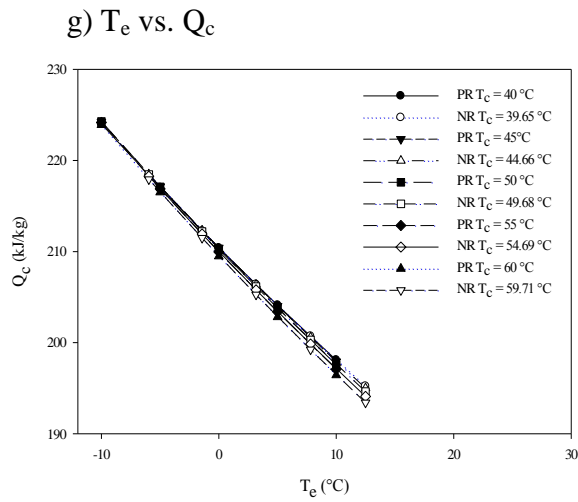
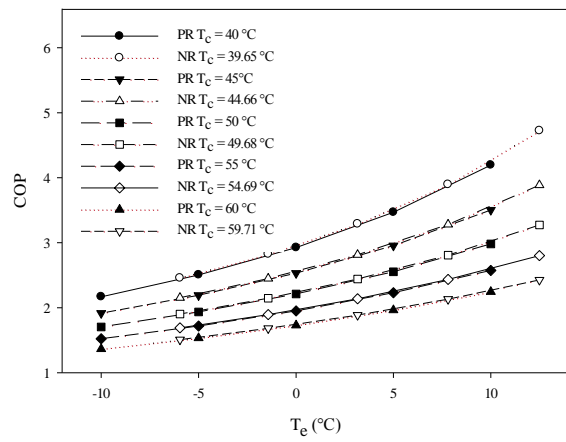
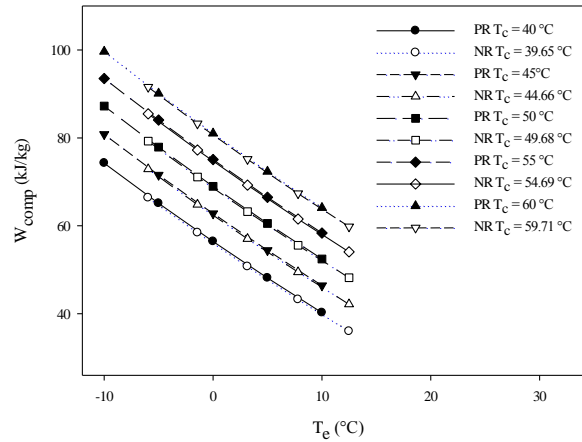


Figure 4.18 Charts of R22 vs R22/Al₂O₃ for non-superheating/subcooling case

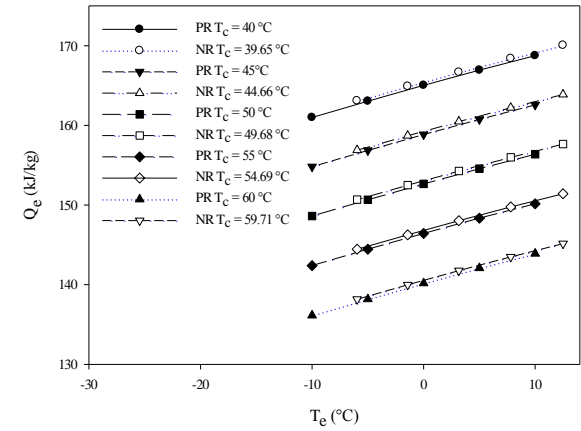
a) T_e vs. COP



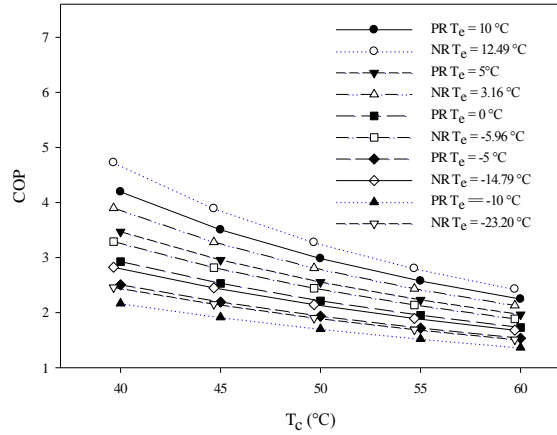
b) T_e vs. W_{comp}



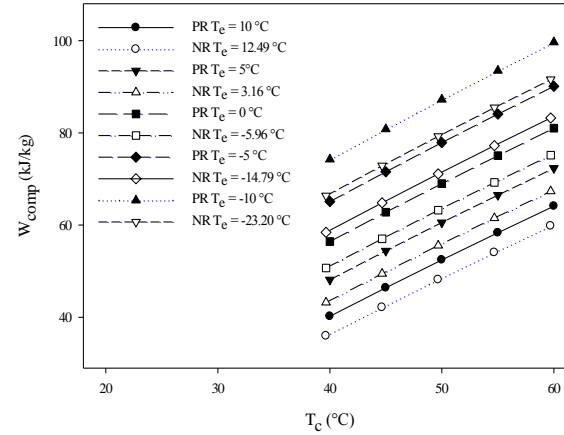
c) T_e vs. Q_e



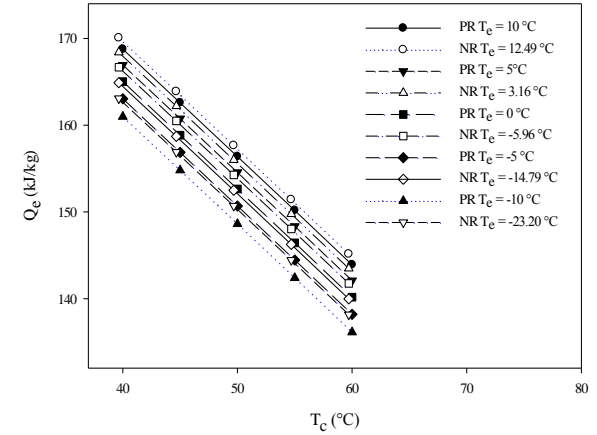
d) T_c vs. COP



e) T_c vs. W_{comp}



f) T_c vs. Q_e



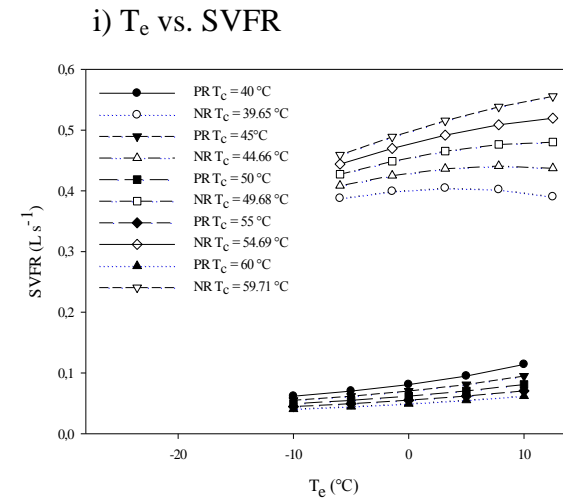
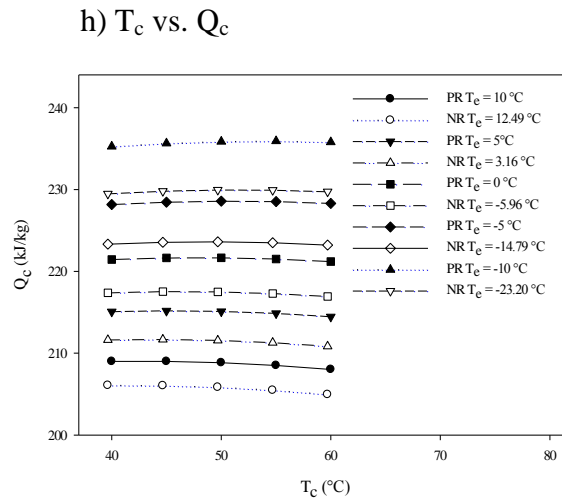
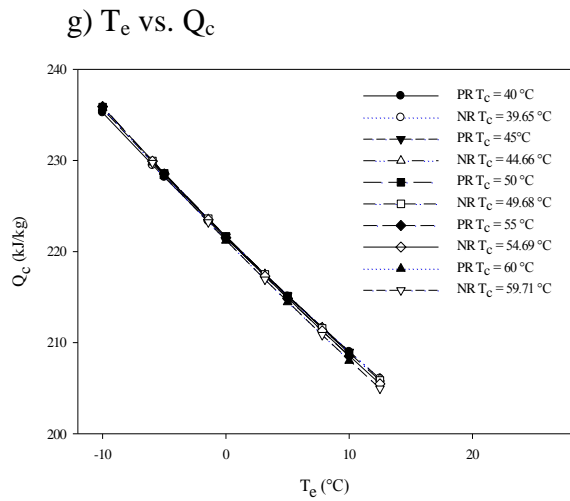


Figure 4.19 Charts of R22 vs R22/Al₂O₃ for 5 °C of superheating/subcooling case

55

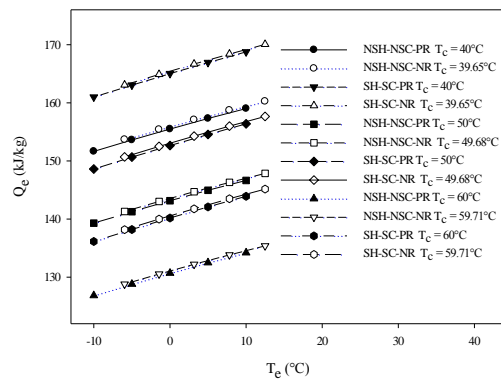
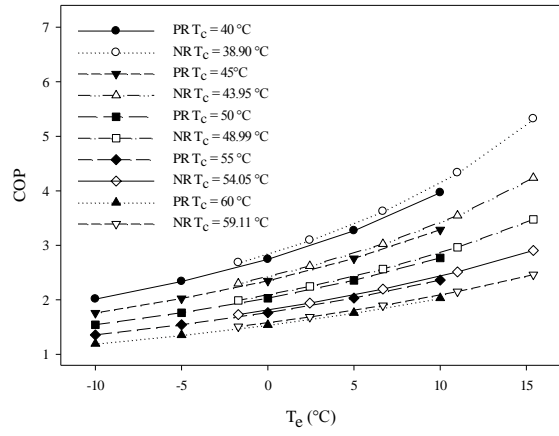
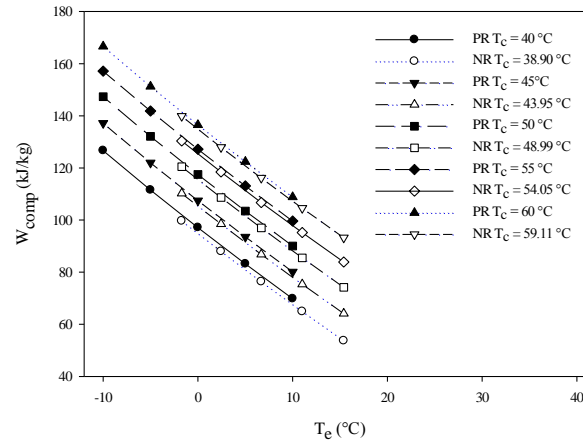


Figure 4.20 Chart of R22 and R22/Al₂O₃ for non-superheating/subcooling vs. 5 °C of superheating/subcooling case

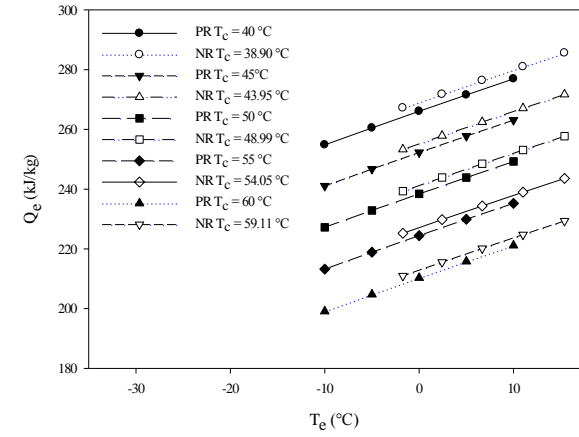
a) T_e vs. COP



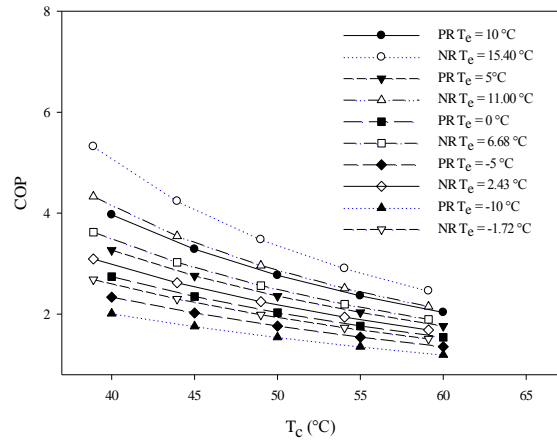
b) T_e vs. W_{comp}



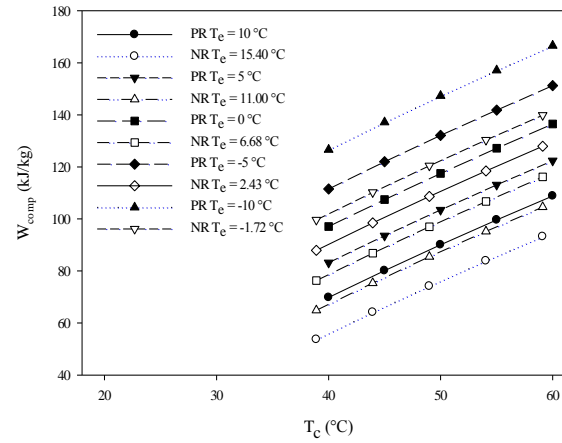
c) T_e vs. Q_e



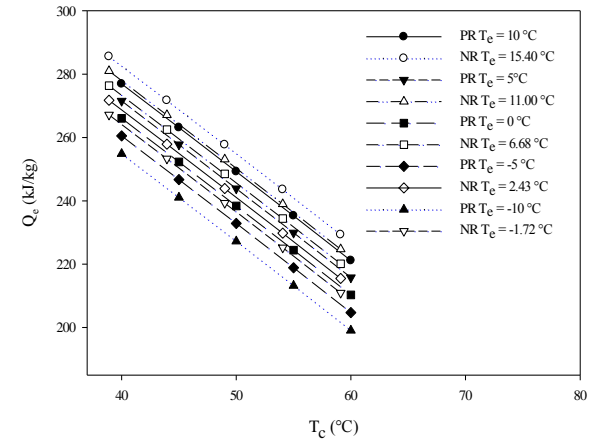
d) T_c vs. COP



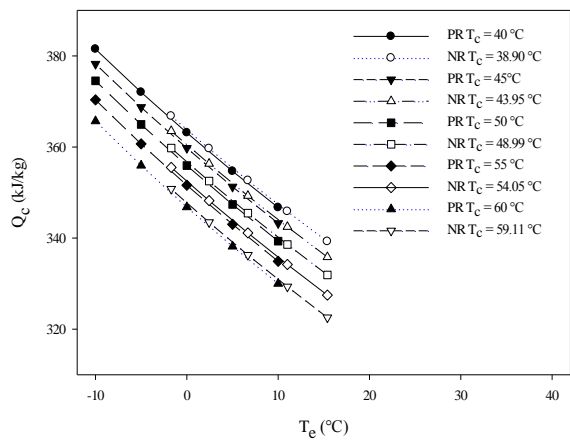
e) T_c vs. W_{comp}



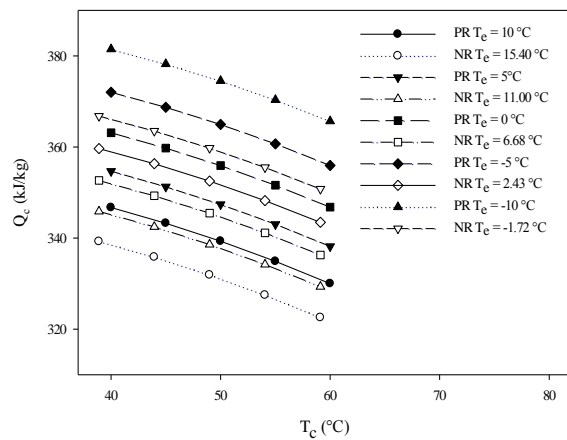
f) T_c vs. Q_e



g) T_e vs. Q_c



h) T_c vs. Q_c



i) T_e vs. SVFR

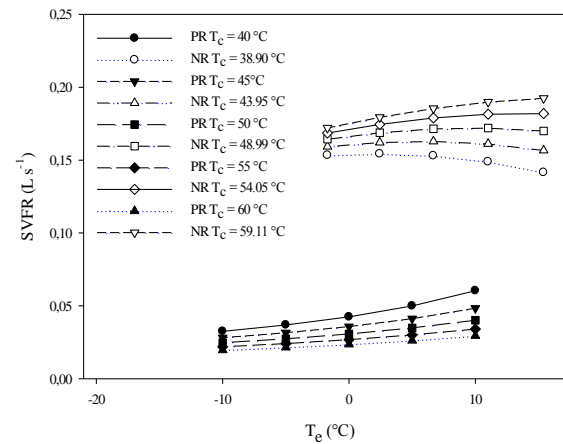
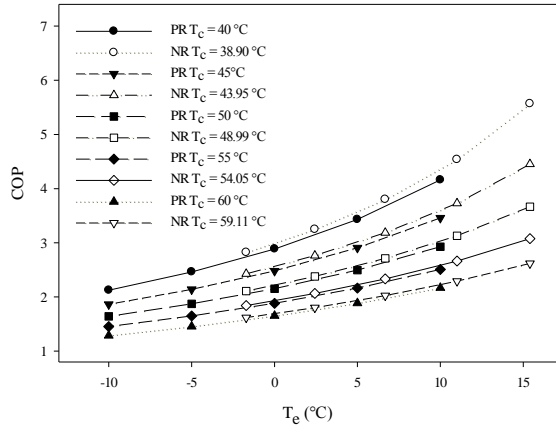
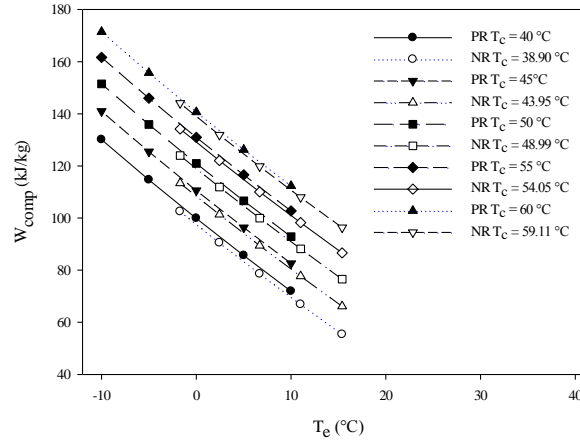


Figure 4.21 Charts of R290 vs R290/Al₂O₃ for non-superheating/subcooling case

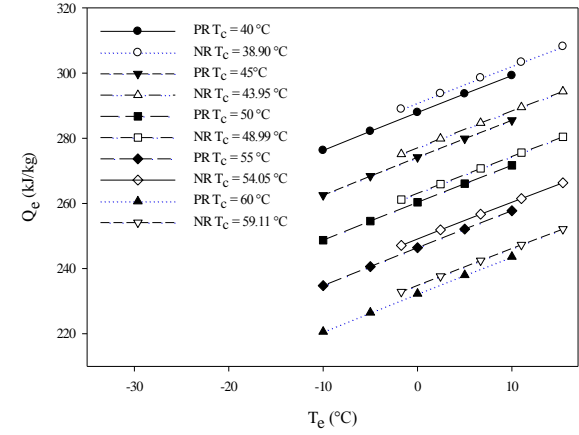
a) T_e vs. COP



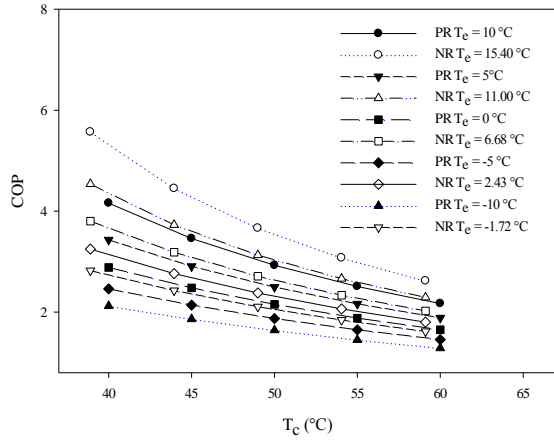
b) T_e vs. W_{comp}



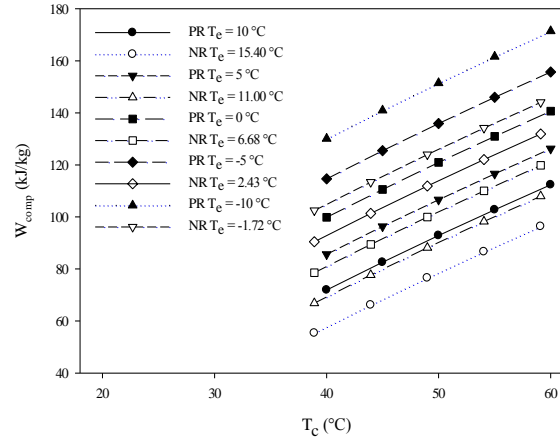
c) T_e vs. Q_e



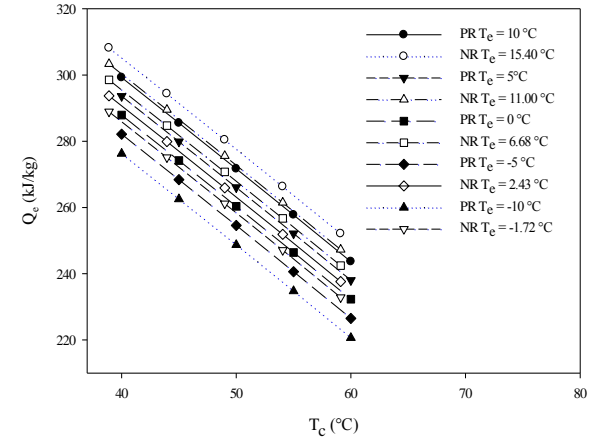
d) T_c vs. COP



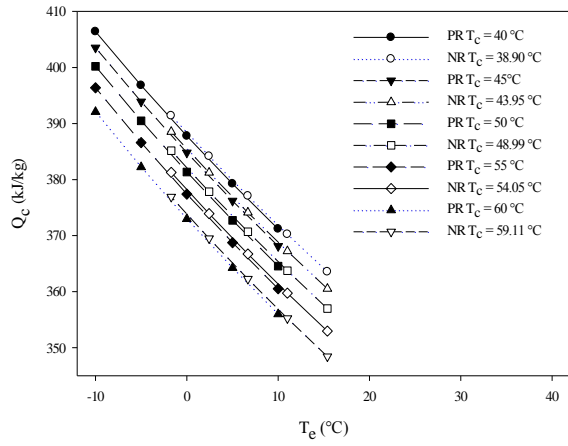
e) T_c vs. W_{comp}



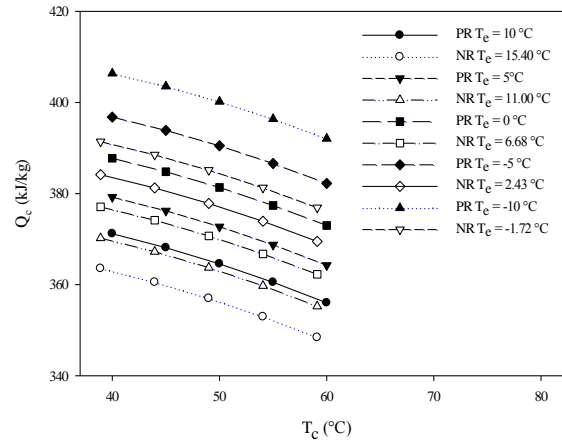
f) T_c vs. Q_e



g) T_e vs. Q_c



h) T_c vs. Q_c



i) T_e vs. SVFR

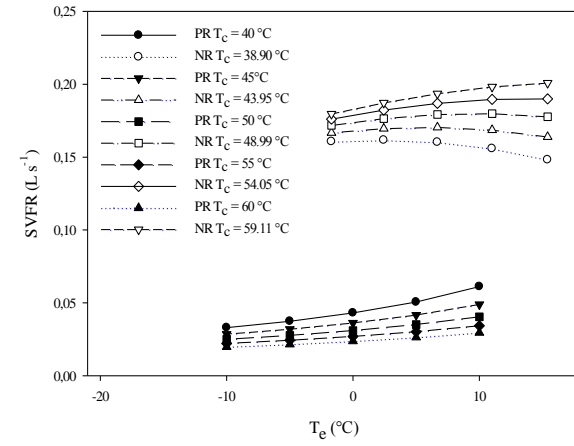


Figure 4.22 Charts of R290 vs R290/Al₂O₃ for 5 °C of superheating/subcooling case

59

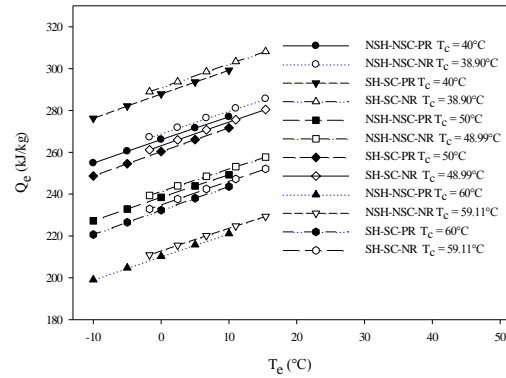
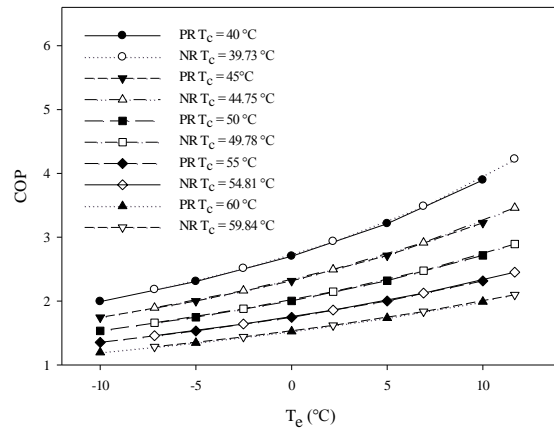
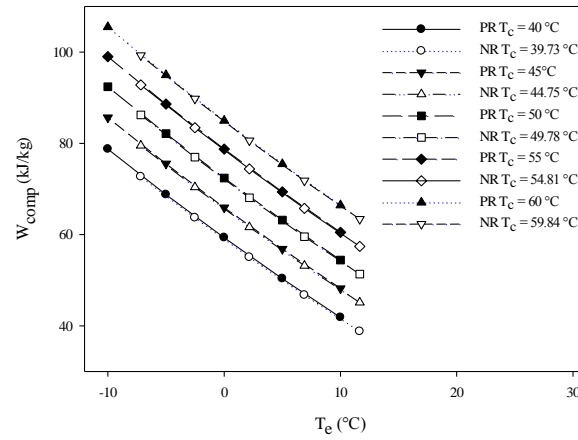
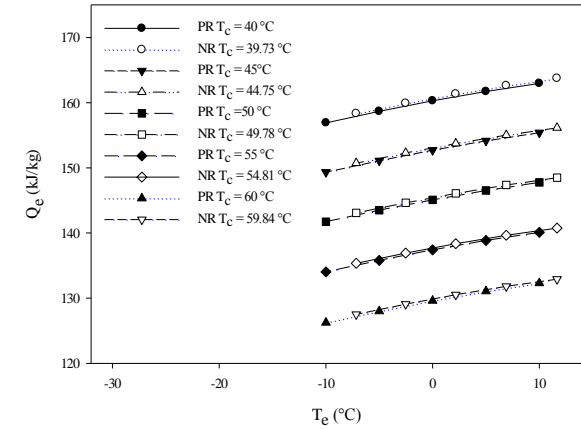
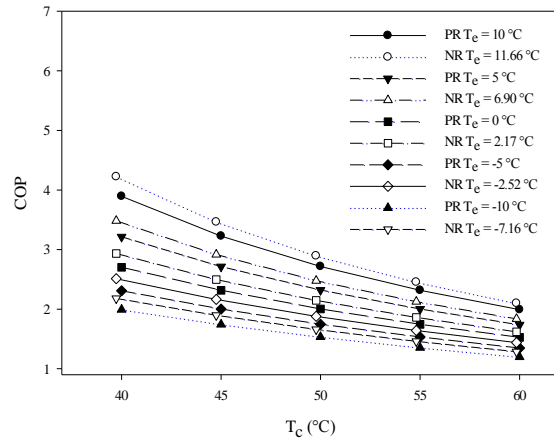
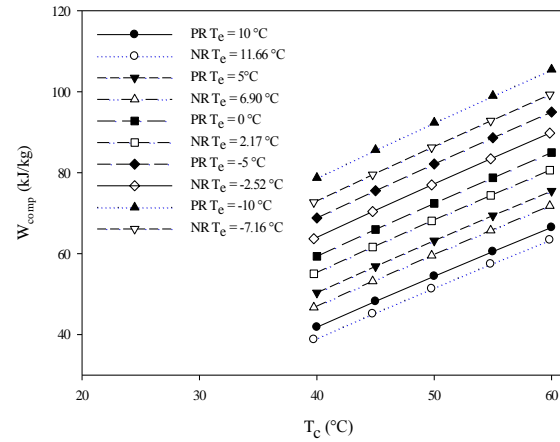
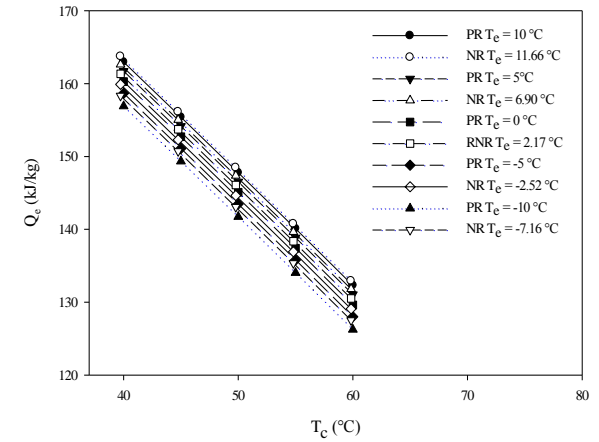


Figure 4.23 Chart of R290 and R290/Al₂O₃ for non-superheating/subcooling vs. 5 °C of superheating/subcooling case

a) T_e vs. COPb) T_e vs. W_{comp} c) T_e vs. Q_e d) T_c vs. COPe) T_c vs. W_{comp} f) T_c vs. Q_e 

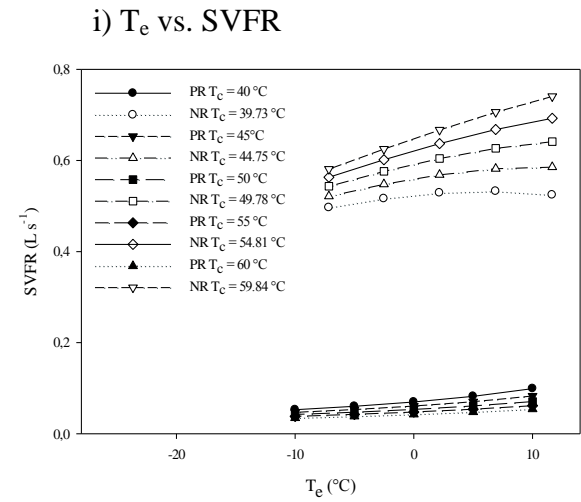
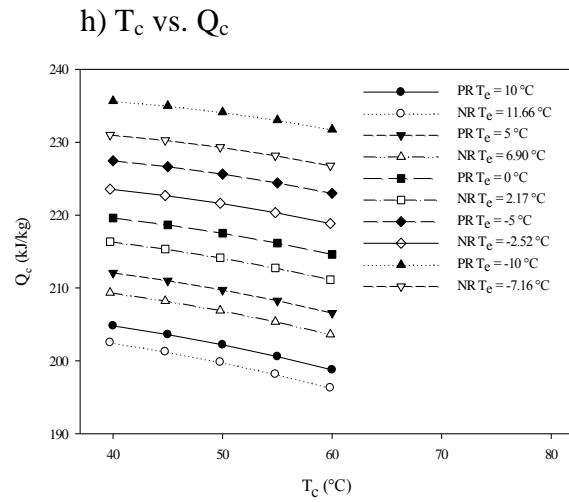
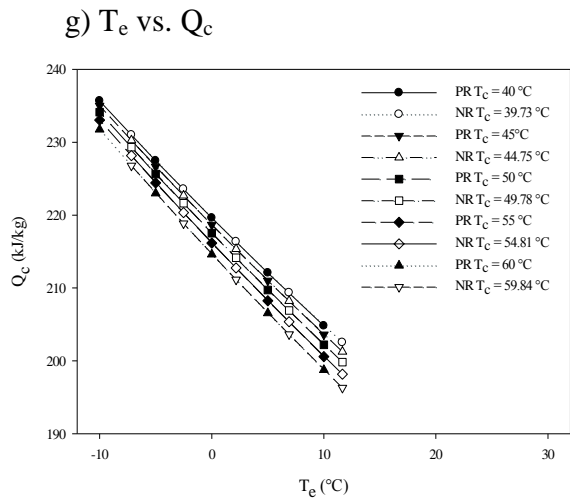
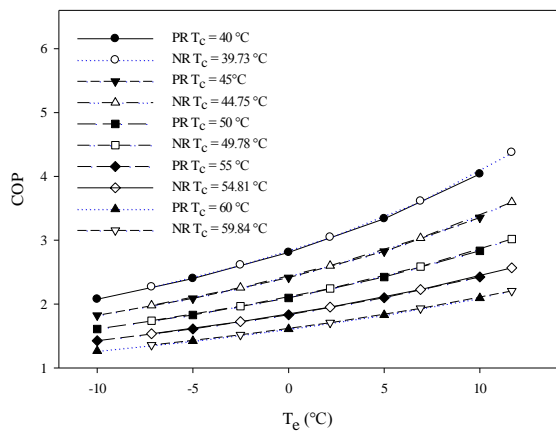
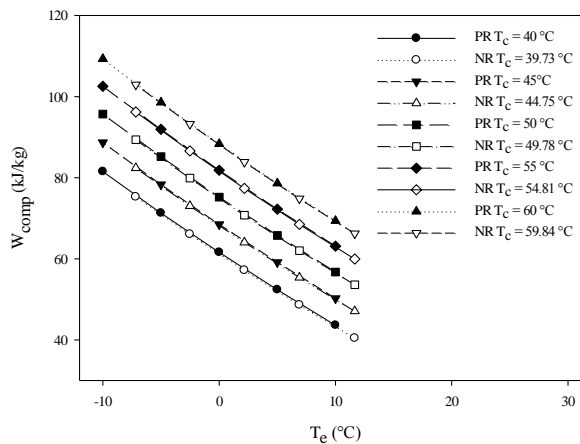


Figure 4.24 Charts of R410a vs R410a/Al₂O₃ for non-superheating/subcooling case

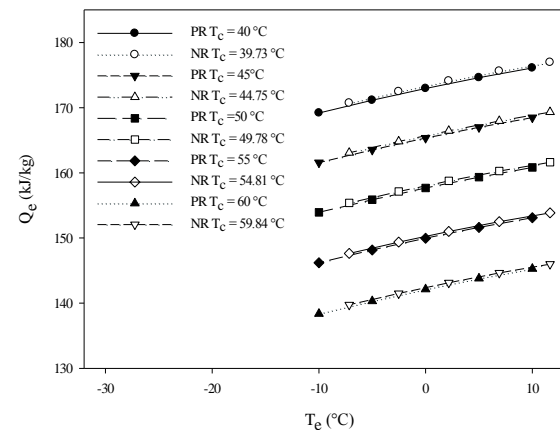
a) T_e vs. COP



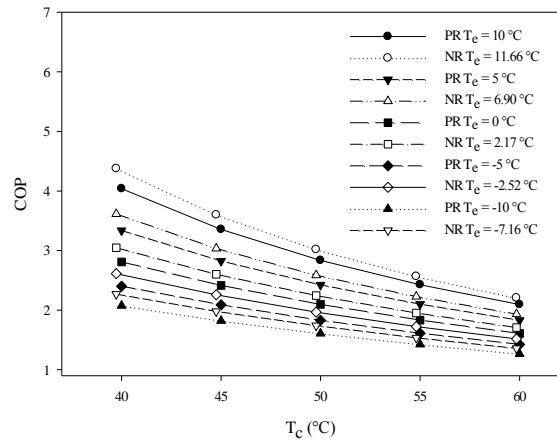
b) T_e vs. W_{comp}



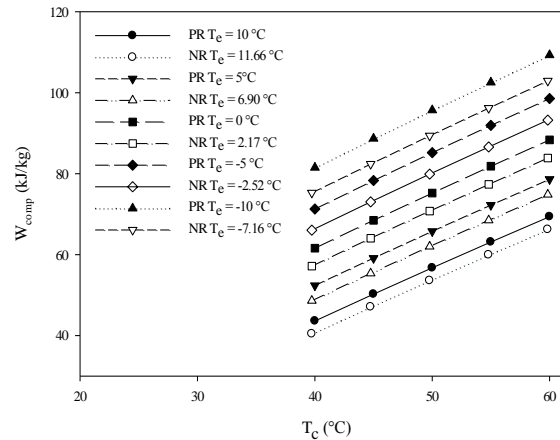
c) T_e vs. Q_e



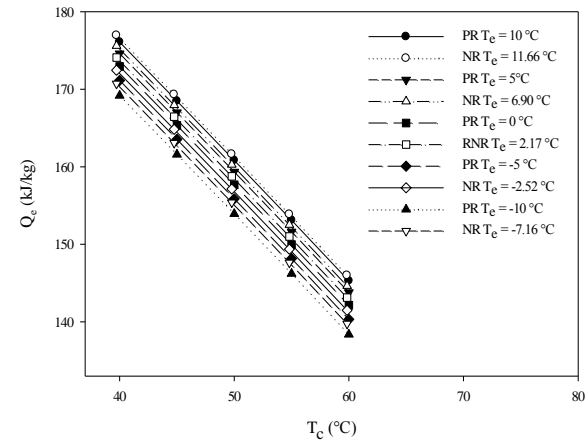
d) T_c vs. COP



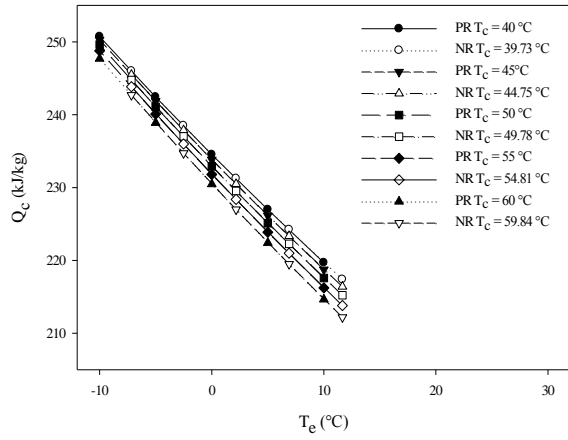
e) T_c vs. W_{comp}



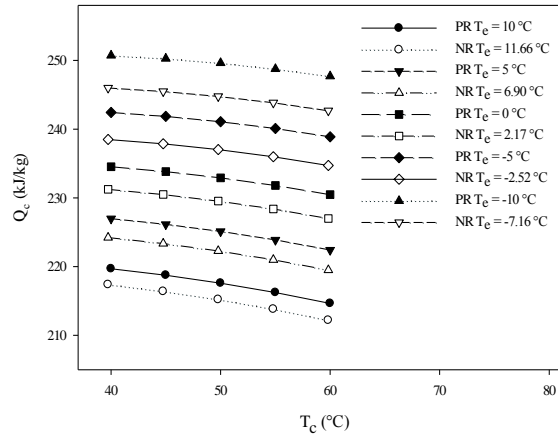
f) T_c vs. Q_e



g) T_e vs. Q_c



h) T_c vs. Q_c



i) T_e vs. SVFR

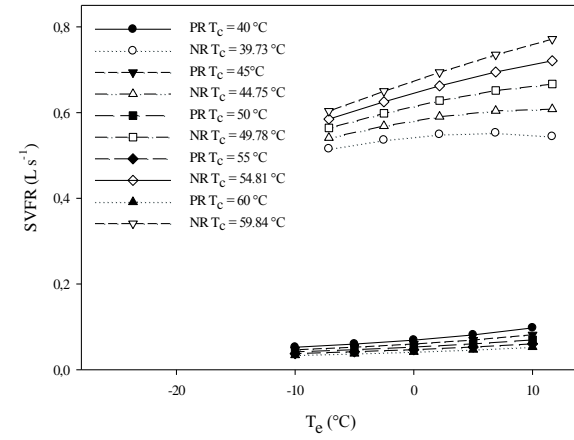


Figure 4.25 Charts of R410a vs R410a/Al₂O₃ for 5 °C of superheating/subcooling case

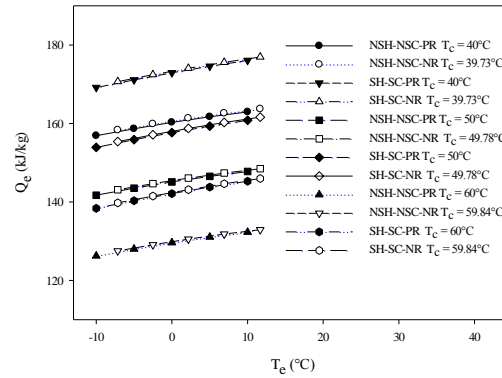
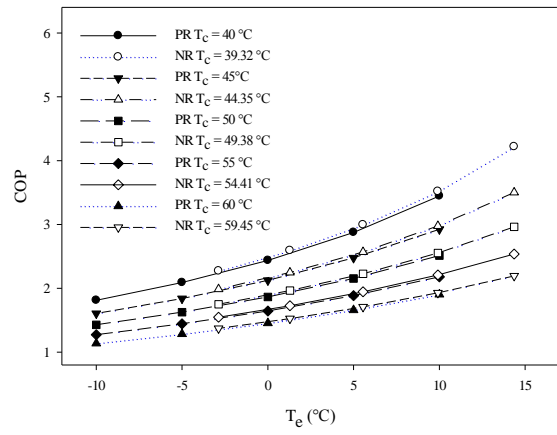
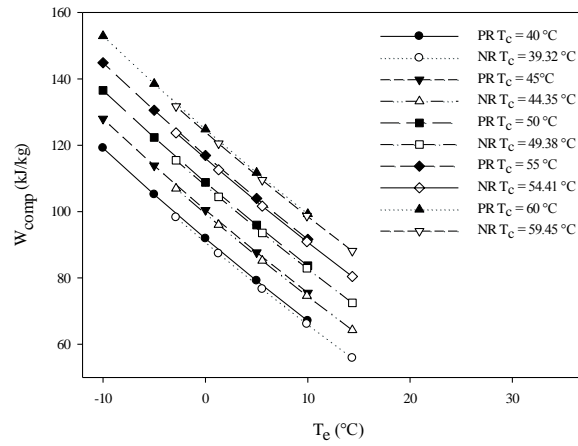


Figure 4.26 Chart of R410a and R410a/Al₂O₃ for non-superheating/subcooling vs. 5 °C of superheating/subcooling case

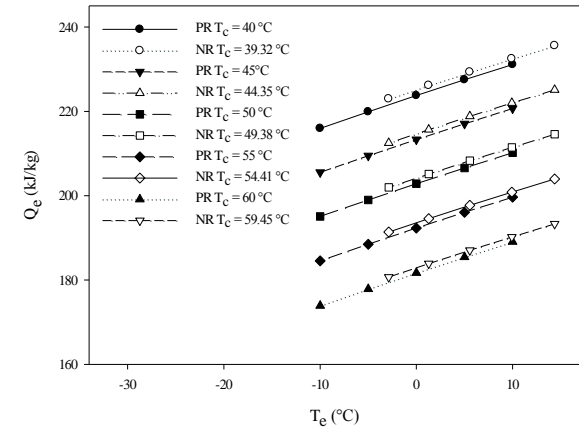
a) T_e vs. COP



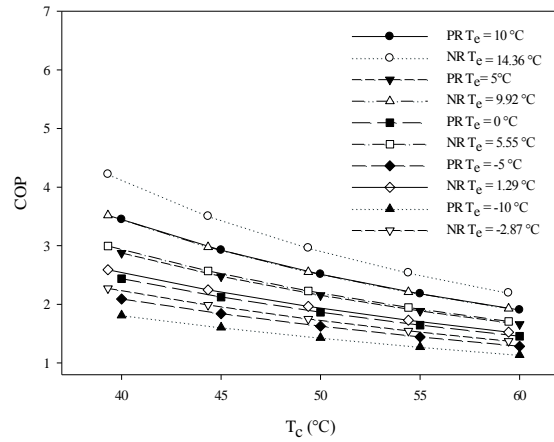
b) T_e vs. W_{comp}



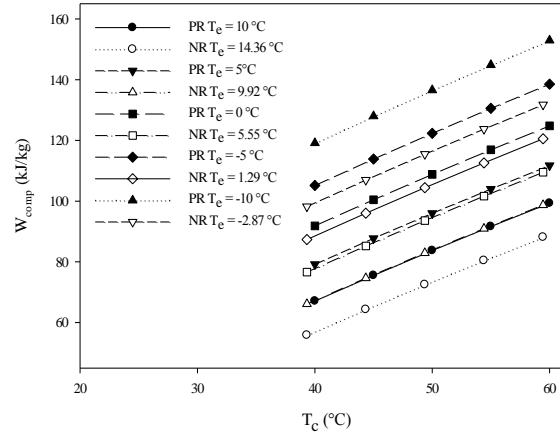
c) T_e vs. Q_e



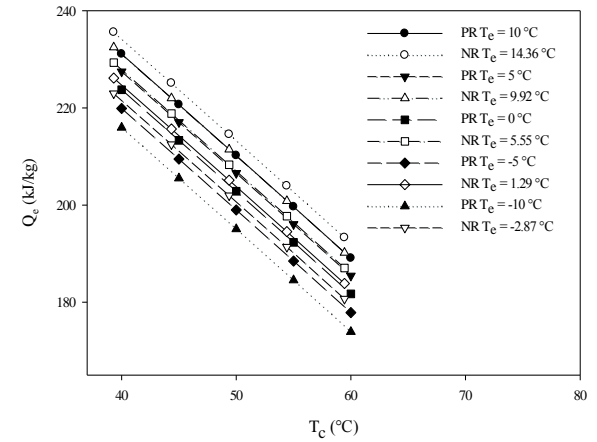
d) T_c vs. COP



e) T_c vs. W_{comp}



f) T_c vs. Q_e



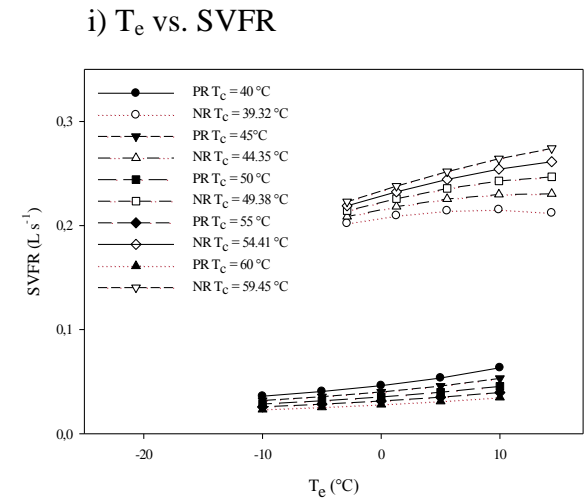
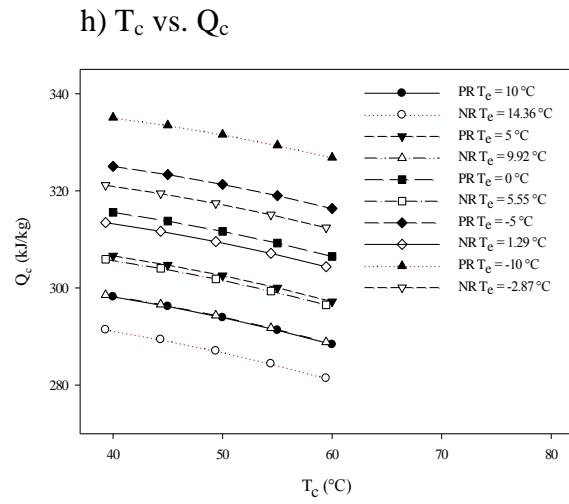
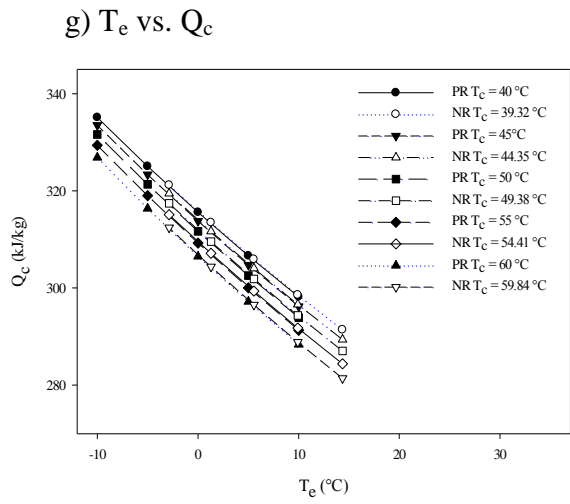
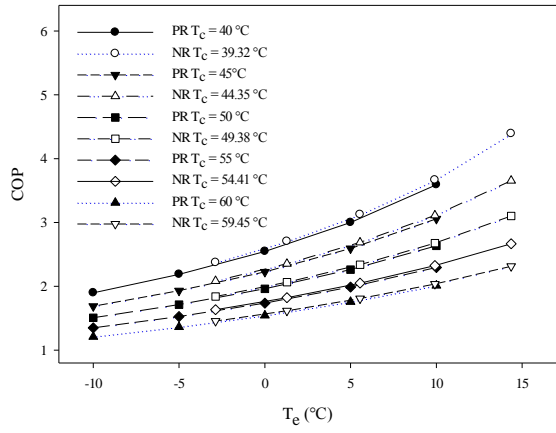
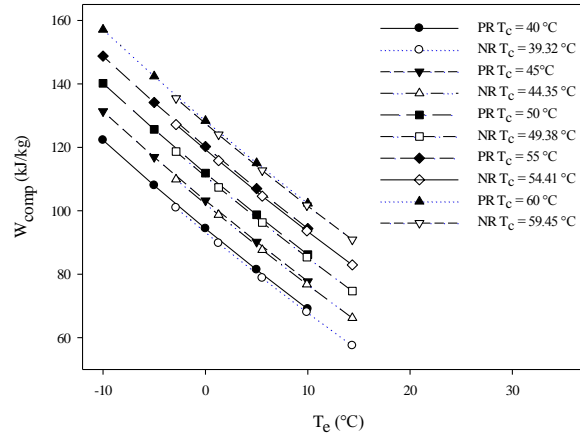


Figure 4.27 Charts of R431a vs R431a/Al₂O₃ for non-superheating/subcooling case

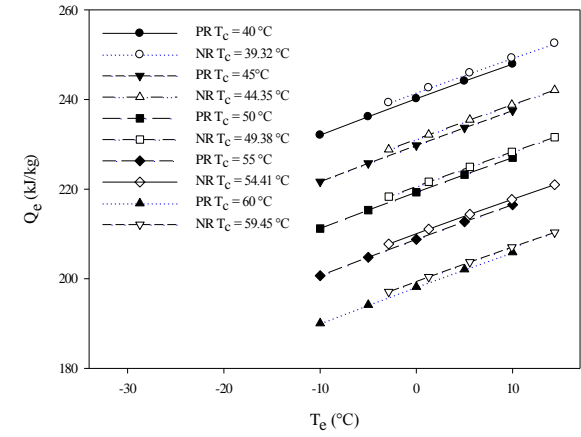
a) T_e vs. COP



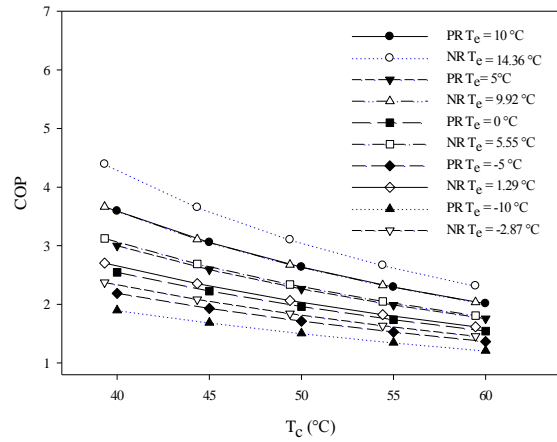
b) T_e vs. W_{comp}



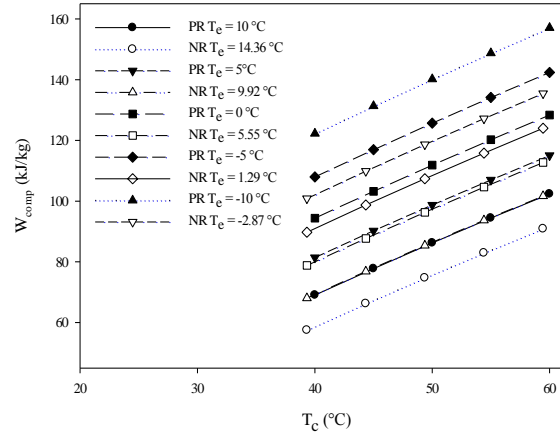
c) T_e vs. Q_e



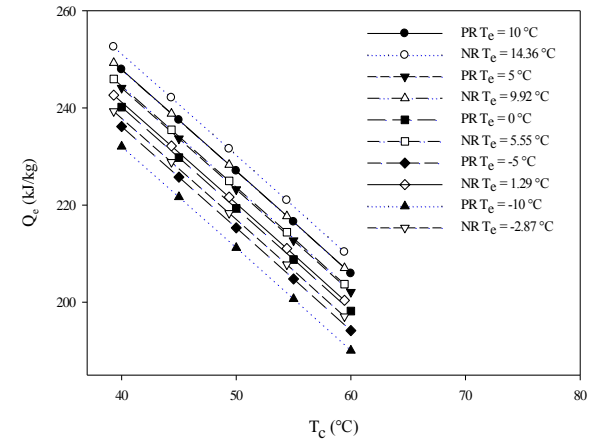
d) T_c vs. COP



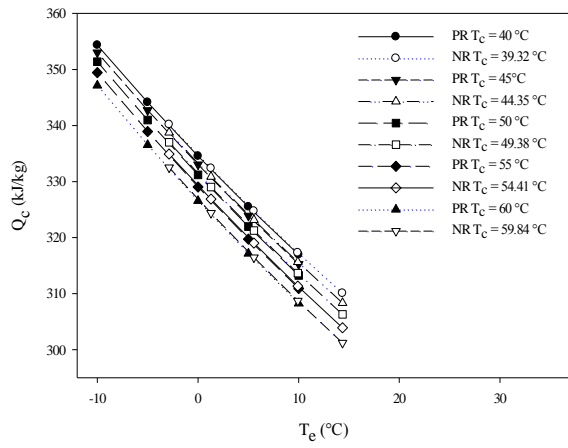
e) T_c vs. W_{comp}



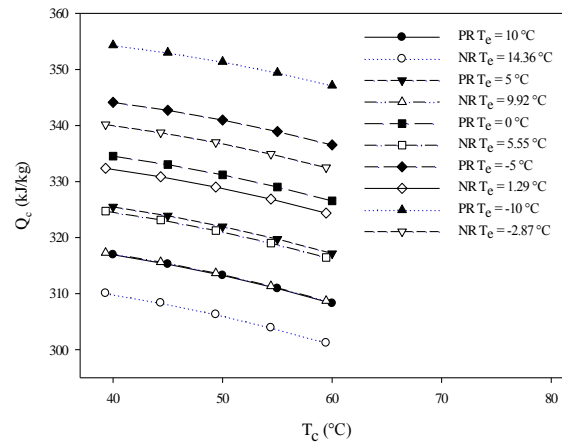
f) T_c vs. Q_e



g) T_e vs. Q_c



h) T_c vs. Q_c



i) T_e vs. SVFR

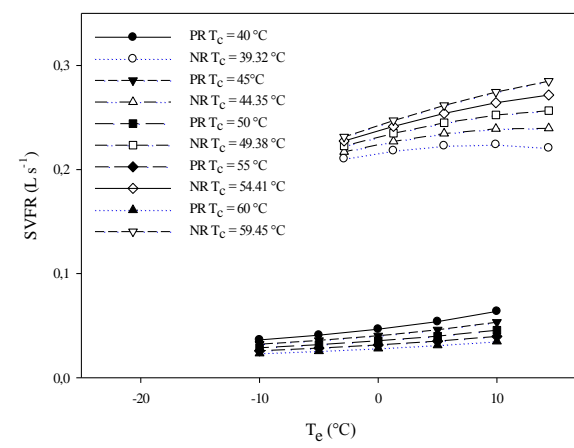


Figure 4.28 Charts of R431a vs R431a/Al₂O₃ for 5 °C of superheating/subcooling case

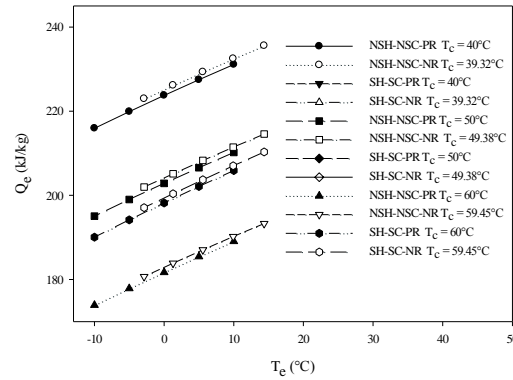
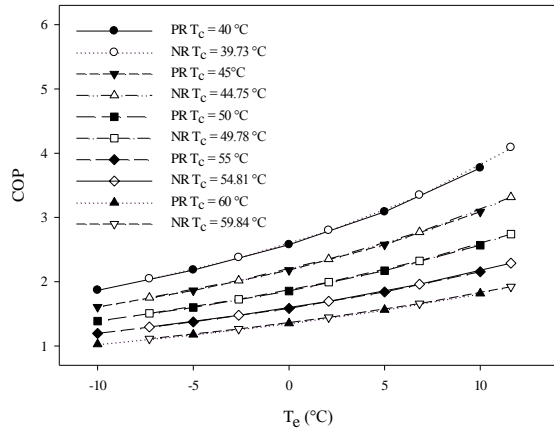
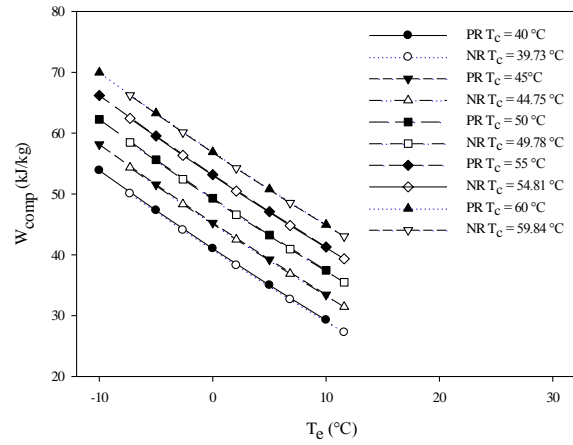


Figure 4.29 Chart of R431a and R431a/Al₂O₃ for non-superheating/subcooling vs. 5 °C of superheating/subcooling case

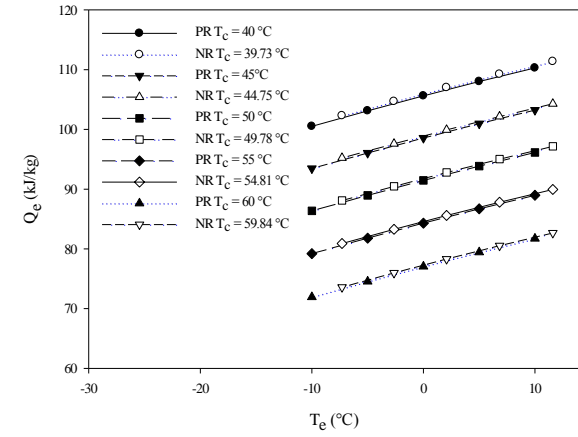
a) T_e vs. COP



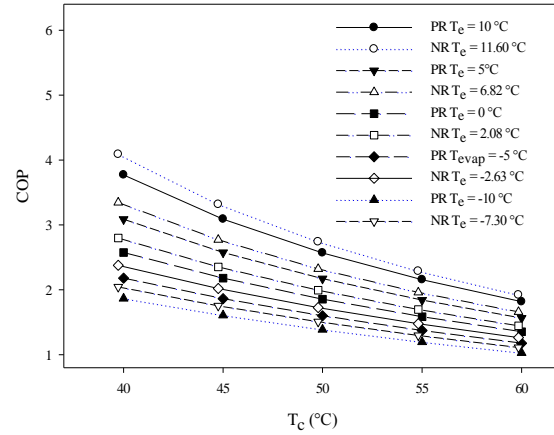
b) T_e vs. W_{comp}



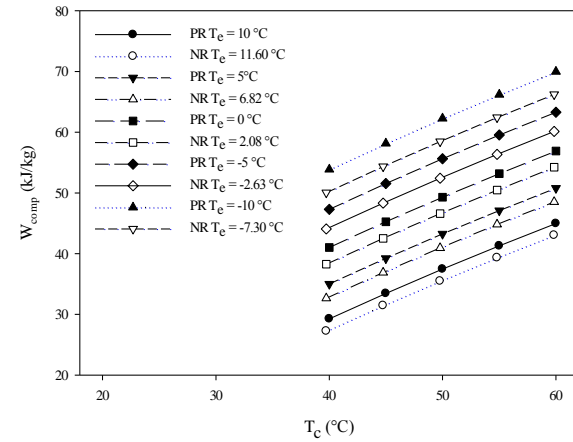
c) T_e vs. Q_e



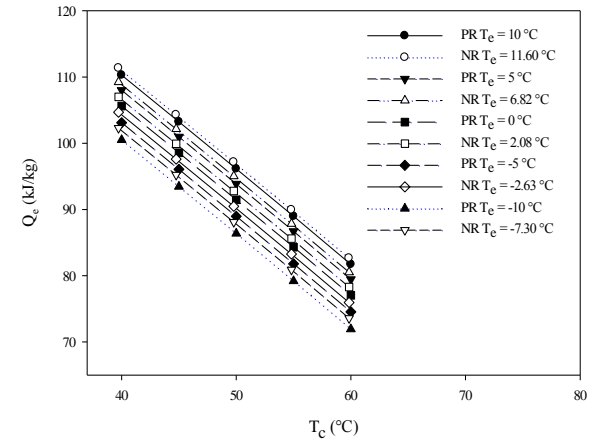
d) T_c vs. COP



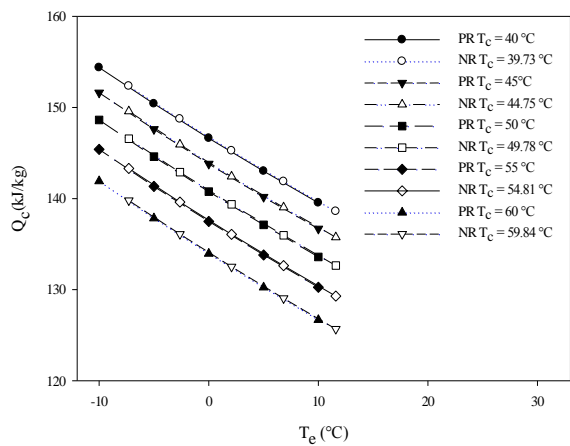
e) T_c vs. W_{comp}



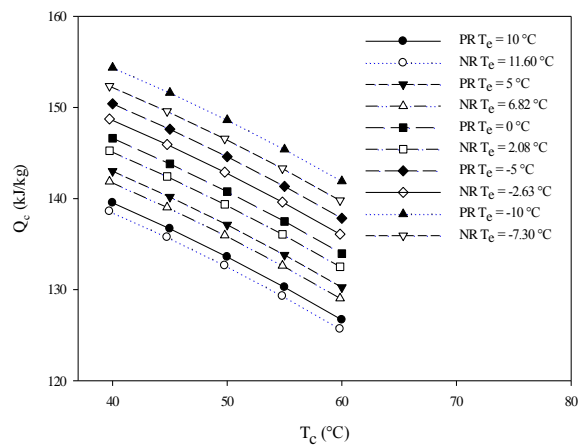
f) T_c vs. Q_e



g) T_e vs. Q_c



h) T_c vs. Q_c



i) T_e vs. SVFR

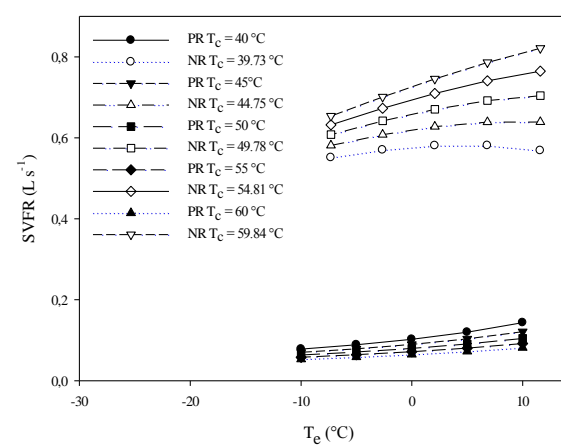
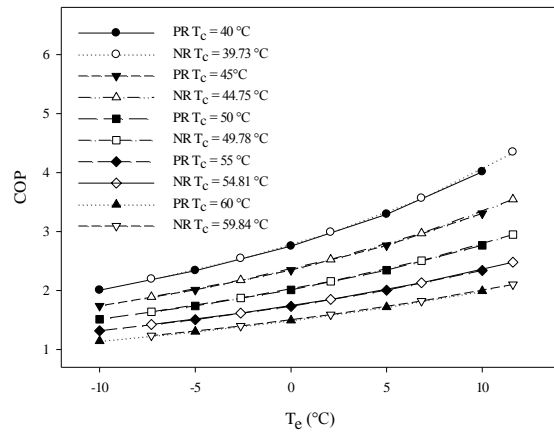
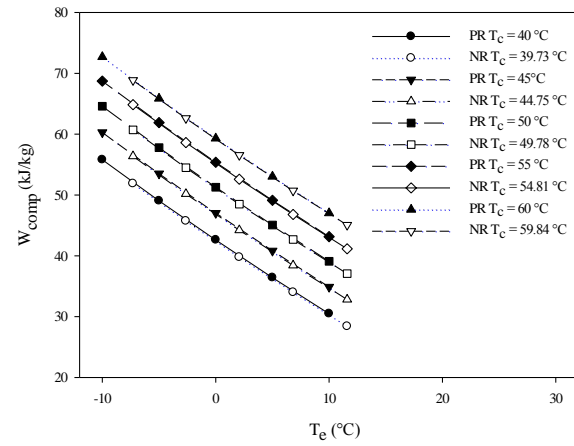
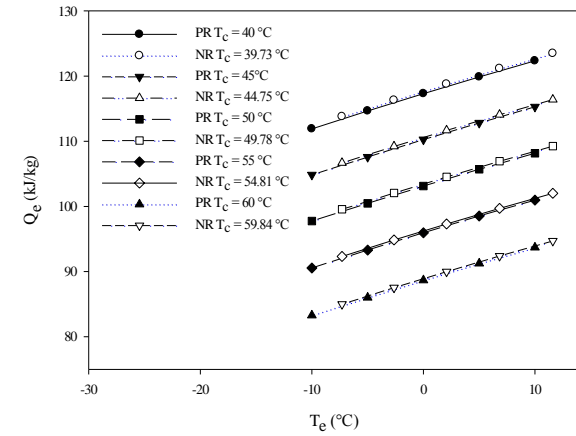
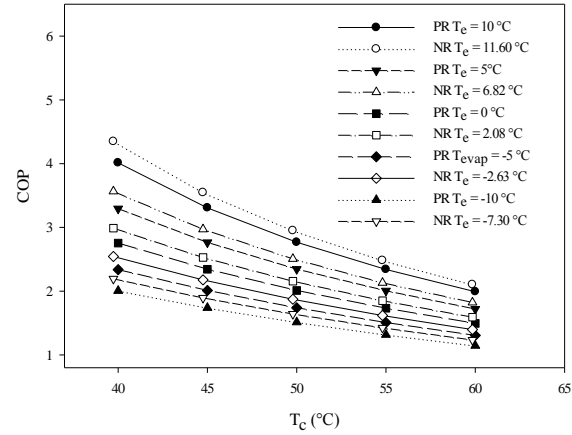
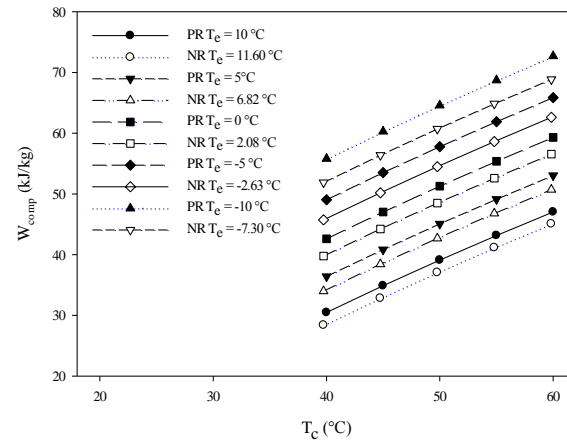
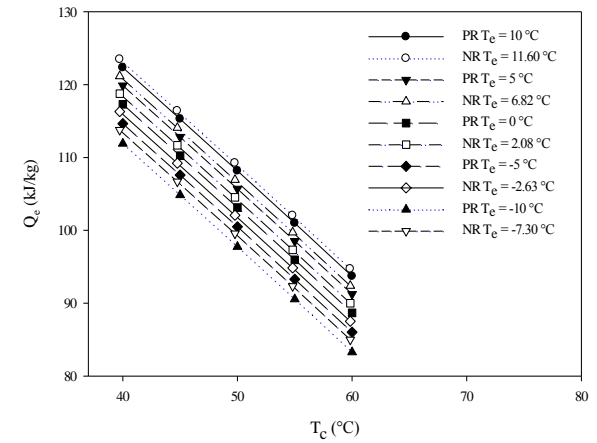
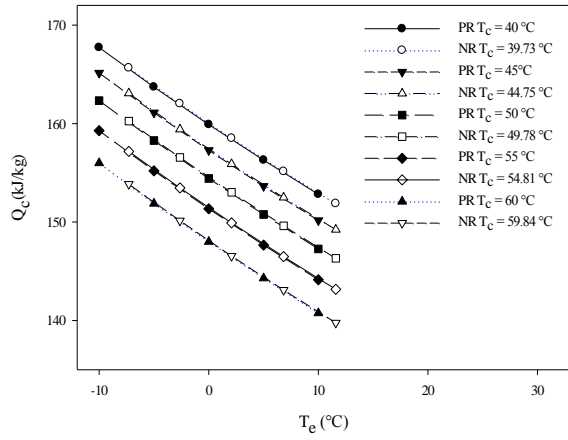


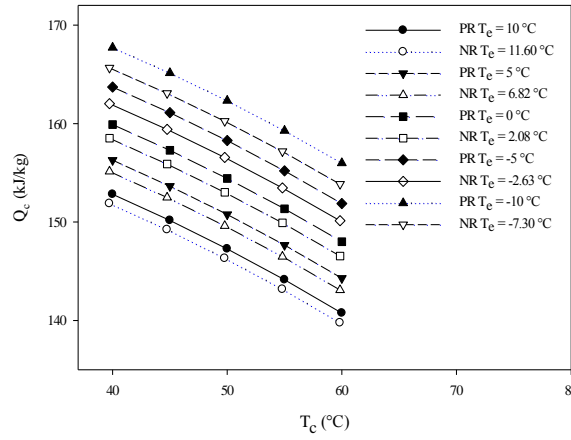
Figure 4.30 Charts of R507a vs R507a/Al₂O₃ for non-superheating/subcooling case

a) T_e vs. COPb) T_e vs. W_{comp} c) T_e vs. Q_e d) T_c vs. COPe) T_c vs. W_{comp} f) T_c vs. Q_e 

g) T_e vs. Q_c



h) T_c vs. Q_c



i) T_e vs. SVFR

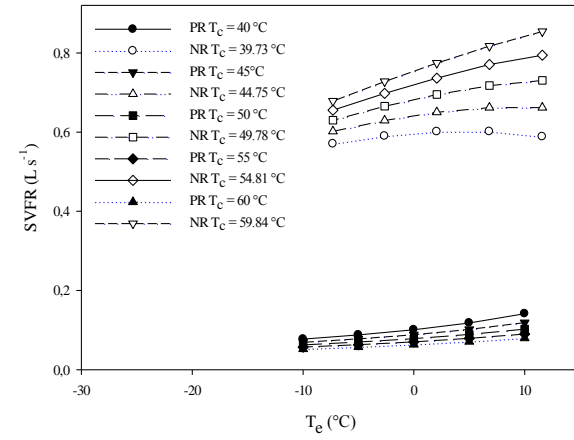


Figure 4.31 Charts of R507a vs R507a/Al₂O₃ for 5 °C of superheating/subcooling case

71

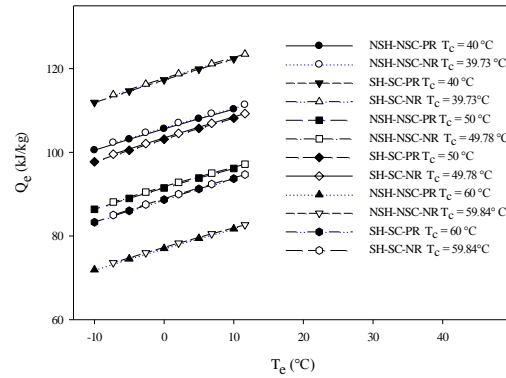


Figure 4.32 Chart of R507a and R507a/Al₂O₃ for non-superheating/subcooling vs. 5 °C of superheating/subcooling case

4.2 Discussion

The results of calculations for refrigerants and nanorefrigerants were used to chart in section 4.1.1 Charts. T_e and T_c temperature ranges were determined, and prediction model was applied to refrigerants and nanorefrigerants for these temperature ranges.

Temperature ranges were selected to realize an healthy comparison. For that purpose, the evaporator and condenser temperatures that ensure normal COP values for vapour-compression refrigeration cycle and the suitable temperatures for the compressor were settled.

Superheating and subcooling the refrigerant or the nanorefrigerant using in the refrigeration cycle increase heat transfer rate of evaporator (Q_e) and compressor work (W_{comp}). Q_e had bigger percental enhancement than W_{comp} . For this reason, COP increased. On the other hand, it was seen that increase of difference between T_e and T_c made Q_e decrease and W_{comp} increase for all the refrigerants and the nanorefrigerants. According to COP equation (2.6), decrease in Q_e and increase in W_{comp} means drop in COP. That is to say, more energy consumption for the same refrigeration capacity.

Although, supplement of the nanoparticles into pure refrigerant increases the pressure drop, the experimental studies was shown that wear in the parts of the compressor decreased with the use of the nanoparticles as refrigerant. The one of the reasons in the COP enhancement can be thought that the effect of mechanical enhancement is more than increasing in pressure drop.

The best percental enhancement in COP of vapour-compression refrigeration cycles using the refrigerants and the nanorefrigerants determined for the lowest condensation temperature with the lowest evaporation temperature for all refrigerants and nanorefrigerants, and for all cases the refrigerants' heat of evaporation increases with decreasing temperature. This can be explain why the best percental enhancement in COP realizes for the lowest evaporation with the lowest condensation temperatures. It can be seen for R134a in Table 4.4.

Table 4.20 Temperature vs. heat of evaporation (h_{fg}) of R134a

T_c (°C)	h_{fg} (kJ/kg)
-20	212.919
-10	205.968
0	198.603
10	190.741
20	182.281
30	173.096
40	163.019
50	151.814

Table 4.21 Comparison of the highest COP enhancement caused adding alumina nanoparticles into R22, R290, R410a, R431a and R507a

Refrigerant	T _c (°C)	T _e (°C)	h ₁ (kJ/kg)	h ₂ (kJ/kg)	h ₃ = h ₄ (kJ/kg)	COP	Nanorefrigerant	T _c (°C)	T _e (°C)	h ₁ (kJ/kg)	h ₂ (kJ/kg)	h ₃ = h ₄ (kJ/kg)	COP	Increase (%)
R22	40	-10	401.20	473.57	249.55	2.096	R22/Al ₂ O ₃	39.65	-5.96	402.79	467.45	249.12	2.377	13.41
R290	40	-10	563.46	690.10	308.61	2.012	R290/Al ₂ O ₃	38.90	-1.72	572.78	672.40	305.59	2.682	33.27
R410a	40	-10	417.46	496.23	260.55	1.992	R410a/Al ₂ O ₃	39.73	-7.16	418.48	491.15	260.14	2.179	9.37
R431a	40	-10	498.69	617.84	282.73	1.812	R431a/Al ₂ O ₃	39.32	-2.87	504.28	602.48	281.31	2.271	25.28
R507a	40	-10	356.37	410.25	255.86	1.865	R507a/Al ₂ O ₃	39.73	-7.30	357.78	407.84	255.48	2.044	9.56

Table 4.22 Comparison of the lowest COP enhancement caused adding alumina nanoparticles into R22, R290, R410a, R431a and R507a

Refrigerant	T _c (°C)	T _e (°C)	h ₁ (kJ/kg)	h ₂ (kJ/kg)	h ₃ = h ₄ (kJ/kg)	COP	Nanorefrigerant	T _c (°C)	T _e (°C)	h ₁ (kJ/kg)	h ₂ (kJ/kg)	h ₃ = h ₄ (kJ/kg)	COP	Increase (%)
R22	60	10	408.56	470.79	274.36	2.157	R22/Al ₂ O ₃	59.71	12.49	409.37	467.40	274.00	2.333	8.18
R290	60	10	585.52	694.36	364.38	2.032	R290/Al ₂ O ₃	59.11	15.40	591.17	684.39	361.85	2.460	21.08
R410a	60	10	423.51	489.97	291.21	1.991	R410a/Al ₂ O ₃	59.84	11.66	423.88	487.26	290.97	2.097	5.35
R431a	60	10	513.84	613.14	324.78	1.904	R431a/Al ₂ O ₃	59.45	14.36	516.88	605.00	323.60	2.194	15.22
R507a	60	10	366.15	411.11	284.43	1.818	R507a/Al ₂ O ₃	59.84	11.60	366.85	409.88	284.20	1.921	5.66

Adding alumina (Al_2O_3) nanoparticles in the base refrigerants made the compressor work (W_{comp}) decreased, heat transfer rate of evaporator (Q_e) and heat transfer rate of condenser (Q_c) increased, as seen Table 4.5 and Table 4.6. SVFR values of refrigeration cycles using nanorefrigerant are bigger than the base refrigerant's for all cases, and SVFR values increases when T_e and/or T_c increased. SVFR is calculated by using equation (3.2). Because of that, increase in heat transfer rate of evaporator causes increase in SVFR.

Outcome of the calculations, the enhancement of COP of the cycle using R600a is the greatest and the enhancement of COP of the cycle using R410a is the least one. It can be noted that the enhancement inflicting the addition of the nanoparticles in COP of refrigerants using instead of or equalized R12 are greater than COP enhancement of R12. This situation is not same for R22 and the refrigerants equalized R22, as well. Some of the refrigerants have larger and some of them have the smaller COP enhancement ratios. The two main reasons for this are that density was the starting point of the prediction model and the thermophysical specification of the refrigerants.

Moreover, it was seen that the nanorefrigerants had bigger evaporator temperatures and smaller condenser temperatures than the pure refrigerants as a result of the estimates. This situation coincides with the experimental studies in literature and confirms the prediction model from this point of view. In addition, decreasing of the difference between evaporator and condenser temperatures reduce isentropic compressor work.

Originally, it can be thought that the decreasing of the evaporator temperature corrupts the heat transfer and refrigeration. However, the higher temperatures for refrigerant means the higher evaporation enthalpy. Therefore, when it is considered that decreasing in evaporation temperature is little, decrease in the evaporator temperature can enhance the refrigeration effect.

In an actual vapour-compression refrigeration cycle, the enhancement in COP and energy-saving arising from the use of nanorefrigerant can be seen as decreasing in on-time ratio and electricity consumption.

The current model is developed to predict enhancement ratios in COP of vapour-compression refrigeration cycle. As there is not enough experimental data about the system parameters working with nanorefrigerant, the correlations available could use for the model. The correlation (3.4) proposed to calculate the density of nanorefrigerant is used for this model. It is enough know the evaporator and condenser temperatures of the system that COP enhancement ratio would estimate to apply the model to a refrigeration cycle. The prediction model gives an enhancement ratio after the calculations.

$$\text{Accuracy \%} = 1 - \frac{(\text{COP}_{\text{NR}})_{\text{experimental}} - (\text{COP}_{\text{PR}})_{\text{experimental}} \times (\text{Increase Ratio}) / 100}{(\text{COP}_{\text{NR}})_{\text{experimental}}} \quad (4.1)$$

This enhancement ratio provides to predict COP of the cycle by using the COP of the cycle using the pure refrigerant, while nanorefrigerant is used as a working fluid in refrigeration cycle instead of pure refrigerant. There is the accuracy above 95%, when

the new COP values obtained compared with experimental results. The percentage accuracy can check equation (4.1).

The migration of the nanoparticles by evaporation and drag can cause the some problems as clogging and stabile working of the system. Despite the nanoparticles become very small particles (1 – 100nm), the some components of the refrigeration systems have tiny sections or tubes. That the rallying of the nanoparticles on a definite place can seal off a part or block the flow of the refrigerant, in time. Moreover, decreasing of nanoparticle concentration in the nanorefrigerant decreases COP and refrigeration effect (RE).

The use of the nanorefrigerant implies dispersion, sedimentation problems. These problems cause that the nanoparticles in the mixture settles in time for stable case. In addition, the agglomeration problems are shown when used in excess of 4 wt. % mass fraction of nanoparticle in refrigerants. Despite the use of some surfactants, the problems are not able to dissolved completely.

CONCLUSION

There are many parameters affect the heat transfer characteristics of nanorefrigerants regarding the nanoparticle concentration ratio, nanoparticle size, nanoparticle type, lubricant type, refrigerant type, refrigeration cycle type, operating conditions, surfactant type etc. Al, Al₂O₃, CuO, SiO₂, Ti, TiO₂ are some of nanoparticle varieties. Generally, spheric and cylindrical types of nanoparticles are produced and used in studies. The serious problems are shown when used in excess of 4 wt. % mass fraction of nanoparticle in refrigerants. There are some evidences on the use nanoparticles with refrigerants that the energy consumption reduces with the using nanoparticle concentration. Sabareesh et al. [45] were reported that compressor work decreased when R12/TiO₂/MO nanorefrigerant used. Javadi and Saidur [51] were also reported that energy consumption of refrigerator when R134a/Al₂O₃ nanorefrigerant used.

As a result of some investigations, it is reported that the freezing velocity and COP in cooling devices increased with the use of nanoparticles. In Kumar et al. [43]'s study, experimental studies in order to reveal effect of R134a/Al₂O₃/PAG were shown that there is an important enhancement in COP.

These sample studies supports the prediction model of this study which based on R134a and R134a/Al₂O₃. In the calculations for ten base refrigerants (PR) and ten nanorefrigerants (NR) are shown that compressor work, energy consumption decreased, and COP increased with adding nanoparticles to the base refrigerant.

That adding nanoparticle to refrigerant or lubricant in compressor of a refrigeration system enhances physical specifications and heat transfer rate and heat transfer coefficient were reported by many researchers. Heat transfer rate of nanorefrigerant

increases with decreasing nanoparticle size, on the other hand, pressure drop decreased with decreasing nanoparticle size, compared with pure refrigerant.

Conductivity and convectional heat transfer of nanorefrigerant is bigger than its pure refrigerant. Enhancement of these physical specifications causes increasing in degree of subcooling and superheating. As removed heat is more than evaporation heat of working fluid, degree of subcooling and superheating increases and less compressor work is needed for the same refrigeration load. You can determine this case by using equation (2.1). Another probable case, heat rate of evaporator is able to increase with increase in mass rate. However, it is difficult to be possible as increasing mass rate increases compressor work. In addition, a nanoparticle relocates heat as the amount of its heat capacity, during heating and cooling, as well.

There are some efforts for the prediction of the long term performances of nanofluids and nanorefrigerants regarding their agglomeration, suspension, dispersion, sedimentation and clogging problems using some surfactants. However, the use of some surfactants is not able to dissolve these problems completely. The surfactant type has a potential to eliminate the problems of nanoparticles regarding their long-term usage. There are many studies on the heat transfer of nanorefrigerants using R11, R12, R22, R134a, R141b, R410a, R430a, R600a in the literature, operating conditions, used nanoparticle types, their concentrations and their sizes. However, findings are shown that nanorefrigerants have not been commercial refrigerants, yet.

REFERENCES

- [1] Xuan, Y. and Roetzel, W., (2000). "Conceptions for heat transfer correlations of nanofluids", *International Journal of Heat and Mass Transfer*, 43:3701-3707.
- [2] Xue Q.Z., (2003). "Model for effective thermal conductivity of nanofluids", *Physics Letters*, 307:313-317.
- [3] Xie, H., Lee, H., Youn, W. and Choi, M., (2003). "Nanofluids containing multiwalled carbon nanotubes and their enhanced thermal conductivities", *Journal of Applied Physics*, 49:4967-4971.
- [4] Liu, M.S., Lin, M.C.C., Huang, I.T. and Wang, C.C., (2005). "Enhancement of thermal conductivity with carbon nanotube for nanofluids", *International Communications in Heat and Mass Transfer*, 35:1202-1210.
- [5] Hwang, Y., Park, H.S., Lee, J.K. and Jung, W.H., (2006). "Thermal conductivity and lubrication characteristics of nanofluids", *Current Applied Physics*, 6S1:e67-e71.
- [6] Park, K.J. and Jung, D., (2007). "Boiling heat transfer enhancement with carbon nanotubes for refrigerants used in building air-conditioning", *Energy and Buildings*, 38:1061-1064.
- [7] Ding, G.L., (2007). "Recent developments in simulation techniques for vapour-compression refrigeration systems", *International Journal of Refrigeration*, 30:1119-1133.
- [8] Ding, Y., Chen, H., He, Y., Lapkin, A., Yeganeh, M., Šiller, L. and Butenko, Y. V., (2007). "Forced convective heat transfer of nanofluids", *Advanced Powder Technology*, 18:813-824.
- [9] Li, C.H. and Peterson, G.P., (2007). "Mixing effect on the enhancement of the effective thermal conductivity of nanoparticle suspensions (nanofluids)", *International Journal of Heat Mass Transfer*, 50:4668-4677.
- [10] Avsec, J. and Oblak, M., (2007). "The calculation of thermal conductivity, viscosity and thermodynamic properties for nanofluids on the basis of statistical nanomechanics", *International Journal of Heat Mass Transfer*, 50: 4331-4341.
- [11] Bartelt, K., Park, Y., Liu, L. and Jacobi, A., (2008). "Flow boiling of R134a/POE/CuO nanofluids in a horizontal tube", *International Refrigeration and Air Conditioning Conference*, 14-17 July 2008, Purdue.
- [12] Bi, S.S., Shi, L. and Zhang, L.L., (2008). "Application of nanoparticles in domestic refrigerators", *Applied Thermal Engineering*, 28:1834-1843.

- [13] Lu, W.Q. and Fan, Q.M., (2008). “Study for the particle’s scale effect on some thermophysical properties of nanofluids, by a simplified molecular dynamics method”, *Engineering Analysis with Boundary Elements*, 32:282-289.
- [14] Chen, H., Yang, W., He, Y., Ding, Y., Zhang, L., Tan, C., Lapkin, A. A. and Bavykin, D. V., (2008). “Heat transfer and flow behavior of aqueous suspensions of titanate nanotubes (nanofluids)”, *Powder Technology*, 183:63-72.
- [15] Ding, G., Peng, H., Jiang, W. and Gao, Y., (2009). “The migration characteristics of nanoparticles in the pool boiling process of nanorefrigerant and nanorefrigerant–oil mixture”, *International Journal of Refrigeration*, 32:114–123.
- [16] Jiang, W., Ding, G. and Peng, H., (2009). “Measurement and model on thermal conductivities of carbon nanotube nanorefrigerants”, *International Journal of Thermal Sciences*, 48:1108–1115.
- [17] Kedzierski, M. A. and Gong, M., (2009). “Effect of CuO nanolubricant on R134a pool boiling heat transfer”, *International Journal of Refrigeration*, 32:791–799.
- [18] Naphon, P., Thongkum, D. and Assadamongkol, P., (2009). “Heat pipe efficiency enhancement with refrigerant–nanoparticles mixtures”, *Energy Conversion and Management*, 50:772–776.
- [19] Peng, H., Ding, G., Jiang, W., Hu, H. and Gao, Y., (2009). “Heat transfer characteristics of refrigerant-based nanofluid flow boiling inside a horizontal smooth tube”, *International Journal of Refrigeration*, 32:1259–1270.
- [20] Peng, H., Ding, G., Jiang, W., Hu, H. and Gao, Y., (2009). “Measurement and correlation of frictional pressure drop of refrigerant-based nanofluid flow boiling inside a horizontal smooth tube”, *International Journal of Refrigeration*, 32:1756–1764.
- [21] Trisaksri, V. and Wongwises, S., (2009). “Nucleate pool boiling heat transfer of TiO₂–R141b nanofluids”, *International Journal of Heat and Mass Transfer*, 52:1582–1588.
- [22] Kedzierski, M. A., (2009)., “Effect of CuO nanoparticle concentration on R134a/lubricant pool boiling heat transfer”, *Journal of Heat Transfer*, 131/043205-1.
- [23] Jwo, C. S., Jeng, L. Y., Teng, T. P. and Chang, H., (2009). “Effects of nanolubricant on performance of hydrocarbon refrigerant system”, *Journal of Vacuum Science & Technology*, 27:1473-1477 .
- [24] He, Y., Men, Y., Zhao, Y., Lu, H. and Ding, Y., (2009). “Numerical investigation into the convective heat transfer of TiO₂ nanofluids flowing through a straight tube under the laminar flow conditions”, *Applied Thermal Engineering* 29:1965-1972.
- [25] Murshed, S.M.S., Leong, K.C. and Yang, C. A., (2009). “A combined model for the effective thermal conductivity of nanofluids”, *Applied Thermal Engineering* 29:2477-2483.

- [26] Wang, R., Wu, Q. and Wu, Y., (2010). "Use of nanoparticles to make mineral oil lubricants feasible for use in a residential air conditioner employing hydro-fluorocarbons refrigerants", *Energy and Buildings*, 42:2111–2117.
- [27] Bobbo, S., Fedele, L., Fabrizio, M., Barison, S., Battiston, S. and Pagura C., (2010). "Influence of nanoparticles dispersion in POE oils on lubricity and R134a solubility", *International Journal of Refrigeration*, 33:1180-1186.
- [28] Henderson, K., Park, Y., Liu L. and Jacobi A. M., (2010). "Flow-boiling heat transfer of R-134a-based nanofluids in a horizontal tube", *International Journal of Heat and Mass Transfer*, 53:944–951.
- [29] Peng, H., Ding, G., Hu, H. and Jiang, W., (2010). "Influence of carbon nanotubes on nucleate pool boiling heat transfer characteristics of refrigerant-oil mixture", *International Journal of Thermal Sciences*, 49:2428-2438.
- [30] Peng, H., Ding, G., Hu, H., Jiang W., Zhuang D. and Wang, K., (2010). "Nucleate pool boiling heat transfer characteristics of refrigerant/oil mixture with diamond nanoparticles", *International Journal of Refrigeration* , 33:347-358.
- [31] Fard, H. M., Esfahany, M.N. and Talaie, M.R., (2010). "Numerical study of convective heat transfer of nanofluids in a circular tube two-phase model versus single-phase model", *International Communications in Heat and Mass Transfer*, 37:91-97.
- [32] Meibodi, M.E., Sefti, M.V., Rashidi, A.M., Amrollahi, A., Tabasi, M. and Kalal, H.S., (2010). "Simple model for thermal conductivity of nanofluids using resistance model approach", *International Communications in Heat and Mass Transfer*, 37:555-559.
- [33] Bi, S., Guo, K., Liu, Z. and Wu J., (2011). "Performance of a domestic refrigerator using TiO₂-R600a nano-refrigerant as working fluid", *Energy Conversion and Management*, 52:733–737.
- [34] Yu, L., Liu, D. and Botz, F., (2011). "Laminar convective heat transfer of alumina-polyalphaolefin nanofluids containing spherical and non-spherical nanoparticles", *Experimental Thermal and Fluid Science*, 37:72-83.
- [35] Peng, H., Ding, G. and Hu, H., (2011). "Effect of surfactant additives on nucleate pool boiling heat transfer of refrigerant-based nanofluid", *Experimental Thermal and Fluid Science*, 35:960–970.
- [36] Peng, H., Ding, G. and Hu, H. (2011). "Influences of refrigerant-based nanofluid composition and heating condition on the migration of nanoparticles during pool boiling. Part I: Experimental measurement", *International Journal of Refrigeration*, 34:1823-1832.
- [37] Peng, H., Ding, G., Hu, H. and Jiang W., (2011). "Effect of nanoparticle size on nucleate pool boiling heat transfer of refrigerant/oil mixture with nanoparticles", *International Journal of Heat and Mass Transfer*, 54:1839–1850.
- [38] Abdel-Hadi, E. A., Taher, S. H., Torki, A.H. M. and Hamad, S. S., (2011). "Heat transfer analysis of vapor compression system using nano CuO-R134a", *International Conference on Advanced Materials Engineering IPCSIT*, 15:80-84.

- [39] Mahbubul, I.M., Saidur R. and Amalina M.A., (2011). “Pressure Drop Characteristics of TiO₂-R123 Nanorefrigerant In A Circular Tube”, Engineering e-Transaction (ISSN 1823-6379), 6:124-130.
- [40] Peng, H., Ding, G. and Hu, H., (2011). “Influences of refrigerant-based nanofluid composition and heating condition on the migration of nanoparticles during pool boiling. Part II: Model development and validation”, International Journal of Refrigeration, 34:1833-1845.
- [41] Kedzierski M.A., (2011). “Effect of Al₂O₃ nanolubricant on R134a pool boiling heat transfer”, International Journal of Refrigeration, 34:498-508.
- [42] Firouzfard, E., Soltanieh, M., Noie, S.H. and Saidi, S.H., (2011). “Energy saving in HVAC systems using nanofluid”, Applied Thermal Engineering, 31:1543-1545.
- [43] Kumar, D. S. and Elansezhian, R. D., (2012). “Experimental Study on Al₂O₃-R134a Nanorefrigerant in Refrigeration System”, International Journal of Modern Engineering Research (IJMER), 5:3927-3929.
- [44] Padmanabhan, V. M. V. and Palanisamy S., (2012). “The use of TiO₂ nanoparticles to reduce refrigerator irreversibility”, Energy Conversion and Management, 59:122–132.
- [45] Sabareesh, R. K., Gobinath, N., Sajith, V., Das, S. and Sobhan C.B., (2012). “Application of TiO₂ nanoparticles as a lubricant-additive for vapor compression refrigeration systems - An experimental investigation”, International Journal of Refrigeration, 35:1989-1996.
- [46] Kedzierski M.A., (2012). “Effect of diamond nanolubricant on R134a pool boiling heat transfer”, Journal of Heat Transfer: ASME DC, 134:051001-1.
- [47] Kedzierski M.A., (2012). “R134a/Al₂O₃ nanolubricant mixture pool boiling on a rectangular finned surface”, Journal of Heat Transfer: ASME DC, 134:121501-1.
- [48] Mahbubul, I. M., Saidur, R. and Amalina, M., A., (2012). “Investigation of viscosity of R123- TiO₂ nanorefrigerant”, International Journal of Mechanical and Materials Engineering (IJMME), 7:146-151.
- [49] Bobbo, S., Fedele, L., Benetti, A., Colla, L., Fabrizio, M., Pagura, C. and Barison, S., (2012). “Viscosity of water based SWCNH and TiO₂ nanofluids”, Experimental Thermal and Fluid Science, 36:65-71.
- [50] Cheng, L. and Liu, L., (2013). “Boiling and two-phase flow phenomena of refrigerant-based nanofluids: Fundamentals, applications and challenges” International Journal of Refrigeration, 36:421-446.
- [51] Javadi, F. S. and Saidur, R., (2013). “Energetic, economic and environmental impacts of using nanorefrigerant in domestic refrigerators in Malaysia”, Energy Conversion and Management, 73:335 – 339.
- [52] Kedzierski, M. A., (2013). “Viscosity and density of aluminum oxide nanolubricant”, International Journal of Refrigeration, 36:1333-1340.
- [53] Mahbubul, I. M., Saidur, R. and Amalina, M., A., (2013). “Influence of particle concentration and temperature on thermal conductivity and viscosity of

- Al₂O₃/R141b nanorefrigerant”, *International Communications in Heat and Mass Transfer*, 43:100–104.
- [54] Mahbubul, I. M., Saidur, R. and Amalina, M. A., (2013). “Thermal conductivity, viscosity and density of R141b refrigerant based nanofluid”, *Procedia Engineering*, 56:310 – 315.
- [55] Mahbubul, I. M.; Saidur, R. and Amalina, M. A., (2013). “Heat transfer and pressure drop characteristics of Al₂O₃-R141b nanorefrigerant in horizontal smooth circular tube”, *Procedia Engineering*, 56:323–329.
- [56] Mahbubul, I. M., Fadhilah, S. A., Saidur, R., Leong, K. Y. and Amalina, M. A., (2013). “Thermophysical properties and heat transfer performance of Al₂O₃/R-134a nanorefrigerants”, *International Journal of Heat and Mass Transfer*, 57:100–108.
- [57] Sun, B. and Yang, D., (2013). “Experimental study on the heat transfer characteristics of nanorefrigerants in an internal thread copper tube”, *International Journal of Heat and Mass Transfer*, 64:559–566.
- [58] Subramani, N. and Prakash, M. J., (2011). “Experimental studies on a vapour compression system using nanorefrigerants”, *International Journal of Engineering, Science and Technology*, 3:55–102.
- [59] Dalkilic, A. S. and Wongwises, S., (2010). “A performance comparison of vapour-compression refrigeration system using various alternative refrigerants”, *International Communications in Heat and Mass Transfer*, 37:1340–1349.

CURRICULUM VITAE

PERSONAL INFORMATION

Name Surname : Melih AKTAŞ
Date of birth and place : 10.03.1987 / Çanakkale
Foreign Languages : English, German
E-mail : melih.aktas@yahoo.com

EDUCATION

Degree	Department	University	Date of Graduation
Master	Mechanical Engineering / Heat – Process		
Undergraduate	Mechanical Engineering	Yıldız Technical University	2010
High School	Science	Çanakkale Fen Lisesi	2005

WORK EXPERIENCE

Year	Corporation/Institute	Enrollment
-------------	------------------------------	-------------------